

Implications of the Late Quaternary Glacio–Eustatic Sea level Changes in the Black Sea Catchment Area

Von der Fakultät für Mathematik und Naturwissenschaften
der Carl von Ossietzky Universität Oldenburg
zur Erlangung des Grades und Titels eines
Doktors der Naturwissenschaften (Dr. rer. nat.)
angenommene Dissertation von

Goran Georgievski
geboren am 09. Februar 1971
in Zagreb

Gutachter: Prof. Dr. Emil Stanev

Zweitgutachter: Prof. Dr. Hans-Jürgen Brumsack

Tag der Disputation: 23. 05. 2008.

Contents

Abstract	iii
Zusammenfassung	v
1 Introduction	1
1.1 Global and regional sea level changes on the glacial time scale	1
1.2 Black Sea region and climate	2
1.3 Shift of the hydrological cycle – conceptual idealization	3
1.4 Figures	6
2 Surface climate response to the glacio-eustatic sea level changes	12
2.1 Introduction	12
2.2 Method and experimental setup	13
2.2.1 Orography and sea - land - ice mask	14
2.2.2 Surface parameters	16
2.3 Results	17
2.3.1 Temperature	17
2.3.2 Hydrologic cycle	19
2.3.3 Correlation between T and $P - E$	20
2.4 Summary and outlook	21
2.5 Figures	22
3 Sensitivity of climatic patterns in Europe	27
3.1 Introduction	27
3.2 Teleconnection patterns dominating European climate	29
3.3 Numerical simulations	31
3.4 Orographic control on the NCP	32
3.5 Conclusions	34
3.6 Figures	35
4 Black Sea level at the last deglaciation	45
4.1 Introduction	46
4.2 Description of Data	49
4.2.1 The Region	49
4.2.2 Hydrological Data	50

4.3	Method and Experiments	56
4.3.1	Water Balance Equations	56
4.3.2	Experimental Design	56
4.3.3	Results	58
4.4	Discussion and Summary	60
4.5	Figures	62
5	Black Sea level sensitivity to the changes of hydrologic cycle	70
5.1	Introduction	70
5.2	Theoretical consideration	71
5.3	Data and methodology	72
5.4	Results	74
5.5	Discussion	76
5.6	Figures	78
6	The Black Sea water balance during the past glacial cycle	82
6.1	Introduction	82
6.2	Black Sea catchment area in the glacial cycle	84
6.3	Data and methods	85
6.3.1	Present-day hydrology	85
6.3.2	Palaeo hydrology	86
6.3.3	Water budget	88
6.4	Experimental setup	89
6.5	Results	89
6.5.1	Sea-land distribution	90
6.5.2	Transport in the passages	90
6.5.3	The Black Sea sea-level	91
6.5.4	Error estimates and discussion	91
6.6	Summary and outlook	92
6.7	Figures	93
7	Summary and further perspectives	99
	Bibliography	103
	List of Abbreviations	109
	Acknowledgments	110
	Curriculum Vitae	112
	Erklärung	113

Abstract

Water balance of the Black Sea catchment area is studied and volumetric analysis of the Black Sea basin is performed in order to estimate sea level fluctuations during the Last glacial cycle. In order to reconstruct the most plausible scenario of the Black Sea reconnection with the Mediterranean, we integrated various data sets available in the literature. These data sets include meteorological re-analysis (ERA-40), as well as more reliable hydro-meteorological observations for the present-day conditions. The latter makes possible to correct the re-analysis data. Hydrological forcing for the past is compiled from various sources including pollen reconstructions and $\delta^{18}O$ oscillations. Eurasian ice sheet extension is inferred from geological observations and modelling reconstruction available in literature. The latter also has a temporal resolution suitable to calculate the corresponding glacial melt water flux at the times of deglaciation. It turns out that about $500 \text{ km}^3 \cdot \text{y}^{-1}$ increase of river discharge into the Caspian Sea is needed in order to enable a transport trough the Manych Pass to the Black Sea. Furthermore, the mechanisms influencing the variability of the global hydrological cycle due to the glacio-eustatic sea level change are investigated with the Earth System Model of Intermediate Complexity (EMIC). It is shown that the redistribution of sea - land can have a significant impact on the regional climate. In particular, in the Mediterranean area, cooling due to mountain uplift would cause the hydrologic cycle to shift towards drier conditions, while warming due to a changed sea-land distribution would cause a shift towards wet conditions. This result and the above mentioned data are combined to perform an extensive sensitivity study of the Black Sea level response to the changes of the hydrological cycle components. It is shown that according to the geological reconstruction of the climate the Black Sea water balance remained positive during the Holocene and the catastrophic flood (the Mediterranean waterfall) is not likely to have happened. However, precipitation and evaporation above the sea remain uncertain at that time. Therefore, we have estimated that the increase of maritime evaporation and decrease of maritime precipitation has to be 1.7 times the present-day values in order to achieve a sea-level drop of 140 m which is hypothesized in the flood theory. These results together with geological observations of the last Quaternary glaciation such as oxygen isotopes ratio ($\delta^{18}O$, maritime and ice core record) oscillations and Eurasian ice-sheet extension as an indicator of hydrological regime change are used to provide theoretical portrayals of likely configurations of the Black

Sea catchment area. Comparing our results with global sea-level, it turned out that reconnection at the penultimate glacial maximum could happen suddenly, while all recent reconnections were more likely gradual. Black Sea water balance was positive during almost all times. Furthermore, we have investigated alternative possibilities that would cause the Black Sea level to decrease, changing each individual component of the hydrologic cycle. Our study indicates that is it possible to have the Black Sea level draw down for about 150 m in a 1000 - 2000 years at LGM or Younger Dryas if precipitation decreases ($450 \text{ mm} \cdot \text{y}^{-1}$ or $150 \text{ mm} \cdot \text{y}^{-1}$ respectively) and evaporation decreases slightly less than precipitation. New, well-dated geological measurements in this area is needed to further constrain changes in the water budgets.

Zusammenfassung

Die Hydrologie des Schwarzen Meeres und seines Wassereinzugsgebietes wurde untersucht. Es war das Ziel, die Veränderungen des Meeresspiegels während des letzten glazialen Zyklus in diesem Meeresgebiet und insbesondere die Wiederverbindung des Schwarzen Meeres mit dem Mittelmeer abzuschätzen. Hydro-meteorologische Beobachtungen wurden verwendet, um ERA-40 Reanalysendatensätze zu korrigieren. Der hydrologische Einträge in der Vergangenheit wurde aus verschiedenen Quellen rekonstruiert, u.a. Pollendaten und $\delta^{18}O$ Variationen. Die Ausdehnung des Eurasischen Eisschildes wurde von geologischen Beobachtungen und Rekonstruktionen aus der Literatur entnommen. Die zeitliche Auflösung dieses Datensatzes erlaubt die Berechnung des Schmelzwasserflusses während des Übergangs von der Kalt- zur Warmzeit. Die Berechnungen haben ergeben, dass ein Anstieg des Flußwassereintrags von $500 \text{ km}^3 \cdot \text{a}^{-1}$ in das Kaspische Meer benötigt wird, um einen Transport durch den Manych Pass zum Schwarzen Meer zu ermöglichen. Mechanismen, die die Variabilität des globalen hydrologischen Zyklus durch eustatische Änderungen des Meeresspiegels beeinflussen, wurden mit dem Erdsystemmodell EMIC untersucht. Es konnte gezeigt werden, dass Änderungen in der Land-Meer-Verteilung einen signifikanten Einfluss auf das lokale Klima haben. Insbesondere im Mittelmeerraum würde eine Abkühlung durch vertikale Verlagerung der Gebirge den hydrologischen Zyklus zu trockeneren Bedingungen verschieben, während eine Erwärmung durch eine veränderte Land-Meer-Verteilung eine Verschiebung zu feuchteren Bedingungen zur Folge hätte. Diese Überlegungen wurden zusammen mit den erwähnten Daten in einer ausführlichen Sensitivitätsstudie zusammengefasst. Es wurde also der Einfluss verschiedener Komponenten des hydrologischen Zyklus auf die Meeresspiegeländerungen im Schwarzen Meer untersucht. Es konnte gezeigt werden, dass aufgrund der geologischen Rekonstruktion des Klimas die Wasserbilanz des Schwarzen Meeres während des gesamten Holozäns positiv blieb und daher die Theorie einer biblische Flutkatastrophe aus heutiger Sicht zweifelhaft ist. Ein unsicherer Faktor für diesen Zeitraum bleibt aber die Summe aus Niederschlag und Verdunstung über dem Meeresgebiet. Aus diesem Grund wurde eine Sensitivitätsuntersuchung gemacht, in welcher der Nettoeffekt aus mariner Verdunstung und marinem Niederschlag mit einem Faktor von 1.7 zu den heutigen Werten verstärkt wurde. So konnte eine Senkung des Meeresspiegel um 140 m reproduziert werden, wie es in den Hypothesen zur Fluttheorie gefordert wird. Diese Ergeb-

nisse wurden zusammen mit geologischen Beobachtungen der letzten Vereisung im Quartär (Verhältnisse von Sauerstoffisotopen aus marinen- und Eisbohrkernen und die Ausdehnung des Eurasischen Eisschildes als Indikator für hydrologische Regimewechsel) benutzt, um theoretisch mögliche Konfigurationen des Wassereinzugsgebietes des Schwarzen Meeres zu bestimmen. Der Vergleich der Ergebnisse mit Zeitreihen der globalen Meeresspiegelentwicklung zeigt, dass Verbindungen zum Zeitpunkt des vorletzten glazialen Maximums plötzlich auftreten können, wobei spätere Verbindungen eher einen graduellen Charakter haben. Über die betrachteten Zeitalter war die Wasserbilanz des Schwarzen Meeres positiv. Desweiteren wurden alternative Szenarien untersucht, die durch individuelle Änderung der einzelnen Komponenten im hydrologischen Zyklus zu einer Absenkung des Meeresspiegels im Schwarzen Meer führen könnten. Es stellte sich heraus, dass es zu Zeiten des letzten glazialen Maximums bzw. während des Jüngeren Dryas möglich gewesen wäre den Meeresspiegel im Schwarzen Meer um 150 m in einem Zeitrahmen von 1-2 Millenien zu senken, falls, bei vergleichsweise etwas geringerer Abnahme der Verdunstungsrate, die Niederschlagsrate um $450 \text{ mm} \cdot \text{a}^{-1}$ bzw. $150 \text{ mm} \cdot \text{a}^{-1}$ abnimmt. Neuere, gut-datierte, geologische Messergebnisse werden benötigt, um die Änderungen in der Gesamtwasserbilanz in diesem Gebiet genauer zu bestimmen.

Chapter 1

Introduction

1.1 Global and regional sea level changes on the glacial time scale

The oscillation of the shoreline position along ocean coasts and around inland water basins (lake or sea) varies in amplitude over a broad spectrum of time scales. Those changes, as a response to various geological and climatological processes, influence the relative sea level. On the glacial time scale ($\sim 120\,000$ years, i.e. ~ 120 ka), several processes cause sea level fluctuations:

- (i) changes within the hydrologic cycle, i.e. redistribution of water from liquid to frozen phase;
- (ii) changes in ocean volume, i.e. isostatic adjustment, tectonic uplift or subsidence, coastal erosion (retreat) or accretion (advance);
- (iii) steric effects, i.e. thermal expansion and compression.

All of these processes are global phenomena, but all of them could also have important regional implications, affecting rise or fall of the relative sea level of land-locked basins. Waxing and waning of the continental ice-sheet as well as large-scale changes in the configuration of continental margins and ocean floors will affect global sea level. However, geomorphological changes such as crustal rebound from glaciation, tectonic uplift or subsidence, erosion and deposition, changes in melt-water load, river flow redirection due to ice-sheet damming, thermal expansion of ocean waters could have only regional impact. For example, decoupling the inland basin from the global ocean.

One exceptional case, where all those processes took place during the Quaternary glaciations, are the Eurasian inland basins (Fig. 1.1). In this thesis, the focus is on the Black Sea catchment area and its sea level during the Last glaciation period (past ~ 120 ka).

1.2 Black Sea region and climate

Several various data sets were used in this thesis to describe the Black Sea catchment area and its extension during the past ~ 120 ka. Brief reference is given below to the data compared, analyzed and used to construct forcing functions and further integration and synthesis. Complete data description and their utilization are described in their respective chapters.

(i) Topography and watershed delineation:

- (a) U.S. Department of Commerce, National Oceanic and Atmospheric Administration, National Geophysical Data Center. 2-minute Gridded Global Relief Data (ETOPO2). ETOPO2 dataset is supplemented with the Caspian Sea bathymetry kindly provided by Caspian Environment Programme;
- (b) Borders of the catchment area are constructed and corrected from Total Runoff Integrating Pathways (TRIP) scheme developed by Oki and Sud [1998];

(ii) Present-day hydrology:

- (a) European Center for Medium-Range Weather Forecasts, (ECMWF) Re-analysis data (ERA-40) Simmons and Gibson [2000];
- (b) Black Sea Hydrometeorological Data set (BSHMD), Stanev and Peneva [2001];
- (c) Global River Discharge Centre (GRDC) Composite Runoff Fields v 1.0, Fekete et al. [1999];

(iii) Paleo hydrology:

- (a) Climate conditions in Europe during the mid Holocene (6 ka BP), reconstructed by Cheddadi et al. [1997] using modern pollen analogue technique constrained with lake level data;
- (b) Precipitation over land for the the main Lateglacial/Early Holocene climate oscillations in eastern Europe and Siberia reconstructed by Velichko et al. [2002] and Klimanov [1997] based on analysis of pollen data;
- (c) Paleo-discharges of the North-Eurasian rivers reconstructed by Sidorchuk et al. [2003] using the concept of modern analogue channel geomorphology;

- (d) Precipitation at the Late Glacial Maximum (LGM) reconstructed by Tarasov et al. [1999] based on pollen analysis;
- (iv) Ice sheet extension and sea level proxies:
 - (a) Global sea level rise since LGM reconstructed by Fairbanks [1989] and data for several sites in the Mediterranean are used from Tushingham and Peltier [1993] reconstruction;
 - (b) Eurasian Ice-Sheet extension based on glacial isostatic adjustment from Peltier [2004, 1994] and geological observation in the frame of the Quaternary Environment of the Eurasian North (QUEEN) project [Svendsen et al., 2004, Siebert and Dowdeswell, 2004, Mangerud et al., 2004];
 - (c) global sea level rise for the last glacial cycle from Lambeck et al. [2002];
 - (d) marine isotope stages, $\delta^{18}O$ oscillation from Raymo and Ruddiman [2004];
 - (e) $\delta^{18}O$ oscillation from the Greenland Ice Core Project (GRIP), GRIP Members [1993].

Furthermore, for the completeness a mini atlas of the surface climatology in the region is prepared from ERA-40 dataset. Annual mean and seasonal means (DJF - December, January, February; MAM - March, April, May; JJA - June, July, August; SON - September, October, November) are shown on Figs. 1.2 (2 m temperature in $^{\circ}C$), 1.3 (precipitation in $mm \cdot y^{-1}$), 1.4 (evaporation in $mm \cdot y^{-1}$), 1.5 (mean sea level pressure in hPa , and 1.6 (wind speed in $m \cdot s^{-1}$).

1.3 Shift of the hydrological cycle – conceptual idealization

Even today, we are witnessing dramatic climate changes. In particular in polar regions, they resemble similar phenomena that appeared on glacial time scale even in mid-latitudes. At present day these changes include unusual melting of glaciers, sea ice, and permafrost, shifts in patterns of rain and snow fall, freshwater runoff which also influence changes in vegetation pattern. However, on the glacial time scale (120 ka) those changes were even more dramatic, and not only in polar regions but also in mid-latitudes. In this work, we have tried to quantify shifts in the hydrological cycle during the glacial cycle, in particular, for the Black Sea catchment area.

The hydrologic cycle, in particular distribution of evaporation and precipitation over the ocean is one of the least understood elements of the climate system. Even the most up to date data sets, such as meteorological re-analysis, do not close regional water balances as they should [Dai and Trenberth, 2002]. According to efforts in the frame of the Paleoclimate Modelling Intercomparison Project (PMIP), the understanding of hydrological cycle variations is now considered as one of the most important issues, especially for ocean circulation changes on decade

to millennial time-scales. The Black Sea and its watershed is an ideal laboratory to study these processes. However, taking into account non-linear interactions between the processes that influence hydrologic cycle and sea level changes mentioned in section 1.1, it is obvious that those phenomena are too complex to be described and predicted by a single unified theoretical model. Actually, that task seems to be impossible at the present state of knowledge and development of computational technology. Therefore, various types of numerical models are employed to understand and quantify physical parameters involved in these processes. In this thesis, an Earth-system Model of Intermediate Complexity (EMIC) – the Planet Simulator (PS) is used in order to understand how eustatic changes of sea level would influence hydrologic conditions. It is shown that redistribution of sea - land can have a significant impact on regional climate. In particular in the Mediterranean area, cooling will favor a hydrologic shift towards drier conditions, while warming will cause a shift towards wet conditions. The same applies for the globe, since reaching towards the stadial (cold) state climate, the global hydrologic cycle (precipitation - evaporation), appears to have deficit in liquid phase, thus resulting in decreasing sea level. Going towards the interstadial (warm) state climate, hydrologic cycle intensifies causing sea level rise. Based on these facts, a conceptual model of the Black Sea water balances for the Late Pleistocene is developed. In the water balance equation, trends towards stadial (cold) state climate are considered as drying periods, while trends towards interstadial (warm) state climate are considered as wetting periods. Using volumetric functions for the Black Sea basin the sea level is estimated from various data sets during the last glacial cycle. The undertaken work is described in five chapters briefly summarized below. In **Chapter 2, Surface climate response to the glacio-eustatic sea level changes** is investigated. In particular, we have investigated the mechanisms influencing the variability of the hydrological cycle. Numerical simulations are performed with EMIC – PS. The model (EMIC – PS) is described in more detail in chapters 2 and 3. We demonstrate that changes of boundary conditions (sea - land mask, orography, surface properties) have significant impact on surface climate (2 m temperature, precipitation, and evaporation). Furthermore, we have investigated how would the changes in regional orography impact the global climate indexes. This work is described in **Chapter 3: Sensitivity of climatic patterns in Europe to changes in coastal line and orography**. The focus is put on the North Atlantic Oscillation (NAO) and East Atlantic/West Russia (EAWR) pattern. The results presented reveal that the orography in the studied region has a crucial role in the control of regional climatic patterns, in particular that of the EAWR. In the following chapters (4, 5, and 6), sensitivity studies of the Black Sea water balances are described. **Black Sea level at the Lateglacial to Holocene transition**¹ is described in **Chapter 4**. Paleohydrological data available for the Black Sea catchment area, analyzed for the period from the Last Glacial Maximum (LGM) to

¹This work is published with Climate Dynamics, full reference is:

Georgievski G. and E. V. Stanev: Paleo-evolution of the Black Sea watershed: sea level and water transport through the Bosphorus Strait as an indicator of the Lateglacial – Holocene transition, Climate Dynamics, Vol: 26:6, 2006, p. 631 - 644, DOI 10.1007/s00382-006-0123-y

the Holocene, indicate that the water balance of the Black Sea should be positive during that period, thus, exporting water through the Bosphorus Strait to the Mediterranean. However, some geological observations indicate that the Black Sea level fell during that period. In the water balance equation of the Black Sea, the maritime components of the hydrological cycle remained the only unknown. Therefore, we have estimated that the increase of maritime evaporation and decrease of maritime precipitation has to be about 1.7 times the present-day values in order to achieve a sea-level drop of 140 m. These results motivated us to perform an extensive **Black Sea water balance sensitivity study** on the changes of hydrological components. This work is described in **Chapter 5**. We have applied hypsometric function and water balance equations with topographic (ETOPO2) and hydrological (corrected ERA-40) data. Results indicate that changes of the continental components have more influence on the Black Sea level than changes of the maritime ones. Furthermore, an increase of maritime evaporation could cause a more significant sea level fall than a decrease of maritime precipitation. It is shown that precipitation has to decrease slightly more than evaporation should decrease in order to draw down the sea level. If they change at the same rate there is no significant change of the sea level. According to geological observation at the LGM there were $450 \text{ mm} \cdot \text{y}^{-1}$ and at Younger Drayas $150 \text{ mm} \cdot \text{y}^{-1}$ less than present-day precipitation. Therefore, it is possible to have the sea level draw-down for about 150 m in 1000 years if evaporation is $350 \text{ mm} \cdot \text{y}^{-1}$ less at LGM and $50 \text{ mm} \cdot \text{y}^{-1}$ at Younger Drayas than the present-day evaporation. In order to provide a possible scenario for the Black Sea level changes during the past glacial cycle, results from Chapter 4 need to be constrained with the geological observations. In **Chapter 6, Black Sea level during the last glacial cycle** water-budget calculations are performed with the data available for the last deglaciation with sensitivity analysis to cover for unconstrained assumptions. Oxygen isotope ratio ($\delta^{18}\text{O}$, ice core record and marine isotope) oscillations indicate variations between cold and warm periods. This feature, together with the method described in Chapter 4 is used to reconstruct the Black Sea hydrological forcing for the past $\sim 120 \text{ ka}$. Geomorphological changes (river redirection due to ice-sheet damming and melt water load) are taken into account according to geological observations. Using hypsometric function and water balance equation enabled us to compute the Black Sea sea level curve and the Bosphorus outflow for the last glacial cycle, during the periods when the Black Sea was isolated from the Mediterranean. Analyses of the results demonstrate that high frequency hydrological variations even with higher amplitudes do not cause substantial sea-level changes. It is moderate hydrological shift towards dry climate that results in sea-level decrease if it lasts for a sufficiently long time period. For the Black Sea level, the duration of the hydrological shifts towards dry climate is more important than the amplitude of change. **Chapter 7: Summary and further perspectives** conclude the thesis.

1.4 Figures

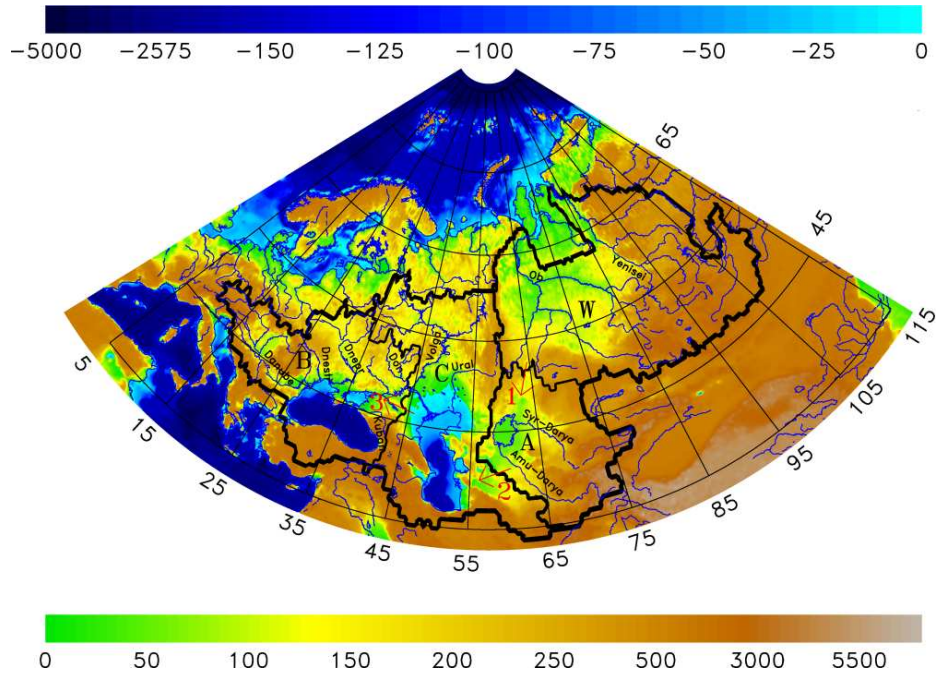


Figure 1.1: Present-day orography and bathymetry (Note that contour intervals are not linear). Thick black line indicates border of the Black Sea catchment area in the past, while thin black line shows borders of the present day watersheds. Bold letters indicate present day watersheds of: B - Black Sea, C - Caspian Sea, A - Aral Sea, and W - West Siberian Plain (Ob and Yenisei rivers). Red numbers with arrows indicate possible paleo-channels: 1 - the Turgay Pass, 126 m ASL, 2 - the Uzboy Pass, 57 m ASL, and 3 - the Manych Pass, 26 m ASL.

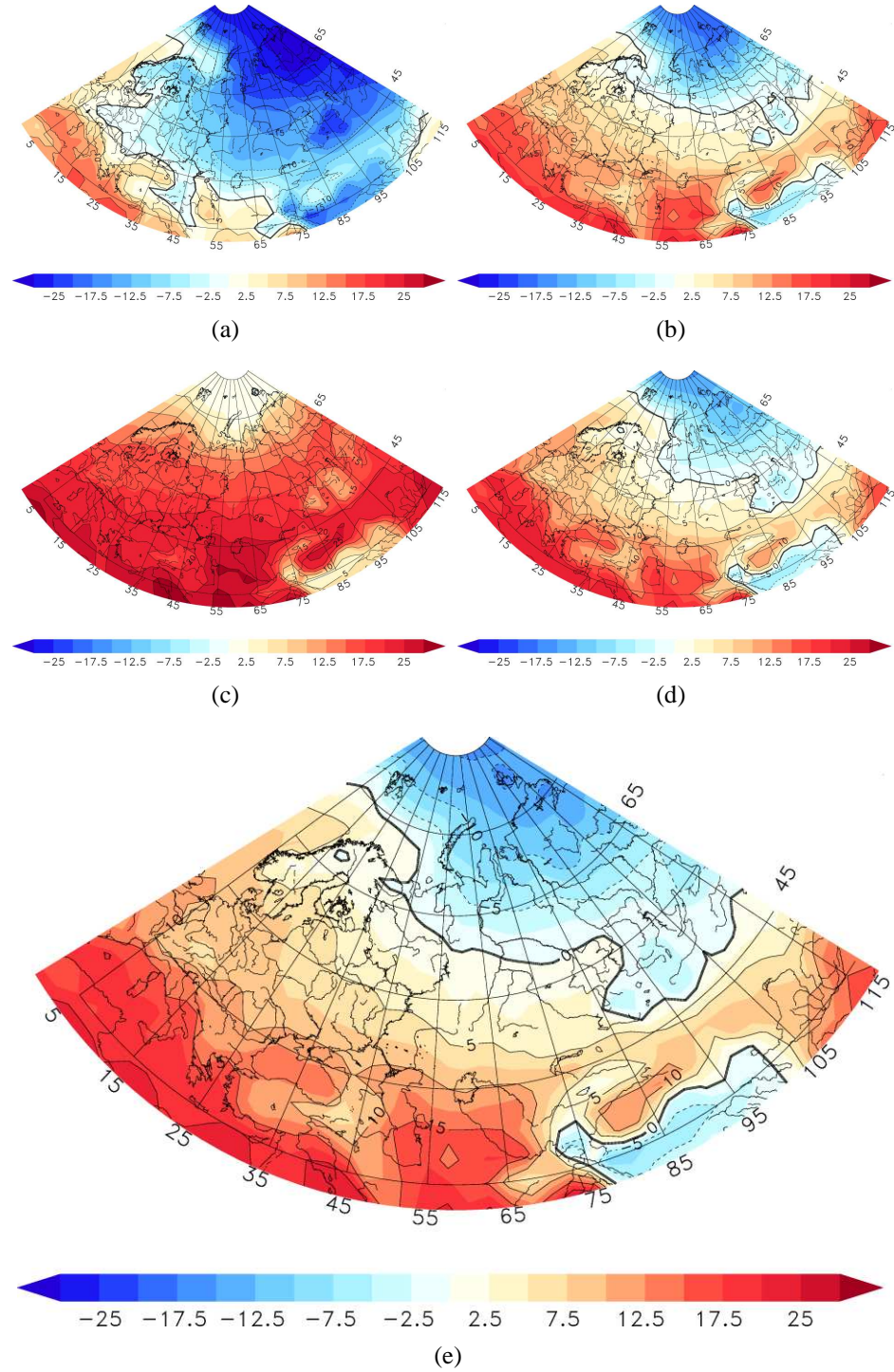


Figure 1.2: Temperature at 2 m (°C) from ERA-40 data (a) DJF, (b) MAM, (c) JJA, (d) SON, and (e) annual mean.

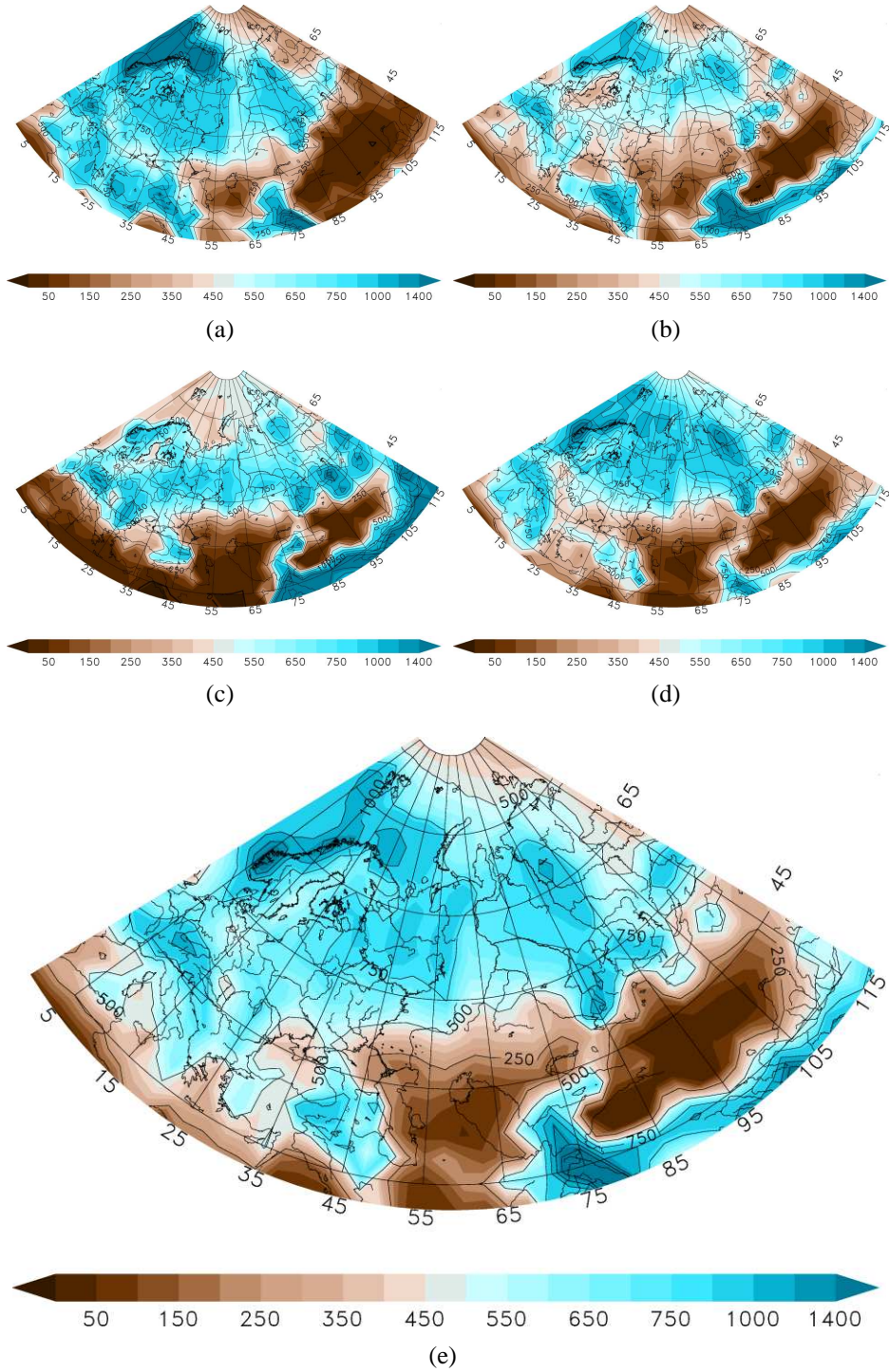


Figure 1.3: Precipitation (mm · y⁻¹) from ERA-40 data (a) DJF, (b) MAM, (c) JJA, (d) SON, and (e) annual mean.

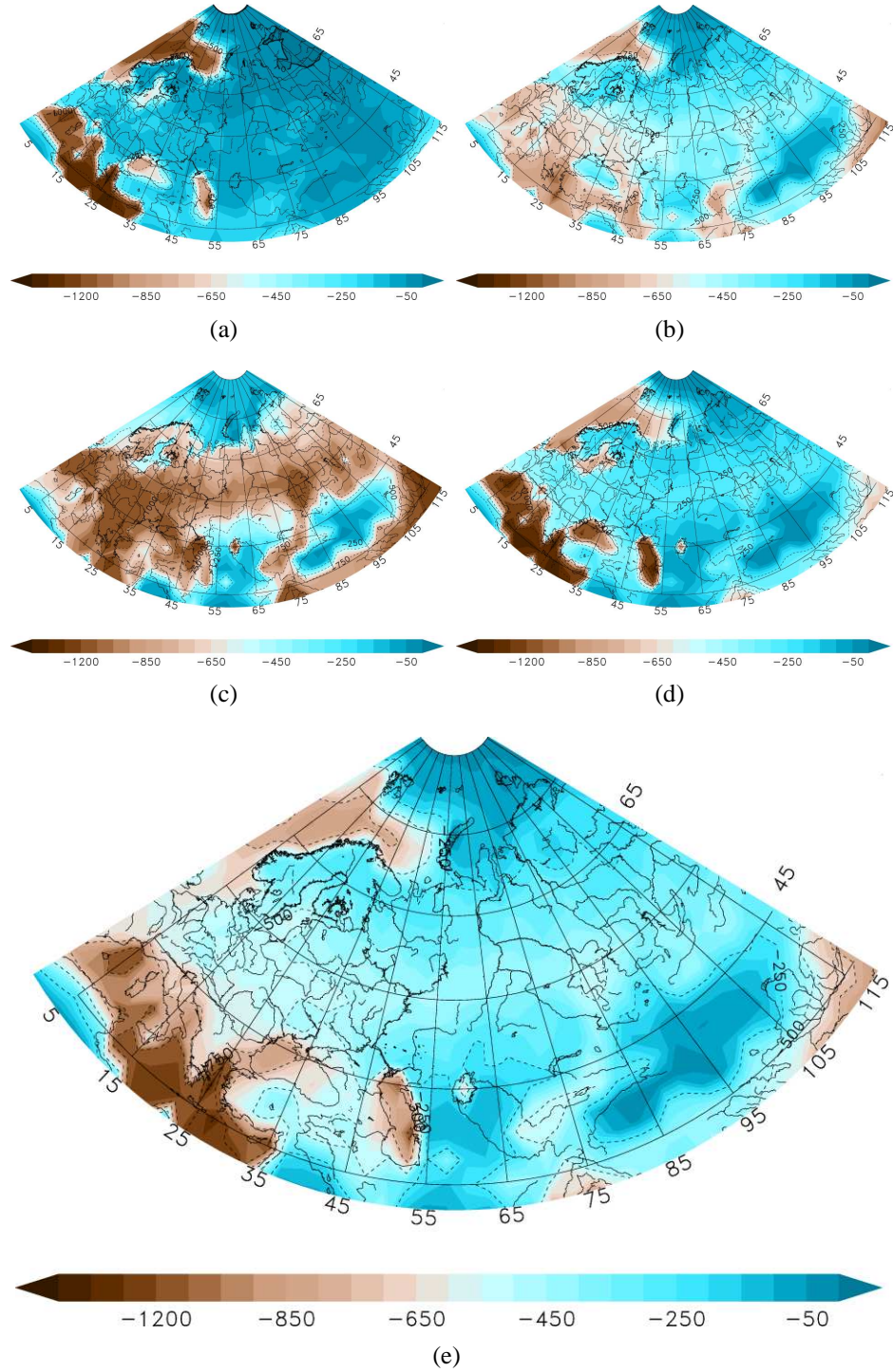


Figure 1.4: Evaporation (mm · y⁻¹) from ERA-40 data (a) DJF, (b) MAM, (c) JJA, (d) SON, and (e) annual mean.

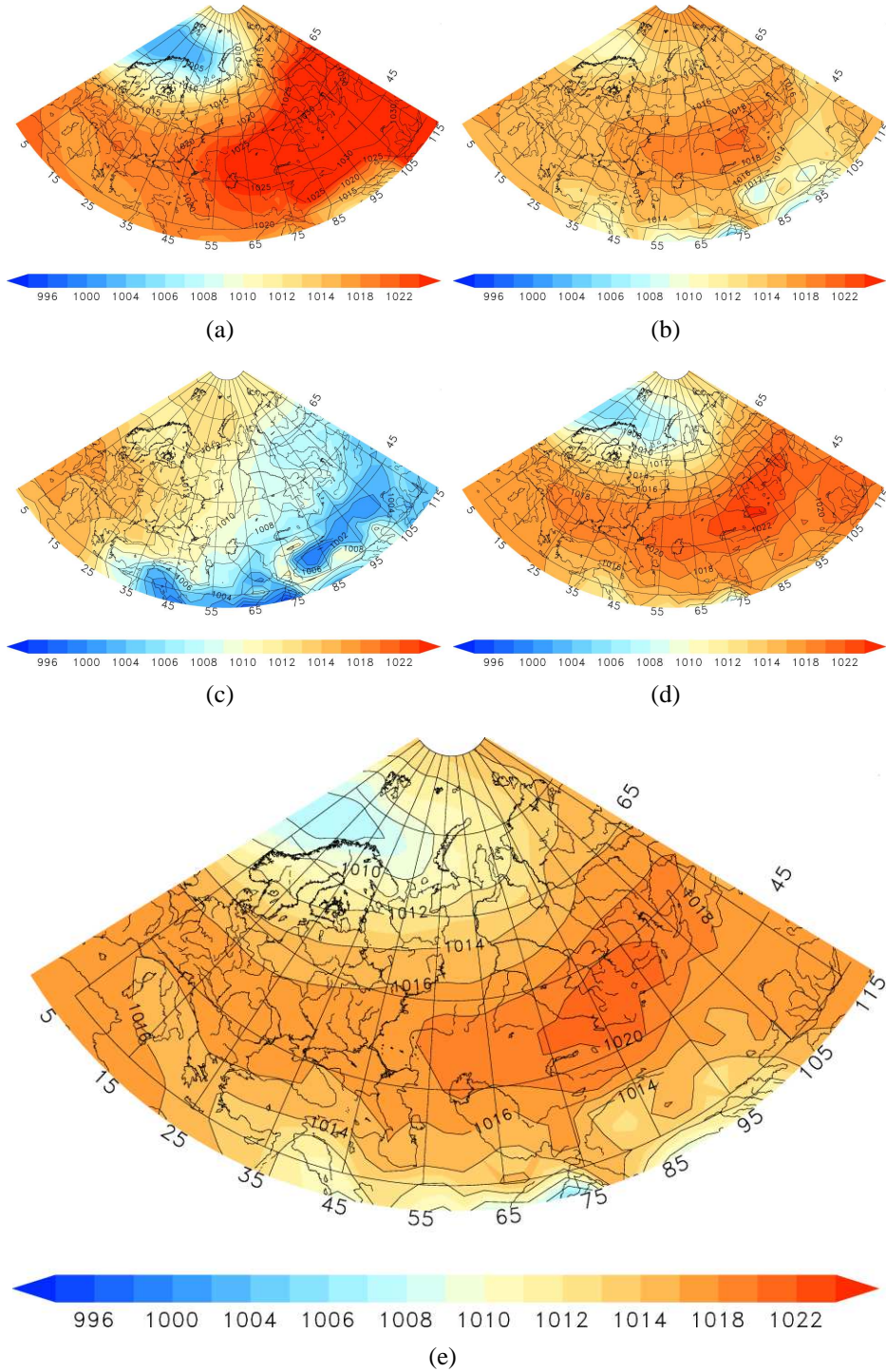


Figure 1.5: Mean sea level pressure (hPa) from ERA-40 data (a) DJF, (b) MAM, (c) JJA, (d) SON, and (e) annual mean.

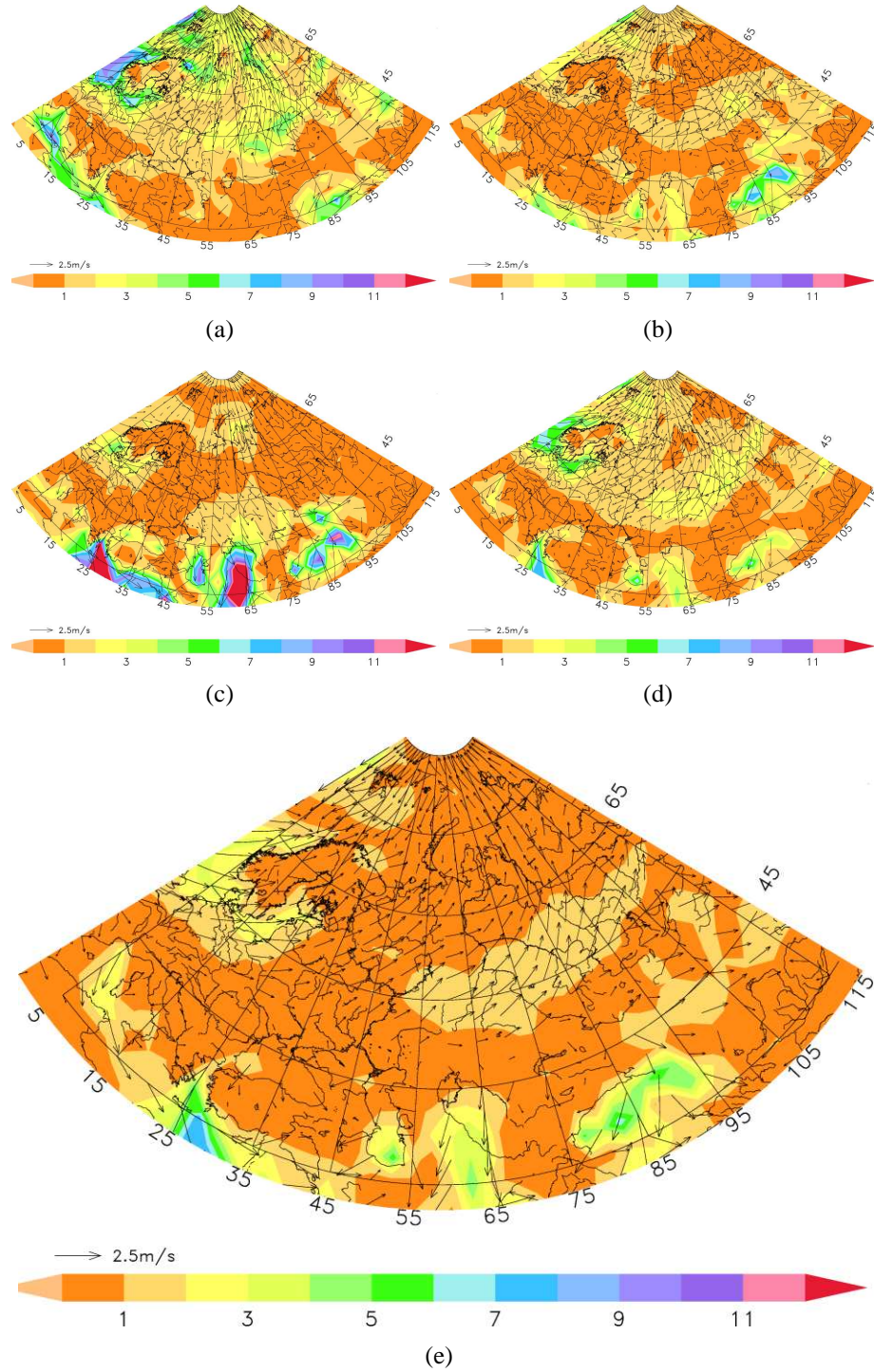


Figure 1.6: Winds at 10 m ($\text{m} \cdot \text{s}^{-1}$) from ERA-40 data (a) DJF, (b) MAM, (c) JJA, (d) SON, and (e) annual mean.

Chapter 2

Surface climate response to the glacio-eustatic sea level changes

Mechanisms governing variability of hydrological cycle on the glacial cycle time scale (125 ka) are not well understood. Here, we investigate sensitivity of the surface temperature and the hydrologic cycle onto sea level changes (125 m lower than present) and corresponding increase of land altitude (237 m). Those changes are tested by running earth system model of intermediate complexity – Planet Simulator. We demonstrate that changes of boundary conditions (sea - land distribution, orography, surface properties) have a significant impact on surface climate (2 m temperature, precipitation and evaporation). Furthermore, we have investigated the regional impact of global change in the Mediterranean catchment area. It is shown that redistribution of sea – land can have significant impact on the regional climate. In particular, cooling due to mountain uplift will cause hydrologic cycle to shift towards dryer conditions, while warming due to changed sea-land distribution will cause shift towards wet conditions.

2.1 Introduction

On the glacial-cycle time scale (~ 120 ka for the past ~ 850 ka) the huge amount of water mass changes its phase from liquid to frozen state and vice versa. Therefore, extension of the ice sheet and topography are interdependent with the global sea level rise and fall (see reviews by Clark and Mix [2002] for the past 20 ka or Lambeck and Chappell [2001] for the last glacial cycle). Going towards a stadial state climate year-round hydrological cycle (precipitation - evaporation) averaged spatially for the globe appears to have deficits in the liquid phase. Thus, it results in decreasing sea level, while melting of the ice-sheet results in relative sea level rise.

Here, we intend to investigate how changes of boundary conditions (orography, sea-land-ice distribution and surface characteristics) affect the hydrological cycle and surface temperature. We are also interested to investigate regional implications of these global processes, in particular the Mediterranean catchment area climate. In the next section, we describe methodology and experimental design, followed by the results in section 2.3, concluding the chapter with summary and outlook in section 2.4.

2.2 Method and experimental setup

Earth System Model of Intermediate Complexity (EMIC), developed at the Hamburg University [Fraedrich et al., 2005a, Lunkeit et al., 2005b,a] – Planet Simulator (PS), i.e. its atmospheric component is utilized to perform several idealized experiments. The dynamical core of the Planet Simulator is based on the Portable University Model of Atmosphere (PUMA), which was developed from the multi-layer spectral model, proposed by Hoskins and Simmons [1975]. Spectral transform method [Orszag, 1970, Eliassen et al., 1970] is used to solve a dimensionless set of primitive equations for the moist atmosphere in the horizontal direction, while finite difference method is employed to integrate equations in the vertical direction. The equations are integrated in time with a leap-frog semi-implicit time stepping scheme [Hoskins and Simmons, 1975, Simmons et al., 1978], with Robert/Asselin time filter [Robert, 1981, Asselin, 1972]. Previously, Fraedrich et al. [2005b] used the Planet Simulator to estimate the maximum effect of vegetation on the Earth’s climate and Romanova et al. [2006] have investigated the relative role of oceanic heat transport and orography on the glacial climate.

Our computations are performed on T21 ($\sim 5.6^\circ$ on Gaussian grid) resolution with 5 non equally spaced σ levels. Integration is completed for 40 model years and averaged for the last 30 years. In order to investigate response of the surface temperature and the hydrologic cycle to the changes of sea-land distribution and orography on the glacial time scale, a set of idealized experiments with prescribed sea surface temperature is designed (Table 2.1). Geological observations [Fairbanks, 1989] indicate global sea level drawdown at about 125 m below the present-day sea level during the Last Glacial Maximum (LGM). Volumetric analysis shows that if equivalent volume of the water (between 0 and -125 isobaths) would be distributed over the land as a solid phase (ice), it would increase the mountain height for additional 237 m. Therefore, mountains are 362 m higher in our idealized experiments. Not only the topography changes but also the surface properties of the new land points. We are interested to investigate trends of hydrological cycle influenced by those modifications.

In our first iteration, testing the response of the hydrologic cycle to the changes of boundary conditions in the glacial cycle, we assume that mountains are 362 m higher than nowadays.

Table 2.1: Boundary conditions in the description of the Planet Simulator runs. *SG* is surface geopotential (orography), α is back albedo, *SR* is surface roughness, *SLM* is sea – land mask and *GM* is glacial mask. *CTRL* is present day control experiment. *TOPO* experiment is characterized by increased topography (362 m). For the *MASK* experiment sea – land mask is constructed to take into account that new land grids will appear for the sea level drawdown of 125 m. *POMA* experiment is a combination of the previous two i.e. *TOPO* and *MASK*. *PELT* is constructed from topography provided by Peltier [2004].

Experiment	SG	α	SR	SLM	GM
CTRL	default	default	default	default	default
TOPO	CTRL + 362 gpm	default	default	default	default
MASK	modified	modified	modified	modified	default
POMA	CTRL + 362 gpm	modified	modified	modified	modified
PELT	modified	modified	modified	modified	modified

Additional height is uniformly distributed over the continents, i.e. it is an idealized case. This experiment is called TOPO run (see Table 2.1). Secondly, we will test the model response to the sea – land mask changes, keeping the same orography as present-day, but changing the sea – land distribution as if the sea level decreased by 125 m. This experiment is called MASK run (see Table 2.1). In the third iteration we combine both of these changes (experiment is called POMA run, see Table 2.1). In order to compare these idealized variations to more realistic ones, we also perform a simulation with LGM topography from Peltier [2004] (the experiment is called PELT run). More details are provided in Table 2.1 and in the following subsections.

Although, PS has some disadvantages [Claussen et al., 2002] in common with coarse resolution EMIC-s (see Table 2.2 to compare area of oceans and continents in various experiments), our preliminary analysis showed that the Planet Simulator can reproduce reasonably well a hydro-logic cycle compared to ERA-40 dataset (compare the PS results from simulation and ERA-40 in Table 2.3). It is noteworthy that ERA-40 dataset has also similar problems [Hagemann et al., 2005], and data quality varies during the whole period (pre-satellite, transitional and satellite era).

Table 2.2: Area ($10^6 \cdot \text{km}^2$) of oceans, continents and globe in various datasets

Experiment	sea	land	globe
ERA-40	363	147	510
CTRL	364	142	506
TOPO	364	142	506
MASK	333	173	506
POMA	333	173	506
PELT	333	173	506

Table 2.3: Global water balance comparison (in $10^3 \cdot \text{km}^3 \cdot \text{y}^{-1}$) and surface temperature ($^{\circ}\text{C}$). Comparison for ERA-40 and Planet Simulator runs.

	sea			land		
	<i>E</i>	<i>P</i>	<i>T</i>	<i>E</i>	<i>P</i>	<i>T</i>
ERA-40	456	460	16.5	74	119	9.1
CTRL	425	435	18.5	104	153	14.4
TOPO	427	433	18.6	102	156	13.3
MASK	390	395	18.6	127	182	15.3
POMA	394	396	18.7	125	183	14.1
PELT	405	402	18.8	109	174	13.5

2.2.1 Orography and sea - land - ice mask

One of the responses of the planet, due to eustatic sea-level change [Lambeck and Chappell, 2001], would be that mountains will appear higher above the new sea level. Two factors will contribute to the higher appearance of mountains in the new configuration. The former would be due to a fall of the sea level and the latter would be hypothetical, if the water mass (in the solid phase) between the lower isobath and the present day sea level is evenly redistributed over the land. Assuming that the sea level decrease for the LGM is 125 m (this estimate varies from 120 to 135 m, check the Clark and Mix [2002] for overview), and according to hypsometric calculation on 5-minute global Digital Terrain Model (DTM), mountains would appear about 237 m higher. This is the volume of the ocean between 0 and -125 m isobaths transformed into solid phase distributed uniformly above the land area. Note that the land area is considered above -125 m isobath at the present day. Therefore, if both effects are taken into account mountains would appear 362 m higher, compared to present.

Fig. 2.1 describes in detail how these changes are taken into account in the model with only positive height axis. Absolute changes of idealized topography are shown in Fig. 2.1(a), while Fig. 2.1(b) and 2.1(c) present two possible approaches how to take into account this change in the model without a negative height axis. Black line presents CTRL topography on all three figures. Green line (MASK) presents changes due to the sea level fall. Fig. 2.1(a) shows the consequences, if suddenly the volume of the water that fills the ocean between -125 and 0 isobaths was taken out of the sea. However, since the model does not have a negative topography axis, new topography will appear 125 m higher then CTRL topography (Fig. 2.1(b)). The red line (TOPO) in the Fig. 2.1(a) shows how much topography would increase, if the volume of the water mass was redistributed uniformly as ice above the land. It will be the same on the model axis (Fig. 2.1(b)). Blue line (POMA) shows the increase of topography, if both of the two effects are taken into account simultaneously in the absolute topography (Fig. 2.1(a)) and in the model topography (Fig. 2.1(b)). However, since we were interested to investigate isolated effects of

topography change and sea-land redistribution, we performed our experiments as described in the Fig. 2.1(c), i.e. in TOPO experiment we account only for 362 m topography increase, MASK accounts only for sea-land redistribution, while POMA combines both of them. Fig. 2.1(d) presents zonal changes along the 40°N latitude of topographies used in simulations.

In the CTRL experiment default orography is used. Since default Planet Simulator topography field does not contain bathymetric data, i.e. all grids representing ocean on the sea - land mask have zero value in the topography field, 5-minute global Digital Terrain Model (DTM) is used to construct the sea - land mask for the 125 m decrease of the sea level.

Modified POMA orography will have heights different than zero in the new land points calculated from 5' global DTM ($9.81 \cdot (237 + \text{present day bathymetry})$ gpm) and in old land grids increased for ($9.81 \cdot 362$) gpm. Modified MASK (125 m lower sea level) sea - land mask would contain more land grids. New land grids would be all those whose topography value is higher than -125 m on the 5' global DTM, those lower or equal -125 m remain ocean. New sea - land mask is re-gridded from fine 5' resolution to T21, using average value of 5' grids in T21 grid. If the average is bigger than 0.5, then T21 grid is assigned land (1). If it is smaller or equal to 0.5, the grid is assigned ocean (0).

Figures 2.1(e) and 2.1(f) present a sea - land mask for various experiments. Blue color presents sea grids while other colors are land or ice. Fig. 2.1(e)) presents topography and mask for the CTRL experiment. For the TOPO experiment, the same mask is used, but orography is 362 gpm higher. Fig. 2.1(f) presents topography and mask for the POMA experiment. For the MASK experiment the same mask was used as for the POMA, but mountains are as high as in the CTRL experiment. In the PELT experiment topography and sea land-mask are constructed from Peltier [2004] reconstruction based on glacial isostatic adjustment theory as suggested by Paleoclimate Modelling Intercomparison Project (PMIP) [Joussaume and Taylor, 2000]. Table 2.1 summarizes the differences in boundary conditions between various experiments.

2.2.2 Surface parameters

New land or ice grids will have a different role in the model depending on their surface characteristic. Below are the rules used to prescribe surface properties in our experiments. Since in this coarse resolution model, the area covered with ice or sea-ice appears north of 75°N and south of 69°S, new land points that appear in that area are assigned to be ice. According to new land and ice points in the sea - land (sea \rightarrow 1, land \rightarrow 0) and glacial mask (ice \rightarrow 1, sea or land \rightarrow 0), new surface properties are assigned to those points in their respective fields. For the new land points 2 m surface roughness, albedo of 0.2 and of 273.16 K soil temperature are prescribed. For the new ice points 0.001 m surface roughness and albedo of 0.8 are prescribed.

2.3 Results

We analyzed global patterns of annual mean surface temperature (T), fresh water balance ($P - E$) (see also Tables 2.2 and 2.3) and the correlation between T and ($P - E$). We were also interested to see how these global processes would impact regional climate, in particular in the Mediterranean catchment area (see Fig. 2.1 for the location and Tables 2.4 and 2.5 for the results). The Mediterranean catchment area was chosen since the border of the region is well defined, it is large enough to be adequately resolved in the coarse resolution and significant changes of the sea–land distribution happen here due to a changing sea level. Although, those changes are exaggerated in this coarse resolution model, they are relevant to some smaller regions where similar processes take place, such as the Black Sea catchment area.

Table 2.4: *Mediterranean catchment area ($10^6 \cdot \text{km}^2$)*

Experiment	sea	land	Mediterranean
CTRL	4.866	8.509	13.376
TOPO	4.866	8.509	13.376
MASK	1.808	11.568	13.376
POMA	1.808	11.568	13.376
PELT	1.499	11.877	13.376

Table 2.5: *Mediterranean water balance ($\text{km}^3 \cdot \text{y}^{-1}$) and surface temperature ($^{\circ}\text{C}$), intercomparison for various Planet Simulator experiments.*

	sea			land		
	E	P	T	E	P	T
CTRL	5883	3006	19.1	5332	6297	22.8
TOPO	6604	3000	18.6	5403	6977	21.1
MASK	1643	735	21.5	5171	6243	24.3
POMA	1998	843	20.9	4788	6073	22.5
PELT	1384	678	22.3	5023	6036	24.2

2.3.1 Temperature

Fig. 2.2 shows 2 m annual mean temperature for CTRL (Fig. 2.2(a)) run and differences TOPO – CTRL (Fig. 2.2(b)), MASK – CTRL (Fig. 2.2(c)), POMA – CTRL (Fig. 2.2(d)) and PELT – CTRL (Fig. 2.2(e)). Comparing anomalies shown on figures (2.2(b), 2.2(c) and 2.2(d)), it becomes obvious that the POMA experiment is almost a linear superposition of TOPO and MASK experiments. Another, not so expected and somehow astonishing result appears when POMA and PELT temperature anomaly patterns are compared. It turns out that they are quite similar,

although in the POMA experiment topographic uplift due to water mass distribution above the earth surface is evenly distributed, while in the PELT experiment distribution is according to Peltier [2004]. Above the land, the temperature of PELT and TOPO experiments are about $1^{\circ}K$ less than in the other experiments. For all experiments sea surface temperature is prescribed from climatological data. Therefore, more or less similar patterns of global temperatures appear in all experiments. However, PELT and TOPO experiments appear to be just a little bit colder than others, even globally. In the MASK experiment the temperature above the land appears to be warmer about $1^{\circ}K$. Since boundary conditions in the POMA experiment are linear superpositions of those from TOPO and MASK worlds, it is to be expected that results would have the same characteristics.

One can conclude from analyzing patterns and numerical values from various experiments that mountain uplift causes land to be cooler. For example, in the TOPO experiment, the temperature above the land is on average $1.2^{\circ}K$ colder. However, taking into account averaged atmospheric lapse rate (6.5 K/km, that is 2.353 K for 362 m) in the TOPO experiment it would be warmer at the same height than in the CTRL experiment, but high northern latitudes show some significant cooling and they will be cooler even on the same height as in the CTRL experiment.

Although coarse resolution models are not primarily designed to study regional climate, some local features in our analysis could not be overseen. Our experiments are designed in that manner that most of the changes of boundary conditions take place in the certain regions of the world. These are also the regions where the dramatic changes took place during the glacial-interglacial changes. One of those regions is the Mediterranean catchment area. TOPO and POMA worlds appears to be colder above the land points, while MASK and PELT warmer than in the CTRL experiment. The biggest cooling is for the TOPO case about $1.7^{\circ}K$, while the highest warming is $1.4^{\circ}K$ in the MASK case.

Comparing results for the globe (Table 2.3) and the Mediterranean region (Table 2.5) one can see that MASK shows warming in both cases (above the sea and above the land for the globe and for the Mediterranean) and TOPO shows cooling in both cases above the land. These two idealized cases (MASK and TOPO) lead us to the conclusion that warming is caused by sea-land redistribution, while cooling is due to topographic uplift. Different temperature distribution between POMA and PELT experiments is not so easy to interpret. These differences indicate non-linear response of temperature change.

One interesting feature that appears in all experiments is the warming above the land along the $40^{\circ}S$ (Australia and South America, it is similar for the northern latitude $40^{\circ}N$). We assume that this happens because significant changes of the surface properties take place in this area, but it would certainly be interesting to perform further investigation with fine resolution model coupled with ocean dynamics.

2.3.2 Hydrologic cycle

When analyzing the hydrologic cycle, we concentrate on the annual mean $P - E$ (precipitation minus evaporation, or net precipitation) anomaly from CTRL run. This value indicates how much arid or humid climate appears in various experiments. Fig. 2.3 shows $P - E$ for CTRL (Fig. 2.3(a)) run and differences TOPO – CTRL (Fig. 2.3(b)), MASK – CTRL (Fig. 2.3(c)), POMA – CTRL (Fig. 2.3(d)) and PELT – CTRL (Fig. 2.3(e)). Similar to 2 m temperature, $P - E$ pattern in POMA run appears to be a linear superposition of the other two experiments. While the PELT experiment shows some similarities in pattern with others it has also some specific features depending on ice sheet extension. Perhaps the most prominent signal in the TOPO run is the drying of high northern latitudes and the Mediterranean region. The drying of northern latitudes is slightly amplified in the MASK experiment and most pronounced in the POMA experiment. From analysis of total water balance fluxes for the globe, it turns out that their values do not change significantly, but rather their distribution pattern (Tab. 2.3). Therefore, regional changes become important.

Analysis of total water balance fluxes for the Mediterranean catchment area provides more insight into processes controlling the region of our major interest (Tables 2.5). The Mediterranean appears slightly wetter in the MASK, POMA, and PELT experiments. Since PELT and MASK appears also warmer in that region (POMA is also warmer above the sea, but slightly cooler above the land), this provides some support to the hypothesis that warming would cause a shift towards a wet hydrologic condition in the Mediterranean area. The TOPO experiment appears colder and dryer. Therefore, cooling in the Mediterranean would cause a shift towards a dry hydrologic condition. An explanation is that sea-land redistribution changes temperature, which further influences the hydrological cycle. There are much more land grids in MASK, POMA, and PELT experiments than CTRL and TOPO. Characteristic of the continent is $P - E > 0$ and for the sea $P - E < 0$, therefore catchment with more land surface grids becomes wetter.

One can argue that results of these idealized experiments are somehow in contrast with reality since low sea level appears during the cold and dry periods such as LGM, while here, for example, MASK experiments with sea level low-stand actually indicate warmer and wetter conditions. In order to understand this, one has to bear in mind that climate change is a non-linear dynamic system meaning that one process could lag behind some condition while under different circumstances the same process could lead to that same condition. Here, we have tried to isolate internal feedback of surface climate (T and $P - E$) to the changes of boundary conditions. Which processes will predominate depends also on external (orbital, solar) forcing and other internal feedback not included in the above consideration.

2.3.3 Correlation between T and $P - E$

Fig. 2.4 presents correlation patterns for the annual mean temperature, precipitation, and evaporation calculated from ERA-40 data. In the tropical latitude, temperature is positively correlated to the precipitation (Fig. 2.4(a)) above the ocean, while the relation is negative above the land. In the sub-polar, region especially in the southern hemisphere, relation is negative, and in the polar region, mostly positive. In the Mediterranean, correlation pattern changes sign. It is negative in the Eastern Mediterranean and positive in the western part of the basin. In the Black Sea catchment area negative correlation is predominant. In the Northern hemisphere, north of 45°N latitude the temperature (Fig. 2.4(b)) is predominately positively correlated with evaporation, especially above the land and in particular above Eastern Siberia and Mongolia. In the southern hemisphere, negative correlation predominates especially above the land, while above the Antarctica, the correlation pattern is positive. In Fig. 2.4(c) the correlation pattern is shown between the annual mean T and $P - E$. Above the land in the Northern Hemisphere, negative correlation is predominant. In particular, in the continental part of the Black Sea catchment area negative correlation is significant at the 5% level and it changes sign above the Black Sea. In tropical latitudes, correlation is positive above the ocean, and negative above the land. Mid-latitude shows predominantly negative correlation, while in the sub-Antarctic region and Eastern Antarctic positive correlation appears.

Fig. 2.5 presents correlation pattern between annual mean T and $P - E$ calculated from various experiments performed with the Planet Simulator. The correlation pattern for CTRL experiment is shown in Fig. 2.5(a) and it is in general agreement with the pattern calculated from ERA-40 data (Fig. 2.4(c)), that there is negative correlation above the land, and positive above the ocean. All the other experiments show similar correlation patterns indicating the robustness of this feature. Furthermore, the TOPO experiment (Fig. 2.5(b)) compared to CTRL shows a significant change of pattern in the Mediterranean region, in particular towards positive correlation above the sea. All the other experiments (MASK, POMA, PELT, Fig. 2.5(c), 2.5(d), 2.5(e)) in that particular region show a weak shift towards positive correlation above the sea and negative correlation above the land. This is in accord with the global pattern. Another important result is that a significant shift toward negative correlation in the new land points appears. This result is in accordance with our previous conclusion. However, one needs to be careful with the interpretation and to keep in mind absolute fluxes and temperature from Tables 2.4 and 2.5. They all show positive correlation in the Mediterranean. Positive correlation means changes of T and $P - E$ in the same direction. For the TOPO experiment that means colder and drier conditions, but warmer and wetter ones for all the other experiments (MASK, POMA, PELT).

2.4 Summary and outlook

We were investigating the sensitivity of the surface climate with the Earth System Model of Intermediate Complexity (EMIC): Planet Simulator to changes of boundary (topography and sea land distribution) condition. We have demonstrated that changes induced only by slightly changing boundary conditions could have significant signals in the net precipitation and 2 m temperature fields. Spatial pattern of $P - E$ changes certainly need deeper consideration and analysis, but this is out of scope in this work. However, important conclusions can be drawn from the analysis presented above. That is that cooling due to an idealized mountain uplift in the Mediterranean catchment area would cause shift towards dry hydrologic regimes,, while warming causes shift towards wet conditions. These changes are connected with global climate change, such as shift in the global hydrological cycle, and they are due to land and sea redistribution on the glacial time scale. Although the correlation pattern between T and $P - E$ may vary above the globe depending on the sea-land distribution, analysis of absolute fluxes and temperature (Tables 2.4 and 2.5) indicates that T and $P - E$ are positively correlated in the Mediterranean catchment area. This result together with the available geological observation provides an useful consideration when developing reconstruction of hydrological conditions in the Black Sea catchment area during the glacial cycle. In chapter 4 we will analyze available hydrological data for the past 20 ka. Experiments resembling glacial conditions (MASK, POMA, PELT) also imply less precipitation and evaporation, therefore, an additional sensitivity study is performed in order to investigate how big changes of P and E in the Black Sea catchment area would be needed in order to cause model changes as big as observed sea level minimum during the past glacial cycle. This analysis is described in chapter 5. In chapter 6, we will synthesize results from chapters 2 and 4 together with available proxies to reconstruct hydrological conditions in the Black Sea catchment area during the past 120 ka. Changes of circulation patterns could also influence T and $P - E$ patterns, therefore, we are also motivated to investigate changes of teleconnection patterns due to changes of orography (chapter 3).

One more puzzle illustrating complexity of the internal dynamics of the climate system could be of interest for the development of ice-age theory. $P - E$ anomaly becomes reduced above the northern high latitudes for each experiment. This univocal result implies that changes in sea - land distribution due to the eustatic sea level drop down could be one of the mechanisms causing the ice-sheet in the high latitudes to stop waxing. Therefore, it could trigger (or at least) amplify termination of the northern hemisphere glaciation.

2.5 Figures

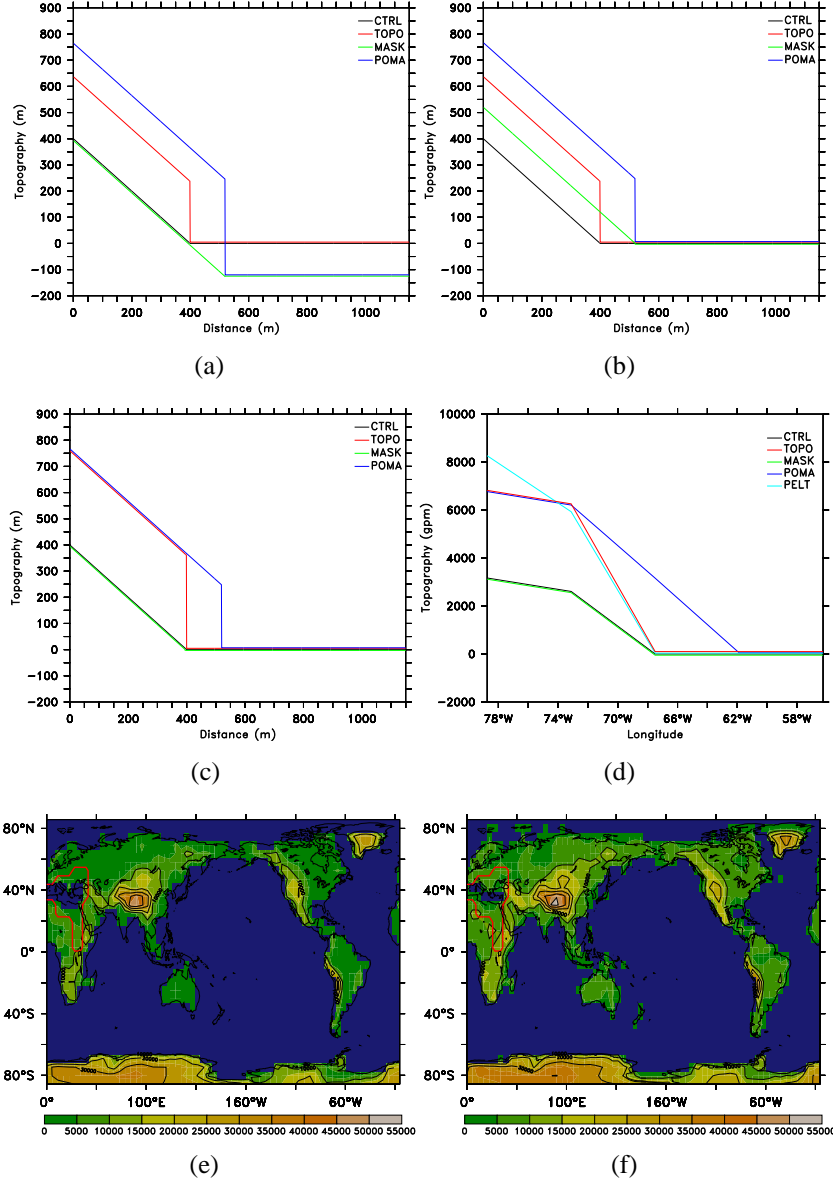


Figure 2.1: Topography and sea land mask: (a) idealized changes of height in an absolute coordinate system, (b) idealized changes of height in model's coordinate system (heights ≥ 0), (c) isolated contributions of idealized changes of height in model, (d) detail of topography changes along the 40N latitude, (e) topography for CTRL run (red is the border of Mediterranean catchment area), (f) topography for POMA run. For TOPO run the same sea-land mask as for the CTRL is used and orography in the land points is the same as for POMA experiment. MASK run uses the same orography as CTRL while the new land points are assigned value of zero orography, sea-land mask is the same as for POMA run. For the PELT run topography is constructed as suggested in the frame of PMIP project.

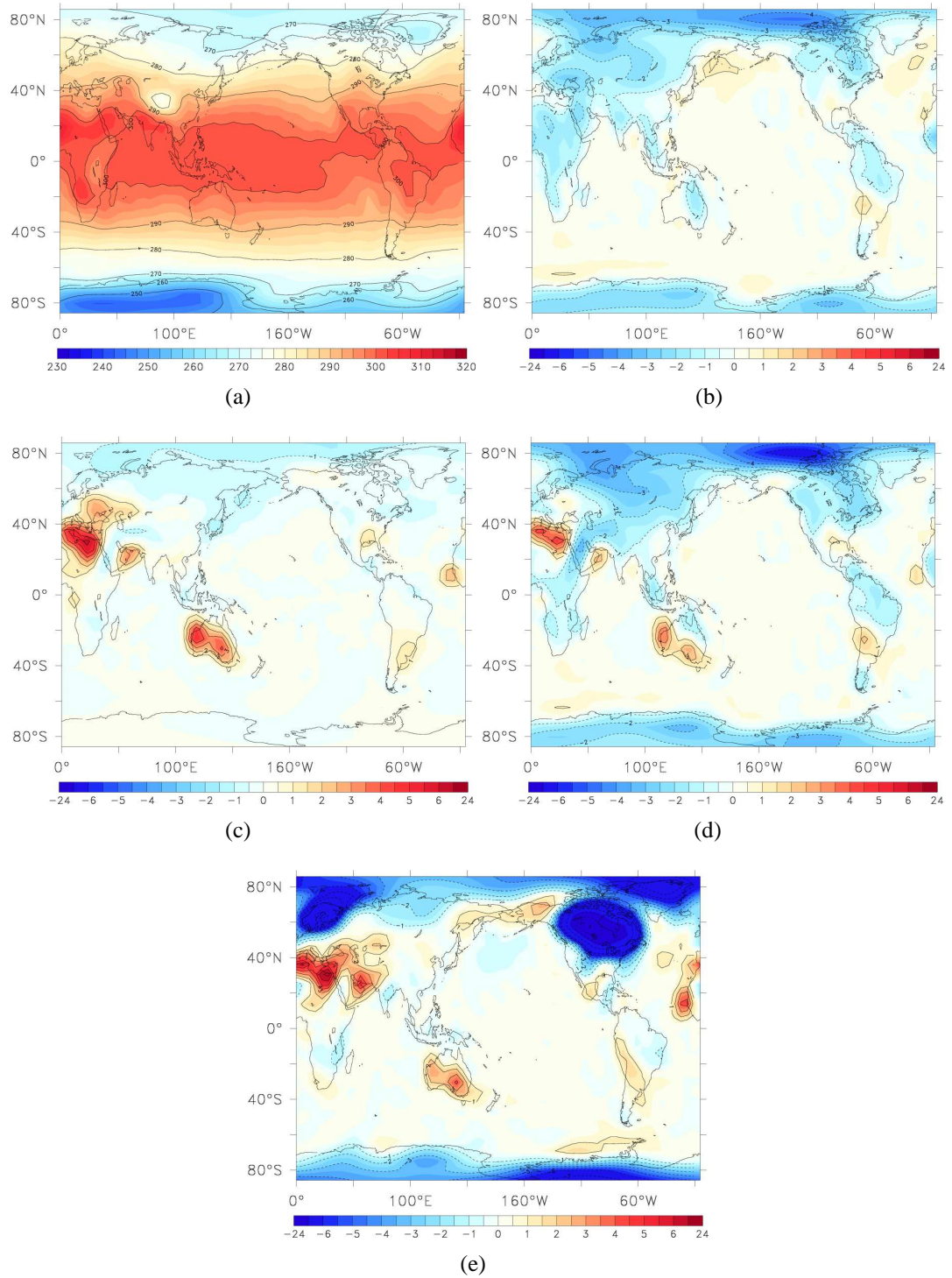


Figure 2.2: Annual mean temperature at 2 m in K for (a) CTRL, and anomalies (b) TOPO – CTRL, (c) MASK – CTRL, (d) POMA – CTRL, (e) PELT – CTRL.

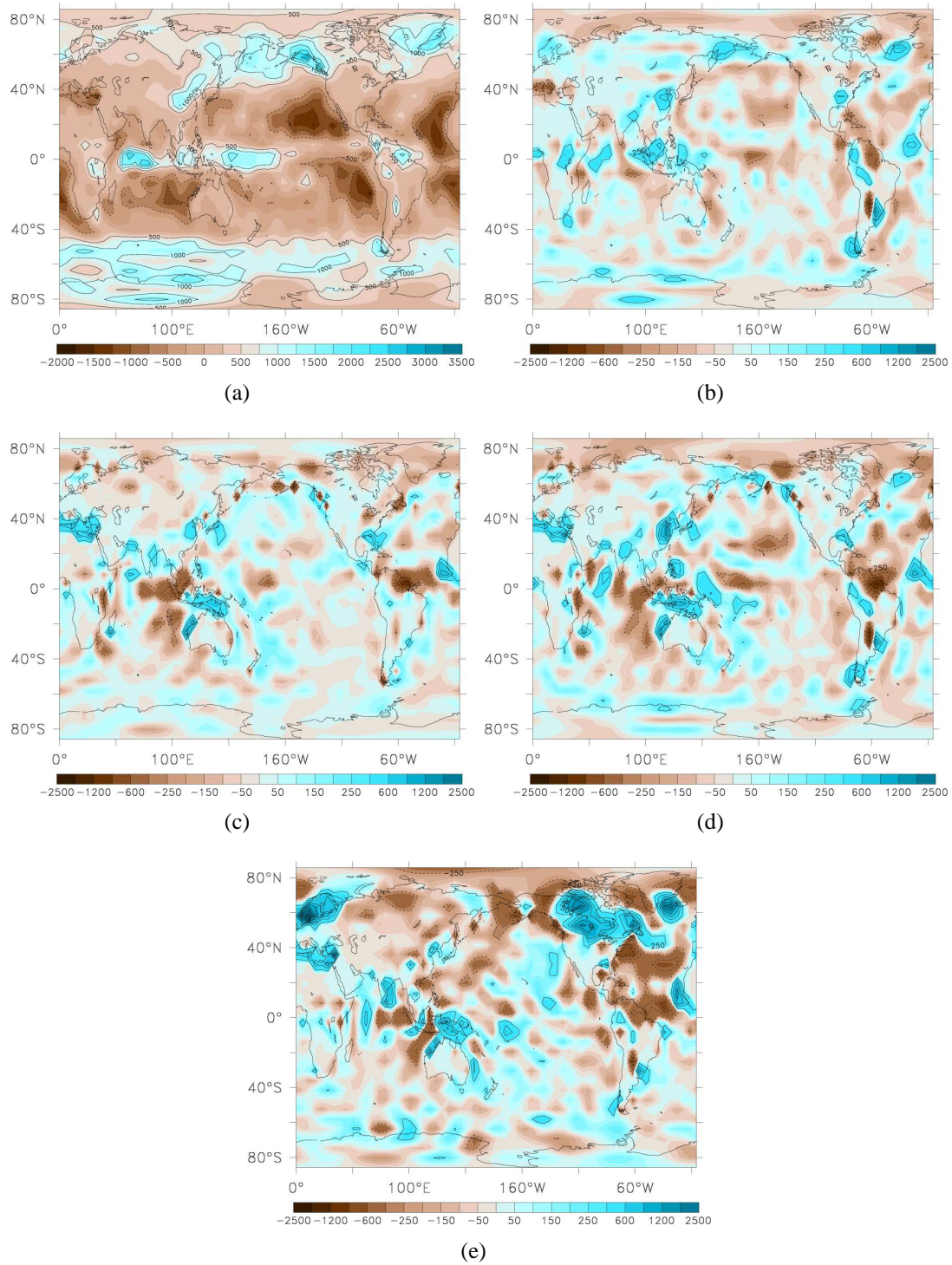


Figure 2.3: Annual mean $P - E$ in $\text{mm} \cdot \text{y}^{-1}$ for (a) CTRL, and difference for (b) TOPO - CTRL, (c) MASK - CTRL, (d) POMA - CTRL, (e) PELT - CTRL

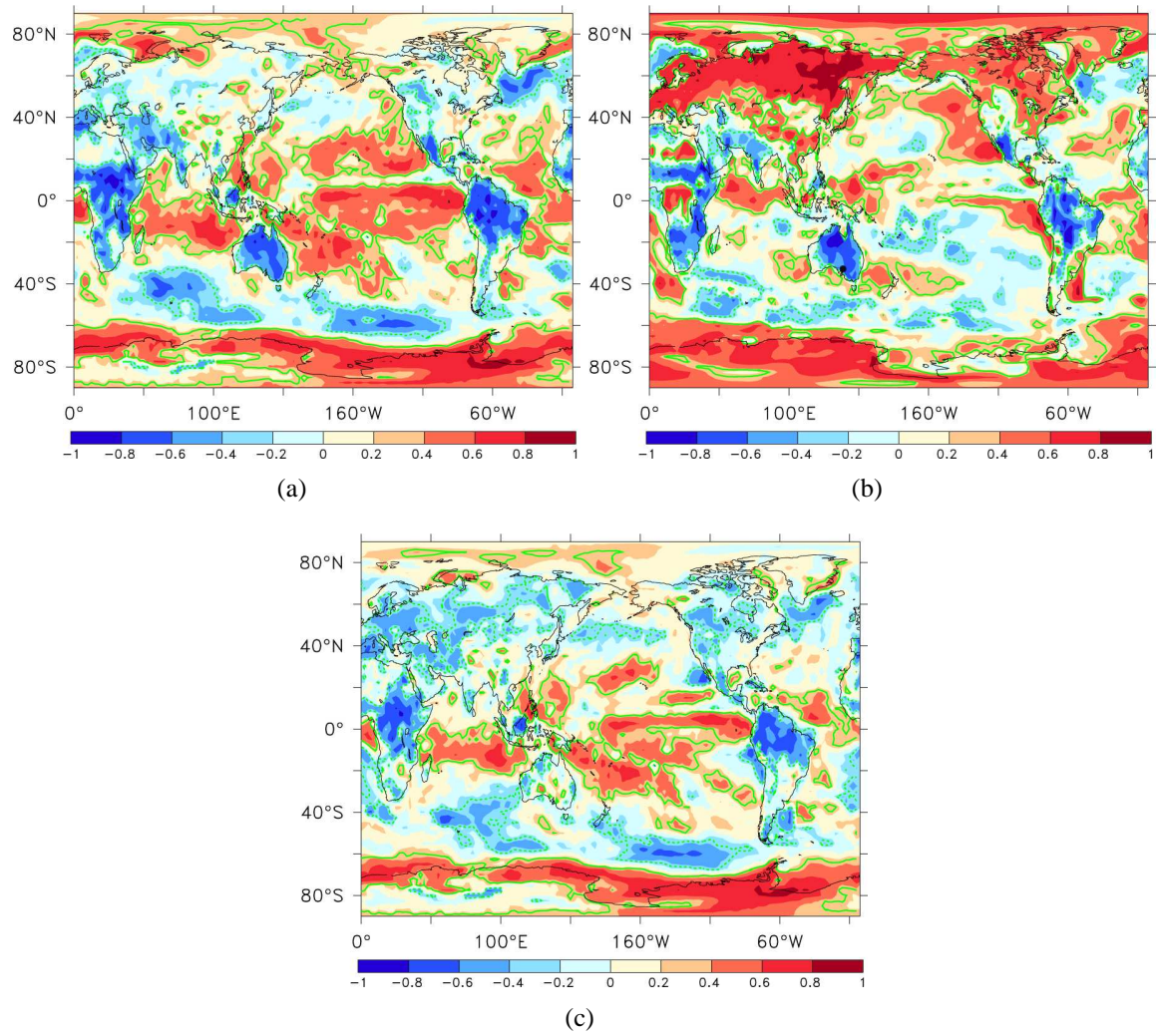


Figure 2.4: ERA40 data, correlation between 2m temperature and (a) P (b) E (c) $P - E$. Green lines indicates correlation coefficient at the 5% level of significance.

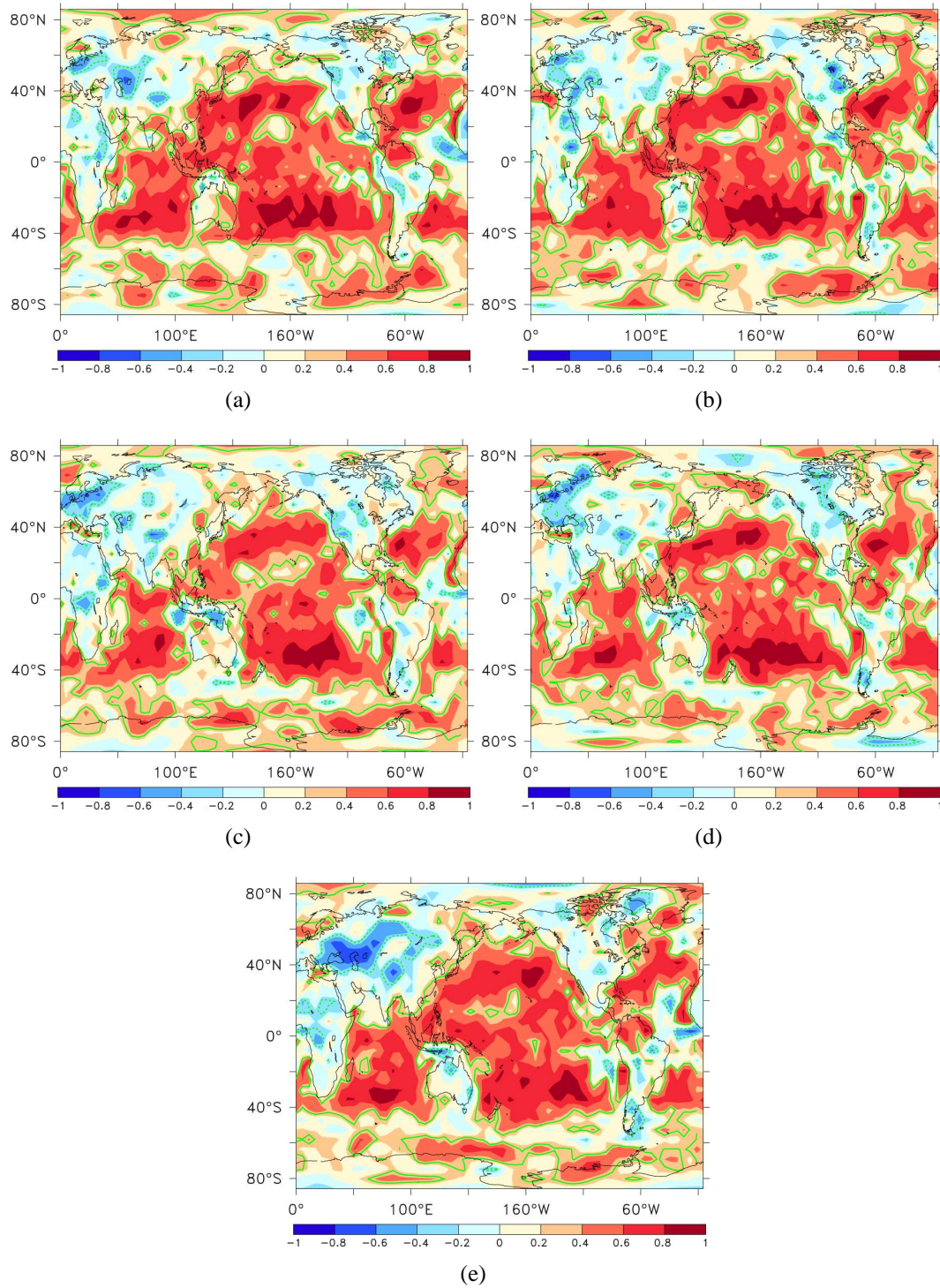


Figure 2.5: Correlation between 2m temperature and P-E (a) CTRL (b) TOPO, (c) MASK, (d) POMA, (e) PELT. Green line indicates correlation coefficient at the 5% level of significance.

Chapter 3

Sensitivity of climatic patterns in Europe to changes in coastal line and orography

The role of the regional orography in the formation of teleconnection patterns dominating the climate of Europe is examined through a series of numerical experiments. The focus is put on the North Atlantic Oscillation (NAO) and East Atlantic/West Russia (EAWR) pattern. These patterns are first identified on the basis of ERA-40 data analysis. An atmospheric component of an earth-system model of intermediate complexity – Planet Simulator, is used to simulate several 40-years long situations with different orography. Changes in the orography in the individual sensitivity experiments have been specified in the region between the Minor Asia and Alps. These changes modify climatic patterns not only locally, but also over areas far from the artificial land (mountain) obstacle. The results presented reveal that the orography in the studied region has a crucial role in the control of regional climatic patterns, in particular that of the EAWR.

3.1 Introduction

Europe is characterised by contrasting marine and continental climates extending between sub-tropical and polar climatic areas. These climates depend largely on the conditions in the North Atlantic, however, inland seas (Baltic, Mediterranean and Black Sea) can not be ignored as an important climatic factor, as they provide sources of air masses. Over large areas, these basins are surrounded by high mountain chains, shaping air masses propagation (Fig. 3.1). Existing observations suggest a complex climatic system, however, its regional functioning is not well known, in particular the feedback to the global climatic system.

ENSO gives the best example of a coupled ocean-atmosphere interaction [Philander, 1983, 1985, Cane and Zebiak, 1985]. The relatively clear signals associated with this teleconnection pattern are due to the large heat capacity of mixed layer, strong atmospheric and ocean transports. Unlike the ENSO-case, it is quantitatively not quite clear how the coupling between ocean and atmosphere over the Atlantic controls the NAO. The signals associated with the NAO shape the European climate, however these signals are less pronounced than the ones associated with the ENSO. Even less clear are the processes controlling some local oscillation patterns as, for instance the Mediterranean Oscillation [Conte et al., 1989, Palutikof et al., 1996] and East Atlantic/West Russia (EAWR) pattern Krichak et al. [2002].

So far, observations and atmospheric modelling have not provided clear evidence of interplay between NAO and EAWR patterns and their physical behaviour is still unclear. The major hypothesis in this chapter is that the European teleconnection patterns are shaped by the local orographies, therefore by using results from numerical modelling with different coastlines and orography, we will try to reveal their sensitivity to these characteristics. A similar issue has been previously addressed by Kitoh (1997, 2002) where it was demonstrated convincingly that changes in orography (e. g. mountain uplift) can substantially change SST and affect the ENSO pattern. Recently, Liang et al. [2005] analysed the role of land-sea distribution in the formation of the Asian monsoon through a series of idealised numerical experiments. Our study is similar to that of Liang et al. [2005], but addresses a different geographical area with different climatic patterns.

The focus in this chapter is on the EAWR pattern, which is associated with the meridional transport over Europe. The dominating concept here is based on the understanding that the NAO, which measures pressure difference between Azores and Island controls the strength of the zonal transport and the position of its axis. The EAWR measures the difference between pressure over the north-western Europe (North Sea) and the Caspian region (Fig. 3.2). Because the line connecting the focal points of the EAWR pattern is almost zonal, it is expected that this pattern reveals the climatic evolution of the meridional transport (almost normal to this connecting line). This transport is expected to be shaped by orography, which acts as an obstacle for the air transport between the northern and southern Europe. There are only several gaps "corridors", which could act as pathways for propagation of air masses in the meridional direction. One of them extends from Ukraine over the Black and Marmara Sea reaching the Aegean Sea to the south (Fig. 3.1). However these "channels" are not well resolved in the numerical models because of insufficient horizontal resolution. Furthermore, in the coarse resolution models orographies are much lower than the real orographies, affecting substantially the meridional transport, and therefore its variability could be underrepresented.

The above idea becomes clear from the following analysis of ERA-40 data [Simmons and Gibson, 2000]. We define the EAWR index as the normalised pressure difference between the North Sea

and Caspian. Then we take the difference between the EAWR positive and negative situation. The corresponding horizontal pattern of wind stress curl (Fig. 3.2) demonstrates clearly that the major changes in the meridional transport are observed around the Black Sea and Balkans, which is associated with the transition of the curl between the two contrasting regions, the one around the British Isles, and the one north of the Caspian (Fig. 3.2). Because the area between the Balkans and Minor Asia is one of the possible corridors enabling the north-south transport (Fig. 3.1), the question which we address here is how sensitive the results from numerical models are to changes in orography, which separates northern from southern Europe.

The chapter is structured as follows: we first discuss in Section 3.2 the teleconnection patterns over Europe derived from ERA data, then briefly present the model used, followed in Section 3.3 and Section 3.4 by analysis of the results from simulations and conclusions at the end.

3.2 Teleconnection patterns dominating European climate

This part aims at introducing the major teleconnection patterns characterising European climate. The analysis will be based on the ERA-40 data [Simmons and Gibson, 2000], which has a horizontal resolution of 2.5° . Earlier, similar analysis based on NCEP/NCAR reanalysis data has been done by [Krichak et al., 2002]. The North Atlantic oscillation (NAO), which refers to a shift in the atmospheric mass between the Iceland low and Azores high pressure systems, is known to be the dominant mode of variability of the northern hemisphere, in particular the Atlantic sector [Hurrell, 1995]. The NAO index quantifies the difference between sea level pressure between two major pressure centres: the Azores and Icelandic ones and represents the phase of the NAO (Fig. 3.3(a)). The North Sea, Labrador Sea, and Sargasso Sea regions were identified by Kushnir [1994] as other dominant centres of action.

In the following, the presentation of the teleconnection patterns will be illustrated using differences between situations having extreme positive (+) or negative (-) indices. We first compute the mean winter (December, January and February) surface pressure for NAO+ and NAO- and then take the difference between them (Fig. 3.4(a)). This difference-pattern reveals positive anomalies over Azores and negative over Island, that gives evidence for Azores high and Icelandic low to be negatively correlated. Thus changes in the mass and pressure fields lead to variability in the strength and pathway of storm systems crossing the Atlantic and Europe. During the negative phase, the Azores high weakens, the Icelandic low shallows, and westerlies also weaken taking a southern pathway (over the Mediterranean). North-western Europe is cold and dry during this period while the Mediterranean area is dominated by mild and wet conditions. During the NAO+ phase the situation is the opposite: westerlies intensify and take a northern path, North-western Europe is warmer and wetter, while the Mediterranean and north-African

region is dry and cold. These patterns (east of the Atlantic) have their counterparts over North America (Fig. 3.4(d)) thus building a quadruple system.

The NAO system alone can not adequately describe all details of climate variability over Europe, in particular Central and Eastern Europe. At least two other atmospheric oscillation patterns are well known for the European region: the East Atlantic/West Russia (EAWR) pattern [Krichak et al., 2002], which is sometimes called North Sea Caspian Sea Pattern (NCP, Kutiel and Benaroch [2002]) and the Mediterranean Oscillation (MO, Conte et al. [1989], Palutikof et al. [1996]).

The EAWR pattern has been referred to as the Eurasia-2 pattern by Barnston and Livezey [1987]. The positive winter EAWR pattern involves a high pressure anomaly centre over the North Sea and a low pressure anomaly over north of the Caspian Sea. Under such conditions the penetration of Arctic air masses over the Black Sea is enhanced, providing colder and drier than normal conditions. The negative NCP is characterised by a positive pressure anomaly north of the Caspian Sea and central North Atlantic and a negative anomaly over the North Sea. Under such conditions warmer and wetter than normal air masses propagate to the north (mainly over the Black Sea-corridor). What has not been addressed in previous studies is the fact that this teleconnection pattern reaches the polar areas. Thus, the anomaly over Asia extending to the Scandinavian separates the two negative temperature anomaly zones over Southern Europe and Mediterranean from one side and Arctic, from another (Fig. 3.4(d)).

Kutiel and Benaroch [2002], who studied the 500 hPa geopotential height level at a monthly timescale, defined the coordinates of pressure centres as: (0°E, 55°N) - (10°E, 55°N), North Sea and (50°E, 45°N) - (60°E, 45°N), northern Caspian. Because the coordinates of these centres correspond better to the proposed by these authors name (NCP), we will use both abbreviations in this chapter for the same atmospheric pattern. According to the scheme of [Kutiel and Benaroch, 2002], the minimum difference between NCP(-) and NCP(+) is expected over Balkans and the Middle East, which is supported by the analysis of surface pressure from the ERA data (Fig. 3.4(a)). This teleconnection, which is active mainly from October to April [Kutiel and Benaroch, 2002], has a major influence on the temperature regime in the Balkans, Anatolian Peninsula and the Middle East (Fig. 3.4(d)). NCP and NAO teleconnections behave almost independently (compare Fig. 3.3(a) and Fig. 3.3(b) and we can not predict one index based on the behaviour of the other.

Although the Mediterranean oscillation (MO) is not the subject of this study it should be noted that the MO index is defined by Palutikof et al. [1996] and Conte et al. [1989] as the normalised pressure difference between Algiers (3.1°E, 36.4°N) and Cairo (31.4°E, 30.1°N). In a similar way to the NAO, changes in this pressure difference may affect wind and rainfall patterns in the region.

3.3 Numerical simulations

The model used to run climate simulations is the Planet Simulator (PS), described into details in previous chapter. For the purposes of the present study a large number of sensitivity experiments were carried out (not all of them are discussed in this chapter), therefore PS is an appropriate model, ensuring relatively low computational requirements, but at the same time helping us to understand climate phenomena and identify key response mechanisms. In the present chapter the emphasis is placed on the interaction of the dominant patterns of atmospheric variability with the land surface.

Three scenarios with different land-mask/orography are formulated aimed at revealing the sensitivity of climatic patterns to local changes of orography in the area between the Alps and Minor Asia (this area connects/separates) the Black Sea and Mediterranean. Our initial idea was based on the consideration that this marine and low-land area provides an important corridor for meridional transport. It was expected that creating a mountain ridge in the model connecting the high mountains in Minor Asia with the Alps would affect the characteristics of climate variability in the Northern and Southern Europe. After carrying out a number of sensitivity experiments, it appeared that another hypothesis is also possible. Mountains in the low-resolution PS are not sufficiently resolved. For these reasons they are much lower in the model than in the real world (the Alps are only about 700 m high in the model and the Balkan mountains and Carpathians are barely resolved (Fig. 3.5(a)). This could largely facilitate the north-south transport thus affecting the dominating teleconnections in this region.

In the Control Run (CR) land sea mask and orography are taken as in the default PS (Fig. 3.5(a)). It is noteworthy that this orography does not correspond well to the real land-sea mask in the region of Mediterranean (too large a sea), which is mostly due to insufficient resolution. In order to keep the present study consistent with the previous approaches using the PS, this default orography was not changed. In the first sensitivity experiment discussed here, which we call Mask Experiment (ME) we change locally only the land sea mask by substituting part of the ocean area with land (Fig. 3.5(b)). In the second experiment, which we call Topography Experiment (TE) we build a mountain ridge of 750 m high connecting mountains in the Minor Asia with the Alps (Fig. 3.5(c)). The individual scenarios differ also through the following parameters in the land surface scheme: (i) the surface background albedo, and (ii) the surface roughness (given by the roughness length). Thus the land cover can be water or land with different albedo, roughness and height. The values prescribed are as close as possible to the ECHAM specifications [Fraedrich et al., 2005c]. The three scenarios are simulated for 40 years overlapping with the ERA-40 period.

In the following we analyse the simulations in CR over Eurasian region and their consistency

with the ERA data (Fig. 3.6 and 3.7). Annual mean surface pressure in ERA-40 data (Fig. 3.6(a)) and in CR (Fig. 3.6(b)) reveal qualitatively similar horizontal patterns in the European region. The two data sources replicate well the major centres of action (Icelandic low and Azores high). It is noteworthy that in the CR the Icelandic low and its extension to the East is over-estimated. The wind field in the two data sets is also qualitatively similar, which is quite satisfactory bearing in mind the low resolution of CR data. The overestimation of the Icelandic low in the CR dominates both the winter and summer patterns (Fig. 3.6(c)- Fig. 3.6(f)). In the CR, winter field is more zonal, while the summer pattern is more elongated toward the Scandinavian Peninsula.

The surface temperature is also similar in the two data sets (Fig.3.7). CR fields are smoother than these in the ERA-40 data set, as well as slightly warmer in the polar regions, particularly over the Greenland. The agreement between ERA-40 data and the ones simulated in the CR (note that the left and right panels in Fig. 3.6 and 3.7 use the same contour levels) allows us to conclude that the PS adequately simulates the major climatic features, which justifies the comparison of the results of sensitivity runs with the ones of CR, which are presented in the following section.

3.4 Orographic control on the NCP

The temporal variability of the simulated atmospheric oscillations in CR (Fig. 3.8) resembles similar variability behaviour as in ERA data. However, the corresponding curves in Fig. 3.8 and Fig. 3.3 are far from identical. This can be expected bearing in mind that the PS-runs barely replicate the weak climatic signals in the real case, which we hope are well represented in the ERA data. While this could be expected in advance, the fact that the variability patterns (both for NAO and NCP) differ substantially in the three simulations was less expected. Although the characteristic periods do not largely differ, the curves corresponding to the three experiments reveal that relatively small (and very local) changes in orography and coastal line affect substantially global and regional teleconnection patterns. This result should motivate further analysis using coupled atmosphere-ocean models in which global and regional teleconnection patterns are expected to be more strongly related to the oceanic variability.

An idea about the impact of changes of orography on atmospheric flow can be gained from Fig. 3.9, where we display the difference between surface wind stress in TE and ME. It becomes clear from this figure that the mountain ridge in TE tends to affect both velocity components. The disturbance due to this obstacle (also seen in the difference between CR and the other two experiments (not shown here)) is confined to Europe and the Middle-East.

The simulated patterns are consistent with the overall expectations based on hydrodynamic considerations: velocity magnitude increases of the two sides of the obstacle. This is more pronounced for the zonal velocity, which is higher than the meridional one. Thus, as seen from Fig. 3.9(a) westerlies decrease to the east and west of the obstacle, while the "compensating" increase is north and south of the obstacle (more pronounced over the northern Africa). Similarly, the dominating northern winds increase east and west of the obstacle (this is better highlighted in the Caspian region and south of it) and decreases over Egypt and south of it. These changes result in large disturbances in the vorticity field, as well as in surface temperature patterns (Fig. 3.9(c)). The region north and south of the obstacle becomes warmer because of the reduction of the meridional velocity and the increase of the westerlies bringing warmer air masses from the North Atlantic. To the east of the obstacle the model simulates a pronounced cooling, extending from the Caspian to the Red Sea.

Because the main interest of this chapter is on the impact of local orography on teleconnection patterns, we will discuss in the following the differences between results of three experiments in this context. To this aim we prepare for each curve in Fig. 3.8 NAO+, NAO-, EAWR+ and EAWR- fields as averages of horizontal maps for winter months (DJF) corresponding to the extreme positive and negative situations. The differences between positive and negative phases are shown in Fig. 3.10 and Fig. 3.11 for surface pressure and 2m temperature.

The overall conclusion from the NAO-pressure maps is that the most persistent feature in the three simulations is the Icelandic low. Azores high is well pronounced both in CR and ME, however in TE this feature is not well resolved. Furthermore, in CR there is a positive pressure anomaly simulated in the northernmost latitudes, which is not observed in the ERA-40 data (Fig. 3.4(a)). This drawback is not (fully) observed in ME, which gives an indication that the water coverage in the Mediterranean area in CR, which seems to be over-represented, could substantially corrupt some atmospheric teleconnections. Therefore ME seems to provide more realistic simulations than CR.

The replication of variability patterns associated with the NCP is not very successful in the CR, particularly in the area of North Sea. Additionally, the pressure anomaly centred over Siberia and extending toward the polar areas in ERA-40 data (Fig. 3.4(b)) is not well resolved over the Greenland and Canada in CR. Changing land-sea mask in ME contributes to resolving the anomaly over the North Sea (Fig. 3.10(c)), however, the simulations over North America are still inconsistent with the analysis of ERA-40 data. One trend worth noting is connected to the artificial mountain ridge in TE. As seen in Fig. 3.10(f) this change in orography contributes to the enhancement of the anomaly over the North Sea. Although relatively small (compared with the global orography) this change critically affects the model behaviour in the polar areas (Fig. 3.10(f)). Finishing with the analysis of Fig. 3.10, we have to mention that orographic changes in ME and TE affect, in a more pronounced way, the patterns associated with the NCP, which

is consistent with the general expectation that this pattern represents north-south transport; the latter being quite sensitive to land-sea mask and orography in Eastern Europe and Minor-Asia

The degree to which the simulated teleconnection patterns replicate the ones in ERA-40 data and their sensitivity to "small" changes in orography are illustrated in Fig. 3.11 on the example of 2m temperature. The NAO pattern is well resolved in CR (compare Fig. 3.11(b) with Fig. 3.4(c)). Almost the same is true for the NCP (compare Fig. 3.11(b) with Fig. 3.4(c)). For this teleconnection, the redistribution of temperature anomalies over Siberia and the Caspian region, from one side and polar regions from another, is the most important. This pattern of variability is associated with the north-south transport of heat, and changing the coastline in ME results in drastic change not only over Asia, but also over the North America.

Although the NAO-horizontal pattern, as seen in 2m temperature seems to sustain the orography change in ME (amplitudes in Fig. 3.11(a) and 3.11(c) are not much different), the changes in TE demonstrates that the artificial mountain ridge reduces the contrasts about two times. The situation as seen in the NCP pattern is much less stable. Here the (zonal) mountain ridge results in changing polarity of temperature patterns between Asia and polar regions.

3.5 Conclusions

The present study can be considered as a sensitivity analysis of the impacts of orography on local and global climatic patterns. Apart from theoretical interest, one can ask the question about whether the results presented here have a practical value. Two aspects can be mentioned in this respect: the first is about how successful models are with different resolutions in simulating processes associated with global teleconnection patterns, and the second is how the land cover being subject to global change (also associated with sea level change) could affect these patterns. In chapter 2 we were investigating how would changes of boundary conditions influence hydrological cycle. This exercise motivated us to perform idealized experiments in order to isolate key mechanism responsible for teleconnection patterns formation. Apart from the fundamental issue that the teleconnection patterns are subject to air-sea exchange, which is a problem motivating further modelling studies with coupled atmosphere-ocean models, one sees clearly that simulations in this study of atmospheric variability over large areas, shows a strong dependence on local changes in land cover. As land cover (not only land-sea mask but also vegetation, which is represented in the model by different roughness and albedo) has changed in the area of interest due to anthropogenic and natural factors (a substantial part of the Black Sea became dry during the LGM), it seems important to be able to adequately simulate and predict atmospheric changes caused by land cover changes. The present study is one initial step in this direction, which must be followed by more comprehensive fine resolving modelling.

3.6 Figures

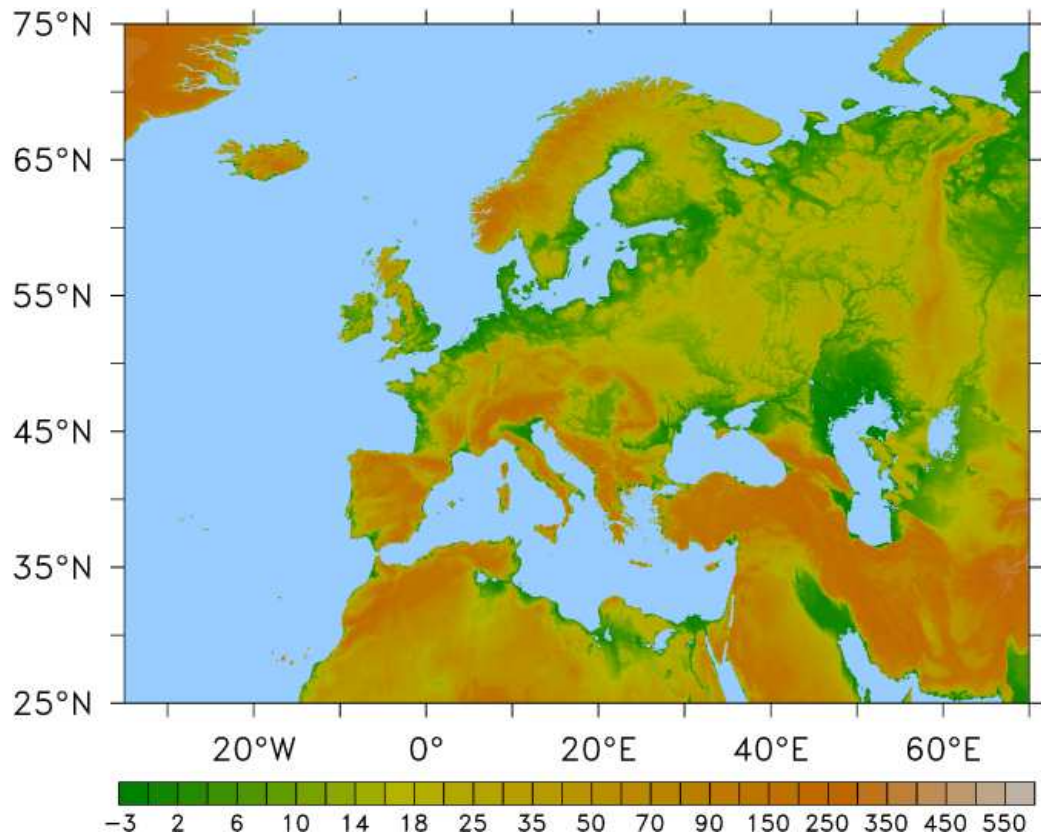


Figure 3.1: *Region of interest and orography in dm*

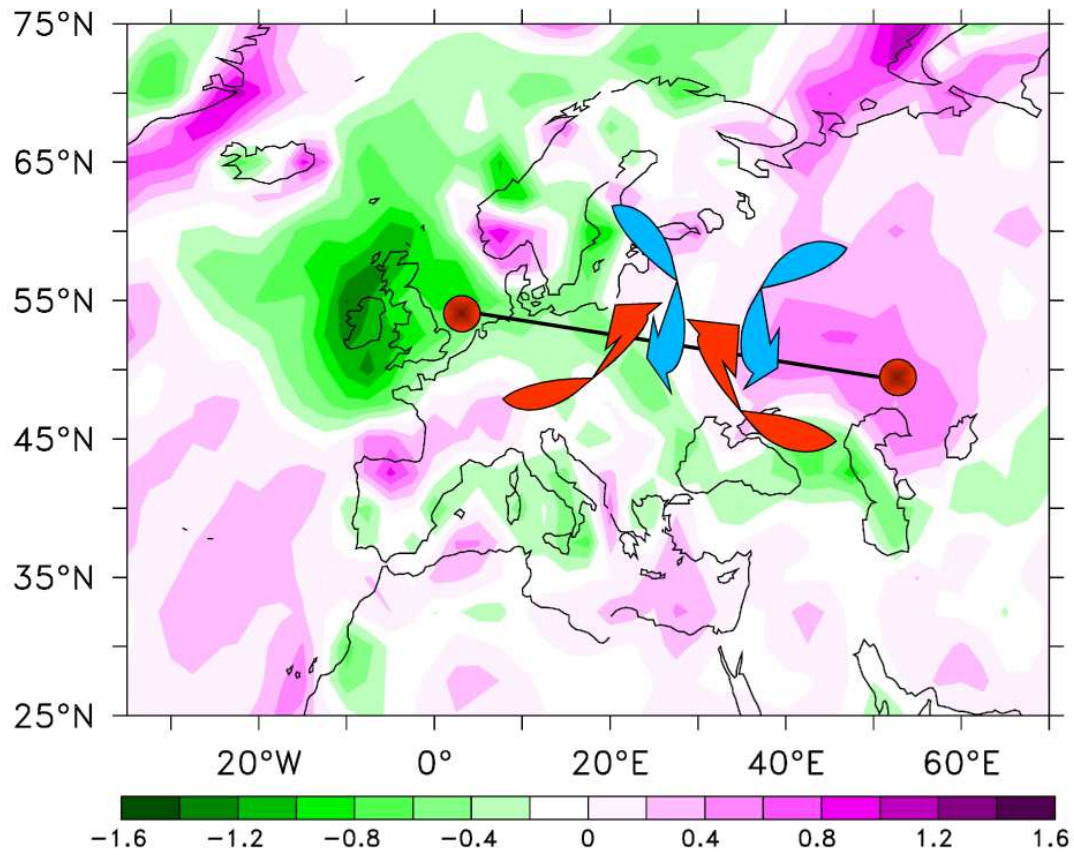


Figure 3.2: Vorticity anomaly in $s^{-1} \times 10^{-5}$, calculated from ERA-40 data defined as the difference between EAWR(+) and EAWR(-) situations in Eurasian region.

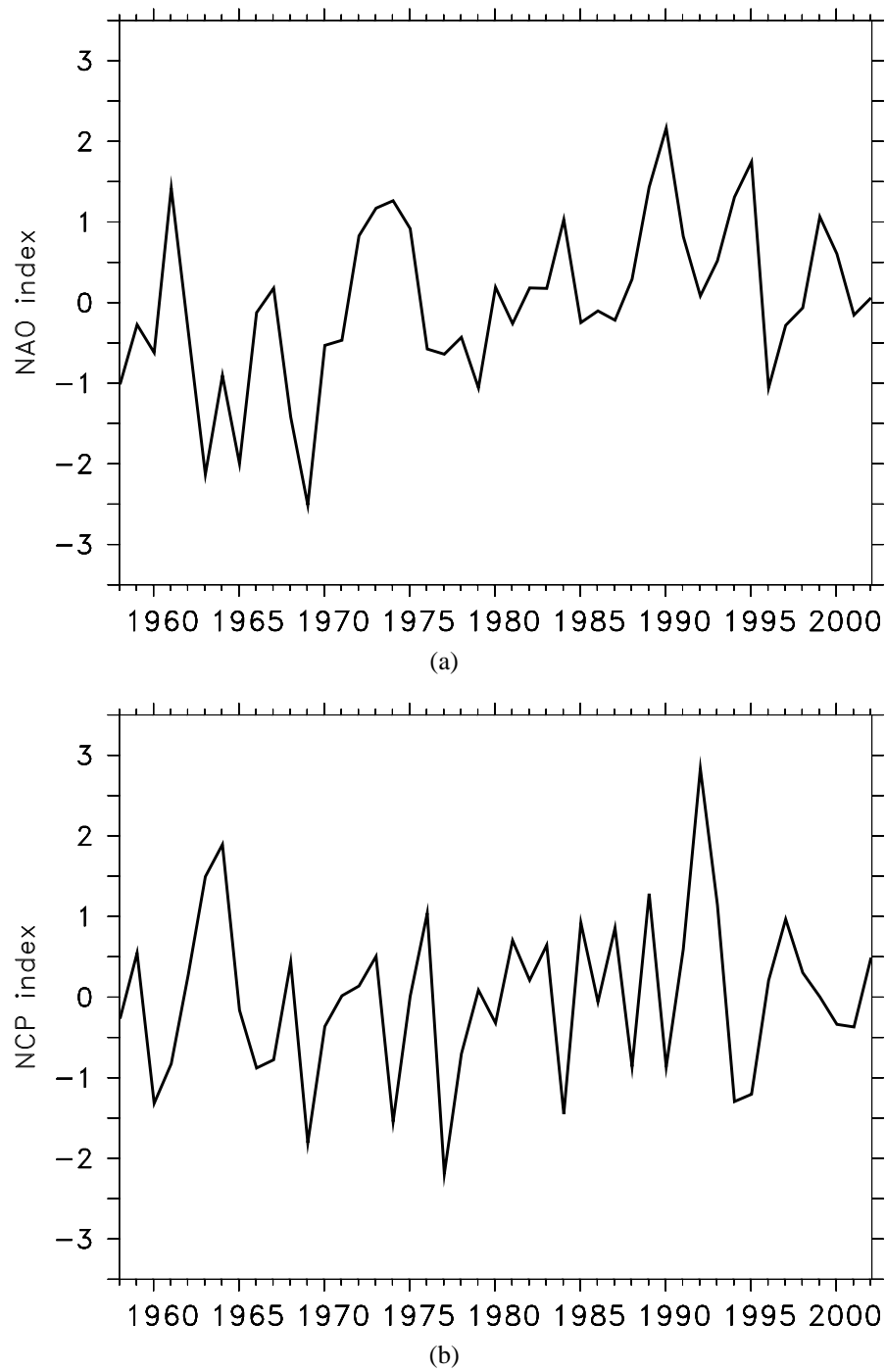


Figure 3.3: (a) NAO index and (b) EAWR (NCP) index based on ERA-40 data.

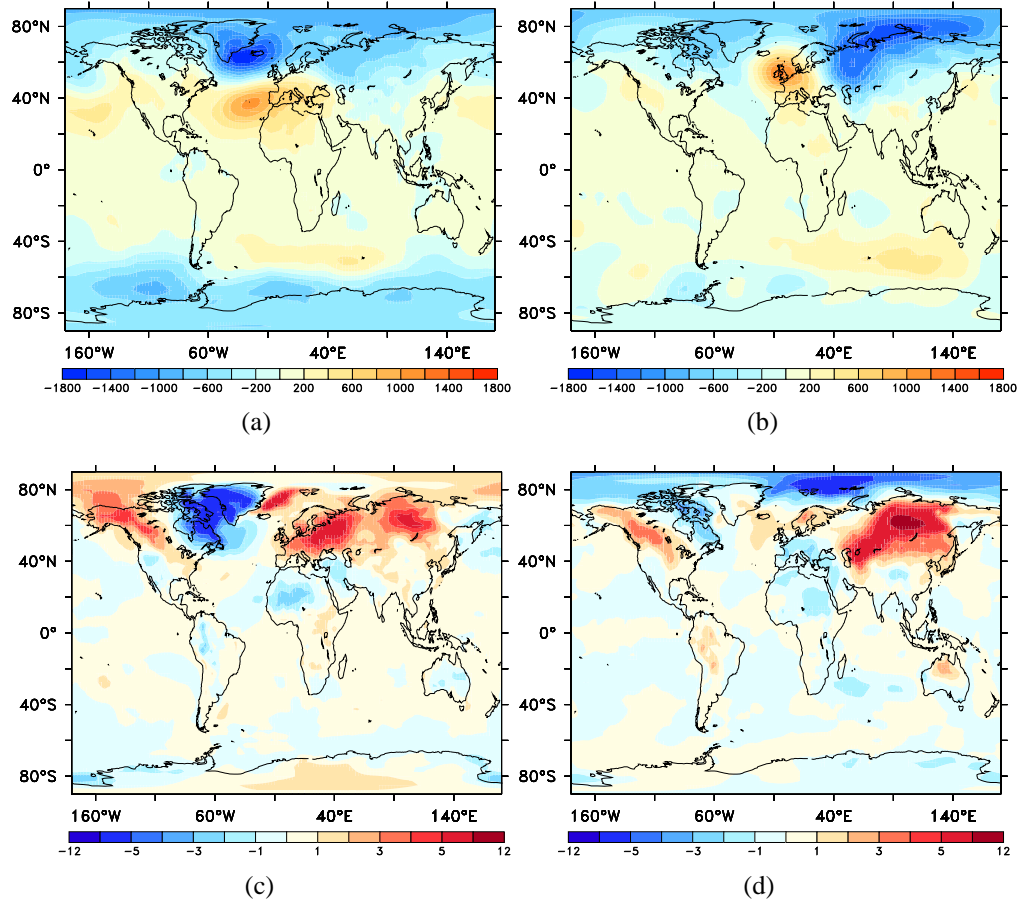


Figure 3.4: NAO and NCP horizontal patterns represented as difference between (a) NAO+ and NAO- surface pressure (hPa), (b) NCP+ and NCP- surface pressure (hPa), (c) NAO+ and NAO- surface temperature (K), and (d) NCP+ and NCP- surface temperature (K).

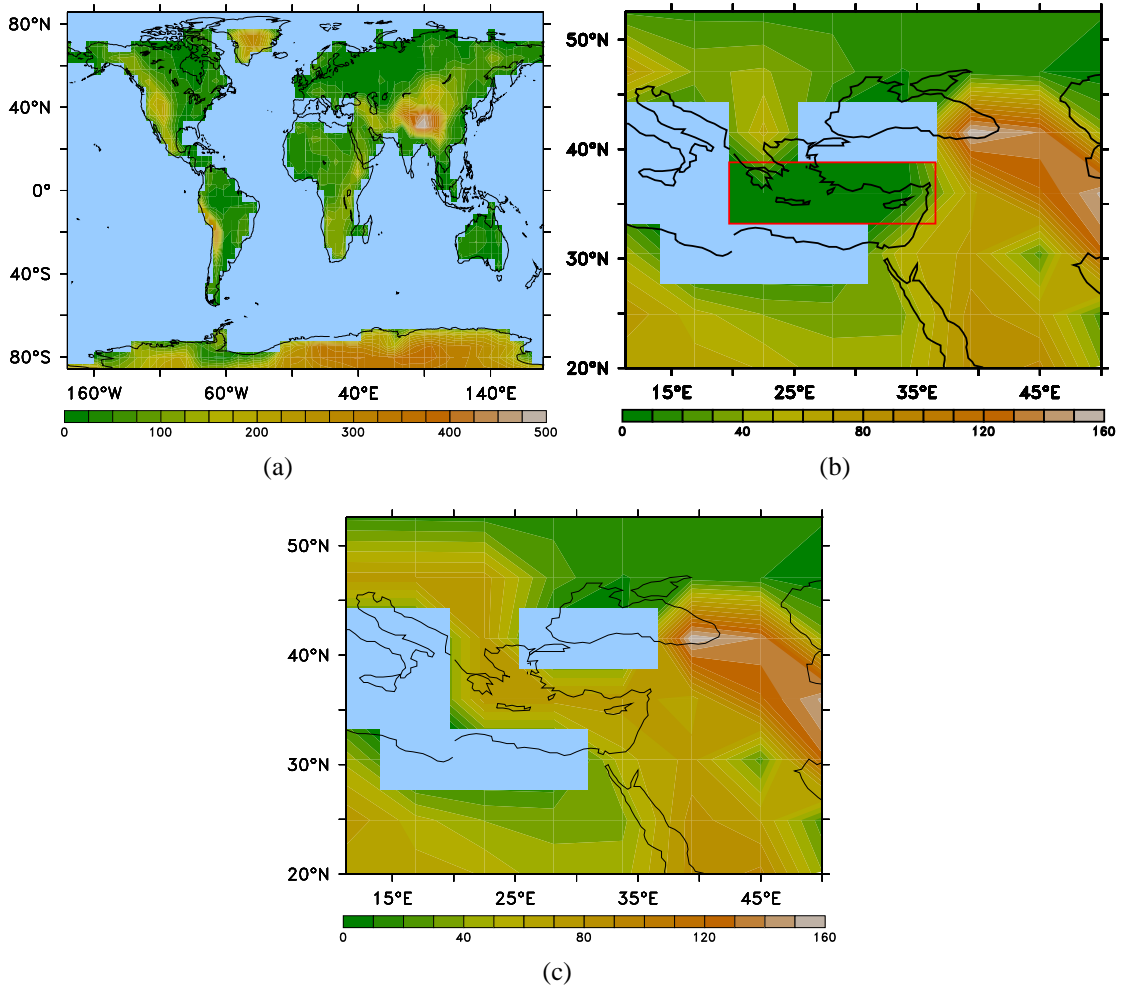


Figure 3.5: Orographies (dm) and land-sea masks in (a) CR, (b) ME, and (c) TE. For the zoomed maps (b, c) only details are shown since they differ from CR only in the region of zooming.

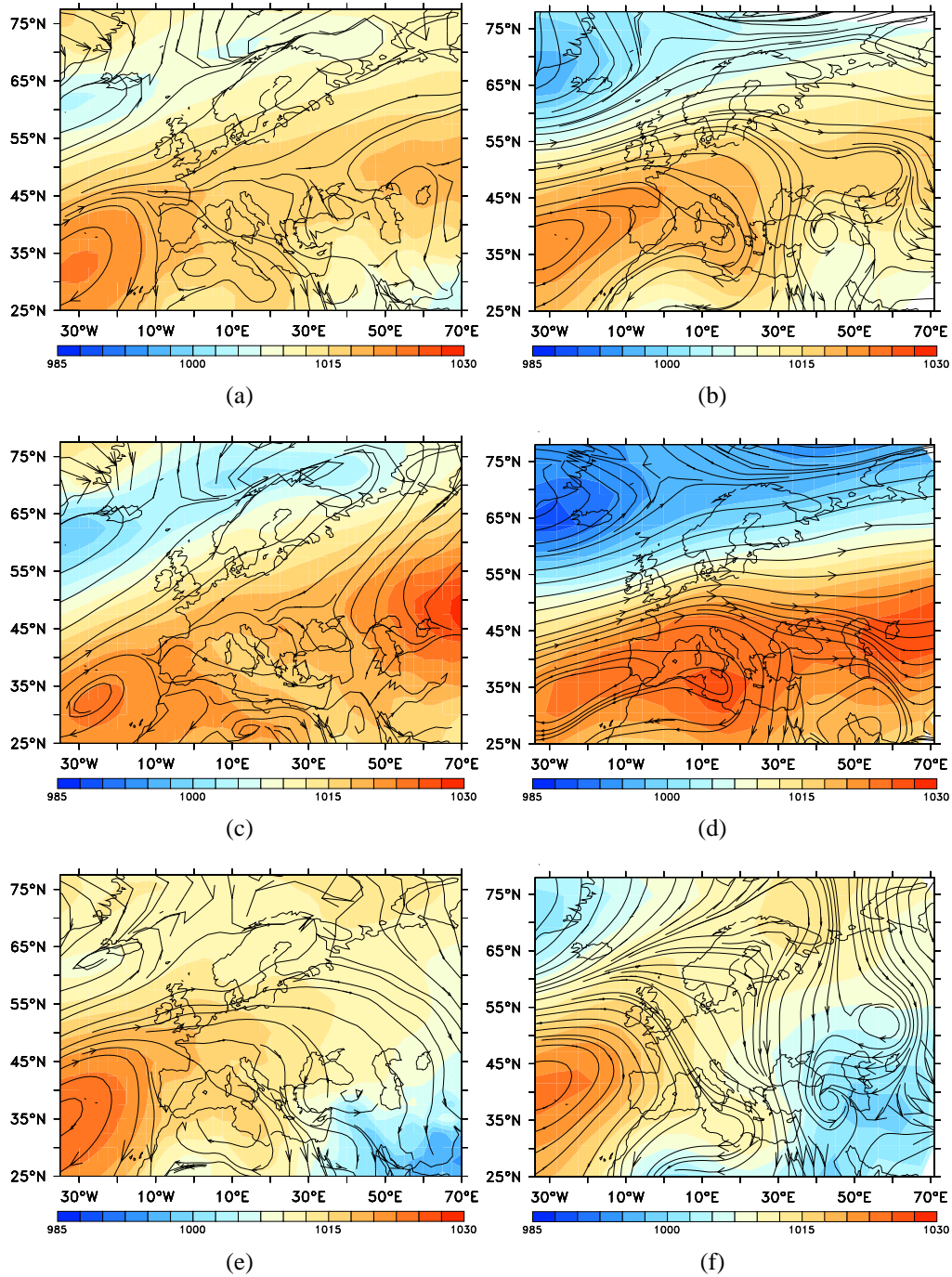


Figure 3.6: Annual mean surface pressure (hPa) in ERA-40 data (a) and CR (b), winter (DJF) mean surface pressure in ERA-40 data (c) and CR (d), summer (JJA) mean surface pressure in ERA-40 data (e) and CR (f). Wind streamlines are also plotted.

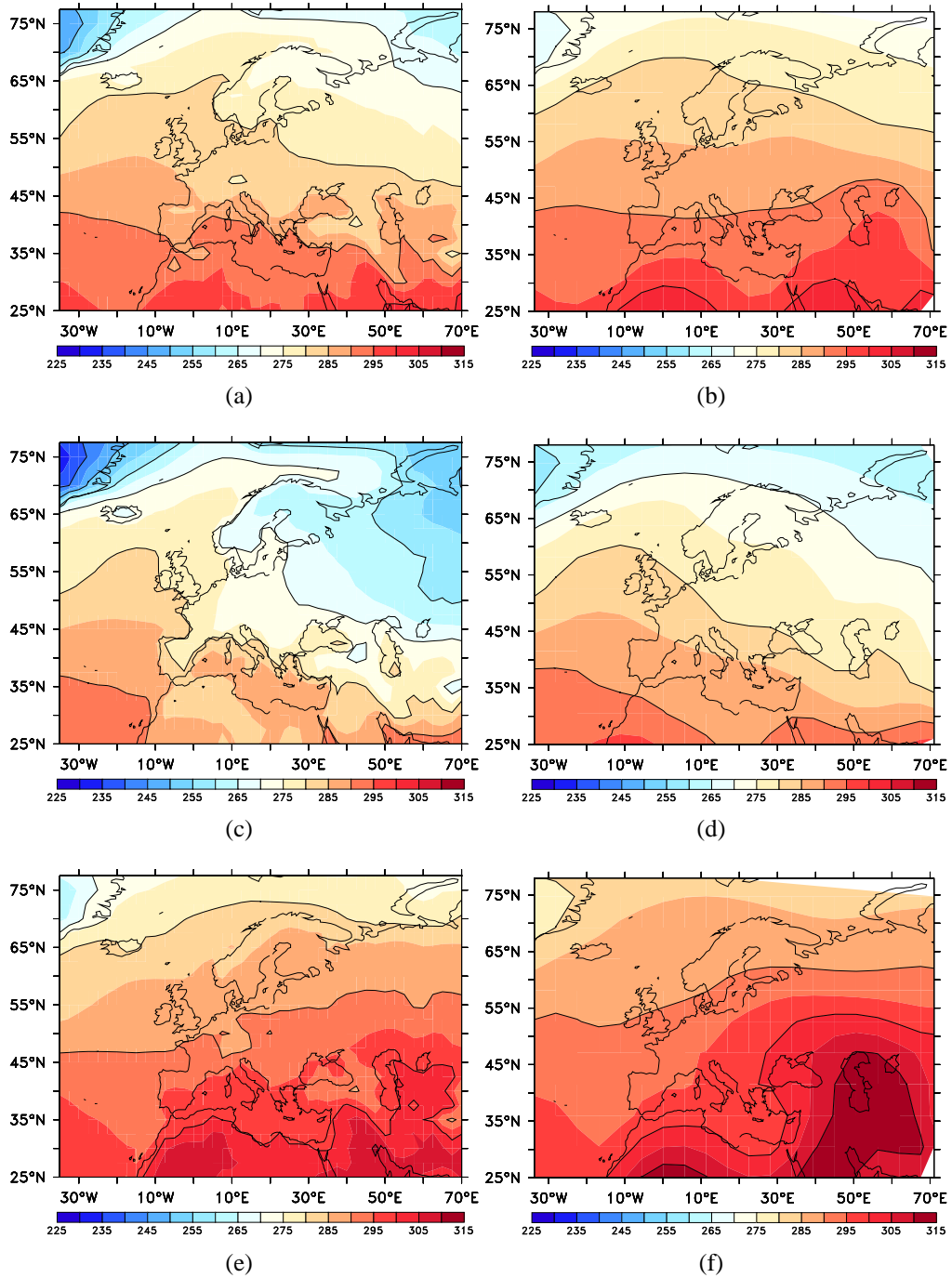


Figure 3.7: Annual mean surface temperature (K) in ERA-40 data (a) and CR (b), winter (DJF) mean surface temperature in ERA-40 data (c) and CR (d), summer (JJA) mean surface temperature in ERA-40 data (e) and CR (f).

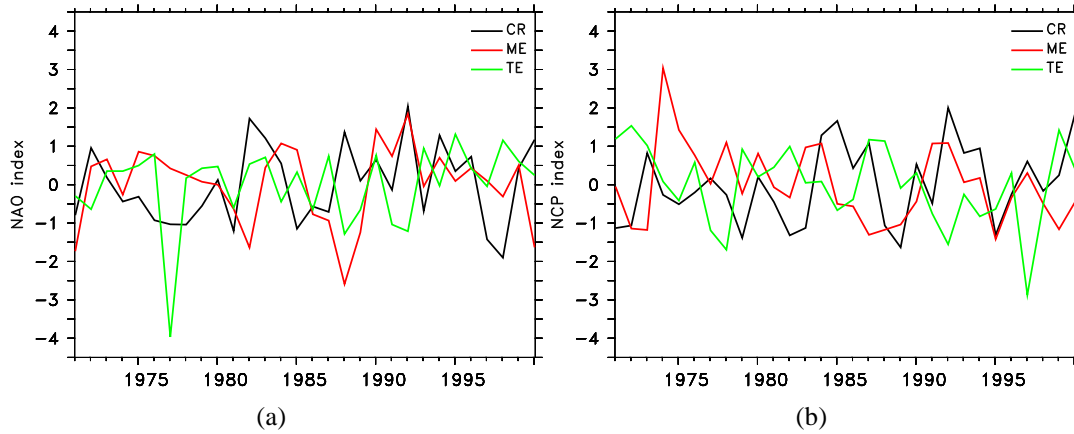


Figure 3.8: NAO (a) and NCP (b) indices. Difference between the simulated atmospheric pressure in Azores and Iceland (a), and North Sea and Caspian (b).

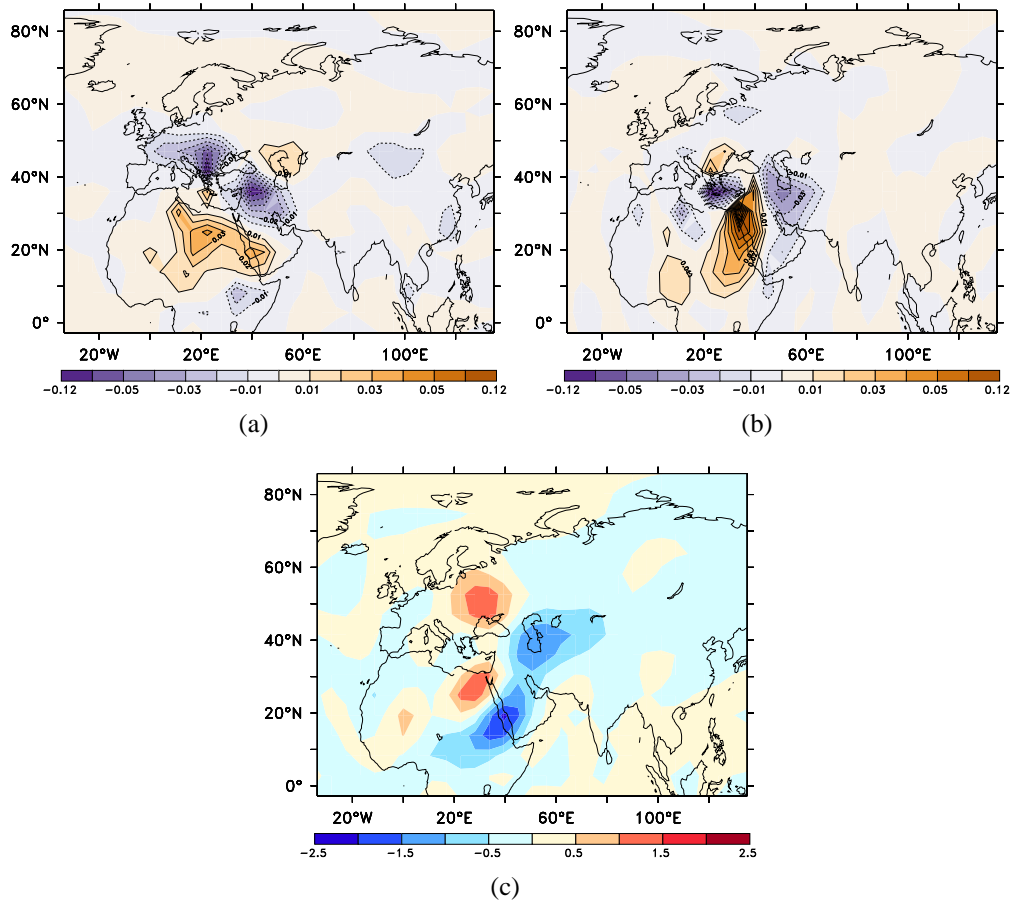


Figure 3.9: Averaged for 30 years difference between TE and ME for u-wind stress in Pa (a), v-wind stress (Pa) (b), and 2m temperature in K (c).

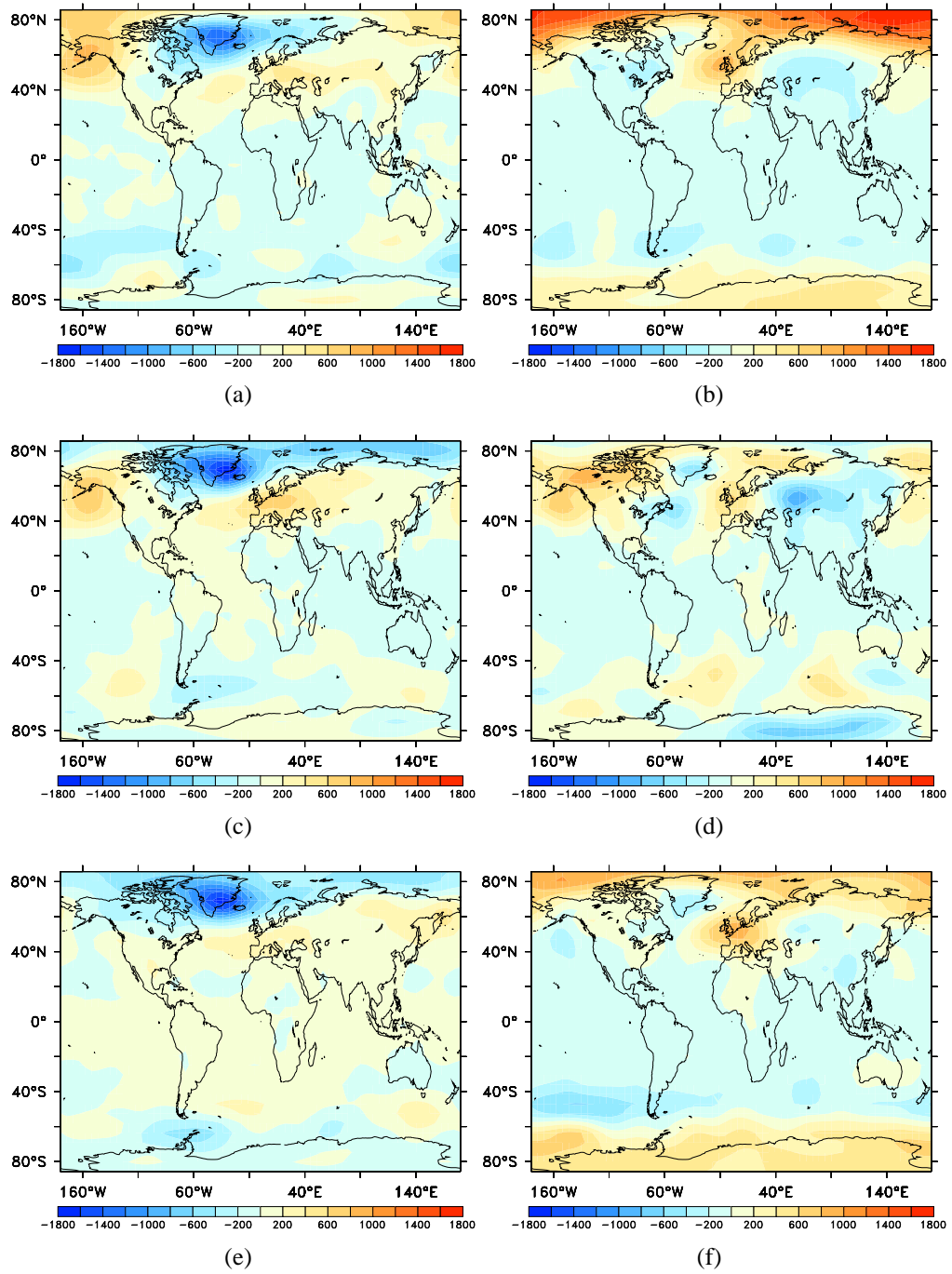


Figure 3.10: Difference between surface pressure (hPa) corresponding to positive and negative NAO (left column) and NCP (right column) phases. Every two plots from top to bottom are for CR, ME, and TE, correspondingly.

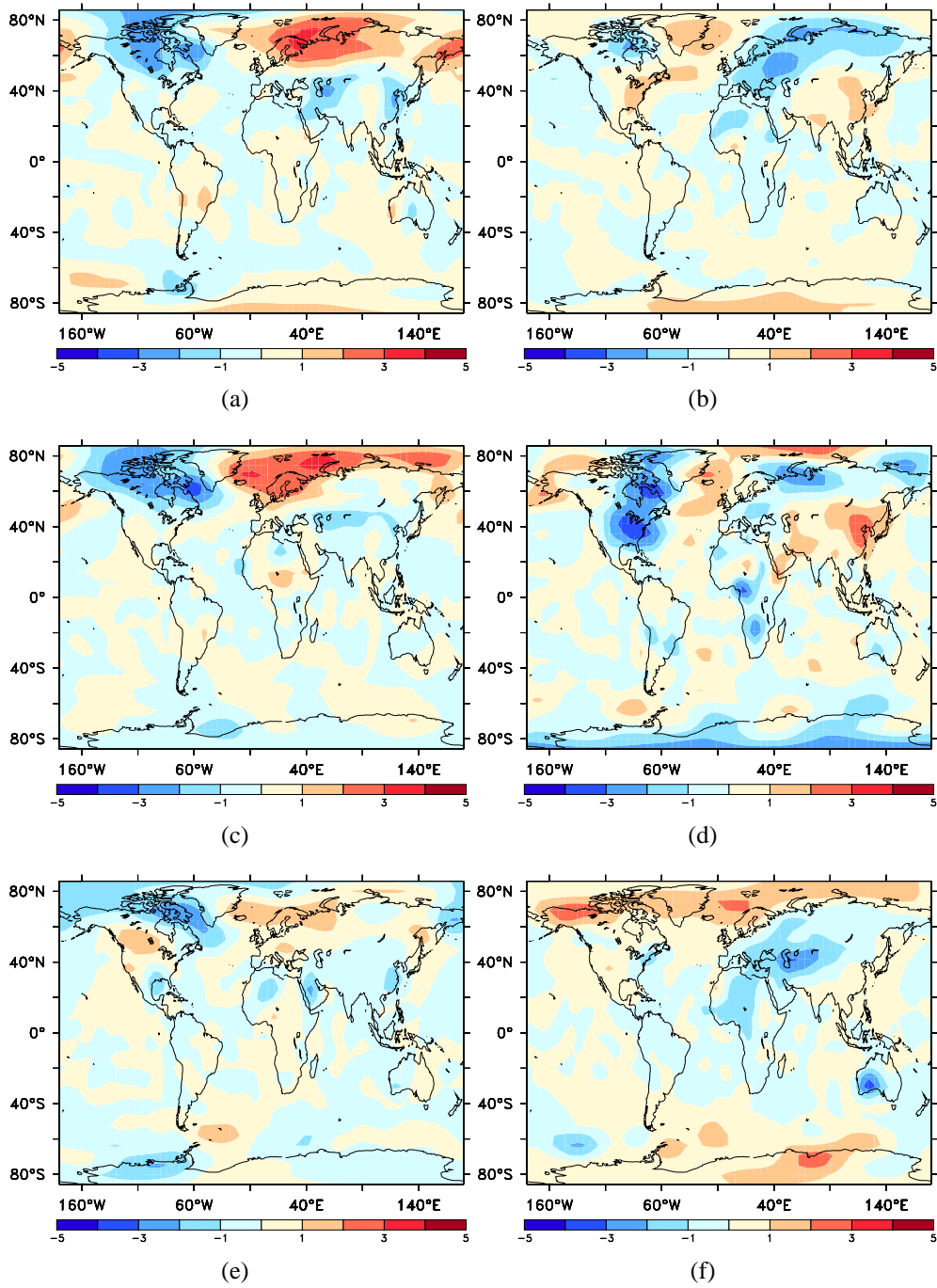


Figure 3.11: Difference between 2m temperature (K) corresponding to positive and negative NAO (left column) and NCP (right column) phases. Every two plots from top to bottom are for CR, ME, and TE, correspondingly.

Chapter 4

Paleoevolution of the Black Sea Watershed: Sea Level and Water Transport through the Bosphorus Straits as an Indicator of the Lateglacial-Holocene Transition ¹

The paleo-evolution of the Black Sea level during the Lateglacial-Holocene transition is still unclear, which motivates us to provide new estimates for that period based on the analysis of water budget. Hydrological conditions in the Black Sea catchment area are reconstructed here using water balance equation, available data, and constraints based on simple theory relating the runoff ratio with climatic characteristics. In order to estimate the impact of the aridity of climate we consider two alternative scenarios: (1) climate change under constant in time gradient in precipitation and evaporation over land and sea, and (2) climate change accounting for changes in the horizontal distribution of precipitation and evaporation. Hydrological data are compiled from available present-day data and paleo-observations. A number of sensitivity experiments is carried out revealing that the hydrological conditions in the Black Sea watersheds should have evolved towards a very arid climate (similar to the present-day climate in the Caspian Sea area) in order to initiate a drop of sea level of ~ 100 m below the sill depth of the Bosphorus Straits, as speculated in some recent research. Estimates of sea-level changes reveal a qualitative agreement with the coast-line evolution inferred from paleo-observations. The Younger Dryas draw-down of the Black Sea starts at about 13.3 - 13 ka BP, with a maximum lowstand of 104

¹This manuscript is published with Climate Dynamics see list of reference or footnote 1 in the section 1.3 for the full reference

m at 11.5 ka BP. In an "arid climate" scenario the sea level reaches the outlet at about 8.8 - 7.4 ka BP. Approximately at that time, Mediterranean sea level was about 10 m higher, making flooding events of the Black Sea possible. However, the nature and exact timing of the Holocene reconnection depends also on other (not well-known) factors; one of them is the Bosphorus sill depth, motivating further research in this field. Estimates of the water transport through the Bosphorus Straits are also provided for the time of Lateglacial-Holocene transition.

4.1 Introduction

The Black Sea level is very sensitive to changes in the surface fresh water fluxes and river runoff. By integrating the variations of global forcing over a vast catchment area, this sea amplifies large-scale climatic signals [Stanev and Peneva, 2001]. This amplification was extremely strong in the past, resulting in either: (1) one-way transport through the Straits of Bosphorus (from the Black Sea to the Mediterranean), or (2) sea-level drop in the Black Sea to a level below the sill depth under extremely dry conditions, facilitating transport in the opposite direction. The evolution of water exchange between the Black Sea and the Mediterranean is largely due to changes in precipitation and evaporation over the Black Sea and its watershed. The possibility that the watershed of the Black Sea has changed dramatically, including the cascading of water from the Caspian Sea (and perhaps, the Aral Sea and the West Siberian Paleo-lake) is not excluded [Grosswald and Hughes, 2002]. According to Mangerud et al. [2004] there were two events of redirecting north flowing rivers by the advancing of the Eurasian ice sheet to the south in the past 100 000 years (100 ka).

The possibility that Black Sea level may at times have dropped below the Bosphorus sill depth is supported by the observations of presently submerged paleo-coasts, caused by periods of significant net fresh-water deficit [Ryan et al., 1997, Ballard et al., 2000]. It has been suggested that at the same time (see below) the level of the global ocean was also below the sill depth, so that the Black Sea had been transformed into an inland lake with no outflow. After global sea level has reached the sill depth, a reconnection with the Mediterranean occurred. Although there were at least eight marine flooding events of the Black Sea during the past three million years [Ryan et al., 2003] it is still not clear how exactly these processes have developed.

For the most recent (Holocene) intrusion of saline water two reconnection scenarios ("catastrophic flood" and "gradual reconnection") have been proposed based on sediment core data (dating, appearance, and composition of sediment) and theoretical studies (hydraulic properties of the flow). The necessary (but not sufficient) condition for the catastrophic flood scenario to take place, is that the Black Sea level should at the time of re-connection be below the sill depth. The reconnection is gradual if the Black Sea level is above the sill (positive water balance). In

this case, there is no counterflow in the connecting strait before the height of sea level reaches some critical value above the sill [Lane-Serff et al., 1997].

Analysis of observations to the east and west of the Crimean Peninsula taken during 1993 demonstrated that euryhaline (tolerant to the wide salinity ranges) species suddenly populated the Black Sea, the vertical profiles indicating an abrupt sedimentation above the 150 m isobath. Based on this evidence Ryan et al. [1997] suggested that the reconnection occurred at 7.15 ka BP (radiocarbon convention age, before reservoir correction) and that the Black Sea level at that time stood more than 100 m below the level of the present-day outlet. Using observations from the continental shelf off the North Turkish coast, Ballard et al. [2000] argue that at the time of reconnection the Black Sea level stood 155 m below the present-day sea level.

The scenario of catastrophic flooding assumes that the global sea-level rise resulted in a spill of Marmara Sea water into the Black Sea. The erosion by gravity currents has led to scouring the material from the bed down to the bed rock, which is at ~ 80 m [Ryan et al., 1997]. Taking for the Black Sea level at this time the value of 120 m below present-day sea level, for the basin area between 120 and 20 m isobaths the value of $370 \times 10^3 \text{ km}^2$, and for the sill height a value of 20 m below the present-day sea level (global sea level at 7.15 ka BP stood at about -20 m [Fairbanks, 1989]), and assuming that this volume has been filled in two years, yields a rate of flood transport of $\sim 370 \times 10^2 \text{ km}^3 \cdot \text{y}^{-1}$. This value was suggested by Ryan et al. [1997] and corresponds to a flow ~ 50 times the present-day freshwater flow (in the opposite direction), that is a "catastrophic flood".

Recently, Siddall et al. [2004] presented a shock-resolving hydraulic model to test paleo-oceanographic implications of such a "catastrophic flood" concept, and concluded that observed sediment waves at 2000 m depth could be explained by a jet stream constrained by bathymetric contours. However, according to their simulations it will take about 34 years to equilibrate the levels of the Black and the Marmara Sea, which is much longer than the estimates of Ryan et al. [1997].

Before the work of Ryan et al. [1997] the "gradual reconnection" scenario was more commonly accepted based on the evidence that the Black Sea has a positive water balance. This idea was first explored by Degens and Ross [1972]. Those authors suggested that the gradual reconnection and salinification of the Black Sea freshwater with salty Mediterranean water occurred in the period from 9 to 7 ka BP. Later, Lane-Serff et al. [1997] and Myers et al. [2003] analyzed results from hydraulic control models, and demonstrated that the time of reconnection could be on time-scales of decades, but not years as proposed in the "catastrophic flood" scenario. Furthermore, they discarded the possibility of a deep Bosphorus sill (80 m or even slightly deeper). The important idea proposed by Lane-Serff et al. [1997] is that the reconnection between the Mediterranean and the Black Sea may have caused a transient effect on the circulation in the

Eastern Mediterranean during the last deglaciation, leading to decreased deep water formation and a higher productivity in the surface water.

The data cored from other locations (near the Sakarya river, Görür et al. [2001], or the Sea of Marmara, Aksu et al. [2002]) reveal that the "catastrophic flood" hypothesis is less probable than the "gradual reconnection", because the Black Sea level appeared to have stood above the sill at the time of reconnection, permanently exporting water into the Mediterranean. Furthermore, Mudie et al. [2004] analysed dinoflagellate cyst assemblages from the Black-Marmara-Aegean Sea corridor, and did not find any evidence supporting the idea of sudden flooding of the Black Sea by 100-m-high waterfall of Mediterranean water at 7.5 ka BP.

The direction of water transport in the straits depends on the water balance of the Black Sea and its watersheds, and on the level of the global ocean. So far, two possibilities have been considered for this sea: (1) estuarine-type basin, and (2) enclosed basin of the type of the present-day Caspian Sea. To the best of the present authors' knowledge, possibilities suggesting functioning like lagoon-type basin (e. g. the Mediterranean) have not yet been considered, except perhaps during short periods of re-connection between the two basins. It seems that the Earth System makes lagoon-type exchange very improbable for the Black Sea, due to large river runoff.

In order to estimate possible Black Sea levels in the past, one needs high-quality paleo hydro-meteorological and glaciological data, or data produced by simulations with climate models. Although there is still much to be desired with respect to their quality and quantity, (see Kohfeld and Harrison [2000] for the data from past periods and Hagemann et al. [2005] for the present-day data, e. g. European Center for Medium-Range Weather Forecasts, (ECMWF) Re-analysis data (ERA-40), Simmons and Gibson [2000]), we intend to develop here a first-order estimate of the paleo-evolution of the Black Sea level based on optimal use of the available data, incl. atmospheric analysis data, the latter providing the spatial patterns of water budget. This chapter can thus be regarded as an attempt to explore the sensitivity of the Black Sea level to climatic (hydrologic) changes in its catchment area. It is thus relevant to global hydrological cycles and brings the attention to the idea that by analyzing consistency of fresh water fluxes in regional (semi enclosed or fully enclosed) seas a further improvement of the estimates of water cycles can be expected. In particular, some problems found in ERA-40 data could motivate further research on the water balances diagnosed by atmospheric analyses.

The chapter is organized as follows: the second section presents a brief overview of the study area, description of the available hydrological data, and their quality in the paleo-oceanographic context. Method and results are described in the third section followed by Discussion and Summary in the fourth one.

Table 4.1: *Area of basins and watersheds (in km²).*

	Sea	Land	Total
Black Sea	471180	2410837	2882017
Caspian Sea	392544	3249154	3641697

4.2 Description of Data

4.2.1 The Region

The extended region of our interest includes the Black and Caspian Sea catchment areas (Fig. 4.1), but we focus in this chapter on the Black Sea catchment area (Fig. 4.2) and its evolution during the past 20 ka. We use a subset of ETOPO2 topography and map of the watersheds adopted from the Total Runoff Integrating Pathways (TRIP) scheme developed by Oki and Sud [1998]. Areas of the basins and watersheds are given in Table 4.1. The Azov Sea and its watersheds are assigned to the ones of the Black Sea.

The margins of the Scandinavian part of the Eurasian ice sheet (Fig. 4.1), as well as the geomorphological characteristics of the West Siberian Plain and Russian Plain provide a possibility for the north flowing rivers to divert to the south in case of extreme glaciations. Paleo observations (Mangerud et al. [2004]) indicate that two such events of river re-routing have occurred in past 100 ka BP. Results from the Project Quaternary Environment of the Eurasian North (QUEEN) have shown that the first event occurred about 90 - 80 ka BP due to the advance of the Barents-Kara Ice Sheet, diverting rivers Ob and Yenisei to the Aral, the Caspian, and the Black Sea. The next event occurred at about 18-17 ka BP. At that time, the drainage towards the Baltic was blocked by the Scandinavian ice sheet and meltwater from a considerable sector of the ice sheet flowed over to the Volga River [Mangerud et al., 2004]. By analyzing gravity cores from the continental slope in the northwestern Black Sea, Bahr et al. [2005] found evidence of meltwater delivery to the Black Sea from 18 to 15.5 ka BP, probably through the Manych Pass (Caspian Sea transgression). Furthermore, according to Sidorchuk et al. [2003] none of the rivers of the Russian Plain were fed with glacial melt water during the Lateglacial to Holocene transition and at that time both the Ob and Yenisei discharged to the Arctic.

Alpine glacier retreat and advance could also influence the Black Sea water balance [Starkel, 2003]. However, the possibility for Danube tributaries to bring Alpine meltwater into the Black Sea existed for a very short time (about 18-17 ka BP, see Bahr et al. [2005] and reference therein). Major et al. [2002] do not exclude the possibility that traces of meltwater in the sediment between 15 and 14 ka BP could be of Alpine and/or Fennoscandian origin, indicating the Younger Dryas cold period. However, to the best of the present authors' knowledge, there

exist no quantitative reconstructions of Alpine and other mountain glaciers that could contribute meltwater to the Black Sea between the last glacial maximum (LGM) and the Present.

Because data which could prove the existence of past lake connections are controversial (ranging from dramatic changes in watersheds [Boomer et al., 2000] to negation of cascading during the Holocene [Mangerud et al., 2004]), and because this possibility is more plausible for earlier times, we do not address this issue in the present chapter. Lake connections (incl. rerouting of rivers) will be addressed in chapter 6. In the present study, we develop a complementary method elucidating paleo water budgets focused on the natural variations of hydrologic regime in the Black Sea catchment area.

4.2.2 Hydrological Data

The Rivers in the Region

The present-day Black Sea catchment area is dominated by the Danube River and the rivers from the North of the Black Sea (Dnepr, Dnestr, Southern Bug, Figs. 4.1 and 4.2). At the easternmost part of the Black Sea catchment area, the River Don approaches the Volga River. Kuban is the biggest river bringing water from Caucasus into the Black Sea via the Sea of Azov. The annual discharge of these six biggest rivers (Danube, Dnepr, Dnestr, Southern Bug, Don and Kuban) is $270.3 \text{ km}^3 \cdot \text{y}^{-1}$ [Fekete et al., 1999]. The annual mean contribution of rivers from the Anatolian mountains is only $36 \text{ km}^3 \cdot \text{y}^{-1}$ and they are not included in the report of Fekete et al. [1999].

Most of the river runoff (about $300 \text{ km}^3 \cdot \text{y}^{-1}$) into the Caspian Sea is due to Volga, Ural and Kura (see Stolberg et al. [2003] for more information on the present-day Caspian Sea hydrological conditions).

Constraining Water Balances

For the purposes of the present study we can assume that precipitation (P), evaporation (E) and river runoff (R) in the individual watersheds averaged over one year or longer times are in a steady state, that is, we will neglect changes in the water storage on land. Then, the flux associated with precipitation less evaporation above catchment areas $Q_c^P - Q_c^E$ (index "c" stands for continent) should present a good proxy of river runoff. However, this is not exactly/always the case with some reanalysis products (e. g. ERA-40 dataset). The problems arise from (1) the coarse resolution, which does not sufficiently resolve the borders of watersheds (the borders usually follow sharp mountain ridges), and (2) possible problems with outflow schemes.

Consequently, the hydrological cycle is not closed for some watersheds ($Q_c^P - Q_c^E \neq R$), as it should be [Dai and Trenberth, 2002, Hagemann et al., 2005]. In this case, we can use independent data (e. g. observations of runoffs R_{obs}) to constrain water budgets over watersheds, that is to calibrate Q_c^P and Q_c^E , which are provided by atmospheric analysis data.

The evaporation ratio $e = \frac{Q_c^E}{Q_c^P}$ is an important climatological characteristic of catchment areas (in the following, if not specifically mentioned, we will refer to mean precipitation and evaporation in km^3 accumulated during one year over catchment area or sea). Taking into consideration that

$$Q_c^P - Q_c^E = R \quad (4.1)$$

it follows that $R : Q_c^E : Q_c^P = (1 - e) : e : 1$. These ratios computed from ERA-40 data scale for the Black Sea watershed approximately as 1:3.8:4.5, that is $e = 0.84$. The runoff ratio $r = 1 - e$ measures the runoff capabilities of watersheds ($R = rQ_c^P$) and the above scaling can be written in a more understandable way as:

$$R : Q_c^E : Q_c^P = r : 1 - r : 1 \quad (4.2)$$

Theoretically there are two extremes: (1) $r \rightarrow 1$, in which case $R \rightarrow Q_c^P$, and (2) $r \rightarrow 0$, that is $Q_c^E \approx Q_c^P$, in which case $R \ll Q_c^P$. The first case corresponds to a very efficient runoff (runoff tends to precipitation), the second corresponds to the case when all water provided by precipitation goes back (directly) into the atmosphere.

Because the evaporation and precipitation from atmospheric analysis data are not perfect we can correct Q_c^E and Q_c^P , using above scaling and R_{obs} , which is usually more accurately estimated from direct observations. The problem of constraining the paleo-data is more difficult because there are no estimates from observations of all components of water balance. Our analysis showed that large inconsistencies exist between ERA-40 data and the data from the Paleoclimate Modelling Intercomparison Project (PMIP) [Joussaume and Taylor, 2000] simulated for the present-day conditions, in particular on regional scales. One possibility to provide paleo-reconstructions would assume that the scaling ($R : Q_c^E : Q_c^P$) holds for past periods. Alternatively, we could suggest scaling factors, corresponding to (different) past climatic conditions.

The total annual mean precipitation over sea and catchment areas scales as

$$Q_o^P = bQ_c^P \quad (4.3)$$

where the index "o" stands for ocean. According to ERA-40 data $b = 0.15$ and 0.07 for the

Black Sea and Caspian Sea catchment areas, respectively. In a similar way

$$Q_o^E = aQ_c^E \quad (4.4)$$

with values for the Black and Caspian Sea areas of 0.28 and 0.27, respectively (note that we work with area integrated-fluxes and not with area normalized values). The above parameters have not changed much during the last 40 years and give a first order estimate of the dryness of climate, as well as of the exposure of basins and their catchment areas to global atmospheric forcing. Obviously, they do not sufficiently describe the responses of local climates to dominating global patterns associated with NAO and ENSO for instance [Arpe et al., 1999, Stanev and Peneva, 2001]. Nevertheless, they are used in this chapter to replicate only some possible long-term trends in climate variability.

For completely enclosed seas (e. g. the Caspian Sea) the balance equation reads

$$Q_o^P + R = Q_o^E. \quad (4.5)$$

Thus it follows from Eqs. 4.1-4.5 that

$$a = \frac{b+r}{1-r} \quad (4.6)$$

that is, the runoff parameter r shapes the contrasts between evaporation and precipitation over land and sea. In the limiting case of zero runoff ($r = 0$) the sea is decoupled from the hydrological cycle over land and $\frac{Q_o^E}{Q_c^E} = \frac{Q_o^P}{Q_c^P}$. Large runoff ($r \sim 1$) is indicative for large evaporation over sea ($Q_o^E \gg Q_c^E$).

As mentioned above, there are inconsistencies between water balances diagnosed from ERA-40 data and the ones originating from analyses based on observations. Therefore the next task is to correct the balances in the atmospheric analysis data using independent observations (e. g. Black Sea Hydro Meteorological Dataset, BSHMD [Stanev and Peneva, 2001], or Global International Water Assessment (GIWA) reports for the Caspian Sea [Stolberg et al., 2003]). The correction assumes that the constants a and b are stable, but not perfect because of problems in the atmospheric analysis data. We correct Q_o^P and Q_o^E adding to the observed (true) values $Q_o^{P\,obs}$ and $Q_o^{E\,obs}$ some part of the misfit between ERA-40 data and observations $m(Q_o^{P\,ERA} - Q_o^{P\,obs})$ and $m(Q_o^{E\,ERA} - Q_o^{E\,obs})$, correspondingly. The value of m is optimized in a way that the river runoffs (relatively well known from observations) and water balance in the corrected data do not differ with more than $1\text{km}^3 \cdot \text{y}^{-1}$ from the observations. Formally, this could be written as:

$$Q_o^{P\,cor} = Q_o^{P\,obs} + m(Q_o^{P\,ERA} - Q_o^{P\,obs}), \quad (4.7)$$

Table 4.2: Black Sea water fluxes (in $\text{km}^3 \cdot \text{y}^{-1}$) and hydrometeorological parameters (non-dimensional) as estimated from various sources.

	R	Q_o^P	Q_o^E	$R + Q_o^P - Q_o^E$	Q_c^P	Q_c^E	a	b	r
ERA-40	$P_c - E_c = 240$	229	356	113	1532	1293	0.28	0.15	0.16
BSHMD	336	241	380	197	-	-	-	-	0.22
corrected	$P_c - E_c = 335$	240	378	197	1719	1384	0.27	0.14	0.20

Table 4.3: Caspian Sea water fluxes (in $\text{km}^3 \cdot \text{y}^{-1}$) and hydrometeorological parameters (non-dimensional) as estimated from various sources.

	$Q_c^P - Q_c^E$	Q_o^P	Q_o^E	$R + Q_o^P - Q_o^E$	Q_c^P	Q_c^E	a	b	r
ERA-40	427	116	342	201	1679	1252	0.27	0.07	0.25
GIWA	300	75	375	0	-	-	-	-	0.18
corrected	299	76	374	1	1569	1270	0.30	0.05	0.19

$$Q_o^{E \text{ cor}} = Q_o^{E \text{ obs}} + m(Q_o^{E \text{ ERA}} - Q_o^{E \text{ obs}}), \quad (4.8)$$

$$Q_c^{P \text{ cor}} = \frac{Q_o^{P \text{ cor}}}{b}, \quad (4.9)$$

$$Q_c^{E \text{ cor}} = \frac{Q_o^{E \text{ cor}}}{a}, \quad (4.10)$$

where the index "cor" stays for correction, "obs" for observation and "ERA" for ERA-40 data. Corrected values for the Black Sea and Caspian Sea are given in Table 4.2 and 4.3. During the budget calibration process, parameters a and b are slightly changed (compare first and third lines of Tables 4.2 and 4.3).

In the remainder of this chapter we will either assume that a and b have been valid during the whole period since the LGM, or propose scenarios assuming that they change. Because no homogeneous hydrological time series exists for the whole period from the LGM to present-day, we use data available for some of the most prominent climatic periods since the LGM (see section 4.2.2), and interpolate them linearly to cover the period from 21 ka BP to the present with time steps of 10 years. All results from computations discussed in the remainder of the chapter are reported in calendar years. Radiocarbon years are converted to calendar years with the radiocarbon calibration program Calib Rev5.0.1. [Stuiver and Reimer, 1993].

Present-day Data

The annual mean net water outflow into the Mediterranean computed from observations (BSHMD, [Stanev and Peneva, 2001]) as precipitation minus evaporation at sea surface plus river discharge into the Black Sea ($Q_o^P - Q_o^E + R$) ranges for the period 1923-1997 between $-4\text{km}^3 \cdot \text{y}^{-1}$

Table 4.4: Normalized by the area surface annual mean components of the hydrological cycle (in mm yr^{-1}) for the Black Sea and Caspian Sea catchment areas (based on corrected values of the fluxes). Note that a^n and b^n (index "n" stands for normalized) differ from a and b in Tabl. 4.2 and 4.3 because of normalization.

	R	P_o	E_o	P_c	E_c	a^n	b^n
Black Sea	139	509	802	713	574	1.4	0.7
Caspian Sea	92	191	955	483	391	2.4	0.4

and $441 \text{ km}^3 \cdot \text{y}^{-1}$. Mean $Q_o^P - Q_o^E$ and R for this period are -138 and $336 \text{ km}^3 \cdot \text{y}^{-1}$. The mean value for the river discharge (from BSHMD) distributed regularly over the catchment area corresponds to $Q_c^P - Q_c^E = 139 \text{ mm} \cdot \text{y}^{-1}$.

Comparison of $Q_c^P - Q_c^E$ calculated for the Black and the Caspian Sea watersheds from ERA-40 dataset with estimates based on observations (e. g. Global River Discharge Centre (GRDC) Composite Runoff Fields v 1.0, Fekete et al. [1999], GIWA reports for the Caspian Sea, BSHMD), demonstrates that water budgets in the global reanalyses do not always give correct first order estimates, which is the case for the Caspian Sea (Tables 4.2 and 4.3). Therefore, it is necessary to constrain reanalysis data with observations. The final results normalized by the areas of individual basins/watersheds are given in Table 4.4.

Paleo Data

There are several climate oscillations recognized on the global scale since the LGM. We will quantify the regional hydrological conditions for the most prominent of them: LGM (~ 21 ka BP) when the ice sheets reached their maximum globally; the onset of the Lateglacial (~ 15 ka BP) when the melt-water flux from ice sheets reached its first maximum (melting water peak, MP-1); Allerød (~ 13.4 ka BP); Younger Dryas (~ 12.4 ka BP), cold stadial and return to the glacial condition; Preboreal (~ 11.2 ka BP), warm interstadial; mid Holocene (~ 6 ka BP), also known as a climatic optimum; and the present-day. We compile below the hydrological data from several sources in the geologic literature. These contain mostly information about precipitation over the catchment area or river discharge. Sometimes even information about evaporation is given. However, no paleo-information is available about $P_o - E_o$ over the lakes/sea. Because such data are necessary in order to estimate the water balance of individual seas, we can, in principle, constrain paleo-data with the present-day ratios $R : Q_c^E : Q_c^P$ and reconstruct precipitation minus evaporation ($Q_o^P - Q_o^E$) over the lakes/seas assuming that a and b do not change. This "linear" approach assumes that the change of climatic conditions does not affect the basic correlations between components of water balance.

Table 4.5: Paleoreconstruction of the water balance ($\text{mm} \cdot \text{y}^{-1}$), used as a base to construct forcing functions in various experiments.

PALEO	Black Sea		Caspian Sea	
	R	$P - E$	R	$P - E$
Present	139	-293	92	-764
mid Holocene	189	-399	142	-1144
Preboreal	134	-283	89	-720
YD	110	-231	65	-523
Allerød	144	-303	99	-798
Lateglacial	279	-588	184	-1484
LGM	51	-108	6	-52

1. Cheddadi et al. [1997] reconstructed climate conditions in Europe during the mid Holocene (6 ka BP) using modern pollen analogue technique constrained with lake level data. His estimates suggest that 6 ka BP $P - E$ in NW Europe including the Alps was $50\text{-}250 \text{ mm} \cdot \text{y}^{-1}$ less than the present-day one (drier conditions), while in eastern Europe and western Asia $P_c - E_c$ was $50\text{-}200 \text{ mm} \cdot \text{y}^{-1}$ greater (more humid conditions). Based on this evidence we use $P - E$ over the land as a proxy variable for the river discharge. In the computations provided below we assume the low-range ($50 \text{ mm} \cdot \text{y}^{-1}$ more humid conditions) based on analysis of patterns of Cheddadi et al. [1997] in the catchment area of the Black Sea. The same trend is assumed for the Caspian Sea. From the above ratios ($R : Q_c^E : Q_c^P$) for the continental part of the hydrological cycle we estimate E_c and P_c , and then from the correlation between $Q_o^P : Q_c^P$ and $Q_o^E : Q_c^E$, precipitation and evaporation above the sea. Results for the Black Sea and Caspian Sea are summarized in Table 4.5 and Fig 4.3.

2. Velichko et al. [2002] and Klimanov [1997] reconstructed total precipitation over land for the main Lateglacial/Early Holocene climate oscillations in eastern Europe and Siberia. To plot his maps, Klimanov [1997] compiled previous reconstructions available in geological literature with his reconstruction based on the information-statistical method analysis of pollen data. Velichko et al. [2002] performed information-logical analysis of pollen data. According to them, precipitation during the Preboreal, was $\sim 25 \text{ mm} \cdot \text{y}^{-1}$ lower. During the Younger Dryas, precipitation was $150 \text{ mm} \cdot \text{y}^{-1}$ less than present. During the Allerød there was $\sim 25 \text{ mm} \cdot \text{y}^{-1}$ more precipitation than at present. With the help of Eq. 4.2 we can reconstruct river discharge and evaporation. Using Eq. 4.3 and Eq. 4.4 we can compute P_o and E_o above the ocean.

3. Sidorchuk et al. [2003] reconstructed paleo-discharges of the North-Eurasian rivers using the concept of modern analogue channel geomorphology. They estimated that river discharge of Severnaya Dvina, Mezen, Pechora, Volga, and Don during the LGM amounted to twice their present values. Channels and river discharge of these rivers start to decrease at 15 to 14 ka BP to reach their present-day values. Here we reconstruct the data in the same way as in (1).

4. Tarasov et al. [1999] performed a similar reconstruction as Cheddadi et al. [1997], but for another time slice and another region - the LGM for the Former Soviet Union and Mongolia. Besides the region and the time slice, there is a further difference in that the lake level record contains only one site for that region at the LGM, which was not enough to reconstruct $P - E$, but only mean annual precipitation. Their estimate is that precipitation in the main area of our interest was $\sim 450 \text{ mm} \cdot \text{y}^{-1}$ less than at present. Here we reconstruct the data in the same way as in (2).

4.3 Method and Experiments

4.3.1 Water Balance Equations

The traditional water balance equation for a lake is extended here by adding the fluxes due to ice melted runoff (IMR) and outflow/inflow from adjacent lakes (sea). It is assumed that after the lake reaches a critical level (H) the water starts to spill over the outlet into the next lake of cascade or into the neighboring sea. The time rate of change of lake volume W

$$dW/dt = \sum_i Q_i, \quad (4.11)$$

where

$$\sum_i Q_i = (P_o - E_o)A_o + R + IMR + D_u - D_l. \quad (4.12)$$

In the above equations A_o is the lake area, D_u is the discharge from the upper lake into the referent lake, D_l the outflow into the lower lake in the cascade. If the lake level z is below H , then $D_l = 0$ and W could change as a result of imbalance of water fluxes. If $z = H$ then $W = W_{max}$ and $D_l = D_u + (P_o - E_o)A_o + R + IMR$. Note that A_o can vary as a function of lake level (computed using topography maps). Although the possibility of Caspian Sea transgression is not excluded in this model our simulation showed that terrestrial fluxes due to river runoff from Volga drainage area and IMR (computed from Peltier [1994] data as the difference between ice volumes discharged into the catchment area per unit time) cannot compensate for the large deficit in fresh water balance at its surface (evaporation minus precipitation). Therefore, the equilibrium sea level remains below the height of the Manych Pass. In view of the specific balances during the Holocene Eq. 4.12, when applied to the Black Sea reduces to

$$\sum_i Q_i = (P_o - E_o)A_o + R - D_l, \quad (4.13)$$

where D_l is the transport through the Bosphorus Straits.

4.3.2 Experimental Design

We perform several experiments in order to estimate the Black Sea level variations since the LGM. The experiments can be divided into two groups depending on the assumptions which we make for the climate parameters a and b : (1) with a and b (or their normalized analogues a^n and b^n , see Table 4.4) corresponding to the present-day land-sea contrasts, and (2) with modified a and b . With (1) we assume that the climate in the individual zones was "similar" to the present-day climate. The second group of experiments can be easier explained considering the difference between a^n and b^n in the Black Sea and Caspian Sea area (Table 4.4). Larger a^n in the Caspian Sea area reveals larger contrast between land and sea evaporation compared to the Black Sea. Larger b^n in the Black Sea area is mostly due to larger (compared to the Caspian Sea) precipitation over the sea. It is obvious that these parameters characterize the Caspian Sea area as much drier. One could then expect that possible changes of the Black Sea climate towards drier conditions (as postulated by many researchers, see Section 4.2.2) could be roughly represented as a trend of the Black Sea a^n and b^n towards the Caspian Sea values. The latter is exemplified in Table 4.6 where the first line corresponds to the present-day Black Sea conditions, and the last line assumes that the Black Sea exhibits as dry conditions as the present-day Caspian Sea. In other words, we assume that the Black Sea climate (expressed by indices a and b) could vary between two extreme states: that of the present-day Black Sea, and that of the present-day Caspian Sea. One way to quantify such changes would be to assume that the climate indices a and b are not stable. This is shown in the $a - b$ phase diagram (Fig. 4.4), where the present-day climatic situations of the two neighboring basins are presented by the empty square and circle. Because the Caspian Sea is enclosed any shift of its state (if the runoff factor does not change) follows the sloped line ($r = 0.19$, Eq. 4.4). Unlike the simpler case of the Caspian Sea, the climatic evolution of the Black Sea level is controlled by the strait transport (D_l , Eqs. 4.12 or 4.13), which is unknown and complicates identifying the transition of climate between sea and lake state. Therefore, we will not attempt to provide here the true values of a and b , but rather (by carrying out sensitivity experiments) computing them using the following "quasi-linear" concept. Only when computing a and b we suppose that during the driest period the values of evaporation and precipitation (in $mm \cdot y^{-1}$) in the Black Sea equal the present-day Caspian Sea ones. Thus the Caspian Sea values integrated over the Black Sea and its watershed are used to compute the extreme indices a and b (during the driest period). The state of the sea corresponding to the extreme a and b indices is represented by the crossed-square. It is also supposed that the values of indices during all times can be computed by linear interpolation between the present-day ones and the "driest" ones. In this way, we postulate one possible evolution scenario presented in Fig. 4.4 by the dashed line.

The $r = const$ lines give the states under which sea level in enclosed basins does not change. This follows from Eqs. 4.5 and 4.4. Under the assumptions above ($D_u = D_l = IMR = 0$) the

Table 4.6: Values of a^n and b^n used in sensitivity (SENSO-1) experiments to modify present-day horizontal distribution of hydrological components in the Black Sea basin and watersheds in order to estimate response of the sea level. Values in the first row ("wet condition") correspond to the present-day situation in the Black Sea catchment area and values in the last row ("dry condition") correspond to the present-day situation in the Caspian Sea catchment area. Other values are linearly interpolated. We assume that during the dry periods Black Sea hydrological regime tends to the present-day Caspian Sea hydrological regime.

SENSO	a^n	b^n
Black Sea 1	1.4000	0.7000
Black Sea 2	1.6500	0.6250
Black Sea 3	1.9000	0.5550
Black Sea 4	2.1500	0.4750
Black Sea 5	2.2750	0.4375
Black Sea 6	2.4000	0.4000

former equations together with Eqs. 4.11 and 4.13 lead to $\frac{dW}{dt} = 0$, that is, sea level is constant. The fastest transition from enclosed basin to estuarine-type basin is along the normal to $r = \text{const}$ lines, thus the one corresponding to the dashed line is close to that state. It is certainly true that the real situation of changing climatic patterns is much more complex (involving multiple non-linear mechanisms), and the above considerations should therefore be regarded as a very coarse approach to reconstructing poorly known (documented) past climate changes.

4.3.3 Results

We perform two control simulations (CTRL-1 and CTRL-2). In CTRL-1, forcing functions (water fluxes) are kept constant throughout the whole period (Table 4.4 and first row of Table 4.5). In CTRL-2, forcing functions are constructed from data presented in Section 4.2.2 (Table 4.5). Standard depth of the sill in our computations is -40 m. Both CTRL simulations show that the Black Sea has a positive water balance if the basic climatic parameters a and b do not change. Therefore its level stays at the sill depth during the time when the Mediterranean (global) sea level was lower. This situation does not accomodate a catastrophic flood at the time of the reconnection with the Mediterranean.

Several sensitivity (SENSO) experiments have been carried out aiming to answer the question: how much should the basic meteorological and hydrological conditions in the Black Sea catchment area change for the Black Sea level to decrease below the sill depth? As mentioned earlier, a low-stand of sea level could make the catastrophic scenario of reconnection plausible. Changes in meteorological and hydrological conditions are described by changes in a and b (not only large-scale evaporation and precipitation, but also land-sea contrasts).

We carry out two sets of sensitivity (SENSO) experiments. In the first one (SENSO-1) present-

day water fluxes are modified using combinations of constant a^n and b^n (Table 4.6). Using the Black Sea topography enables us to compute the evolution of the Black Sea level starting from the sill depth at 21 ka BP. The sea level stays at the sill depth (outflow to the Mediterranean) for the first three pairs of values of a^n and b^n in Table 4.6 (see Fig. 4.5). Only after the indices change so that $a^n > 2.15$ and $b^n < 0.47$ (see also the first row of Table 4.5, which gives the present-day values) the sea level starts to drop below the sill depth. An increase in evaporation and a decrease in precipitation above the sea of ~ 1.625 and ~ 1.6 times, correspondingly, results in a drop of the Black Sea level to ~ 70 m below the present-day sea level (Fig. 4.5). In order to achieve a sea-level drop of 140 m, as speculated in some studies, the increase of evaporation and decrease of precipitation has to be 1.7 times the present-day values, that is the dryness conditions in the present-day Caspian Sea.

Using the "quasi-linear" approach described in Section 3.2 we carry out two SENS0-2 experiments, in which the transition of the Black Sea between the present and lake-state follows the dashed line in Fig. 4.4. In the first experiment (light blue line in Fig. 4.5) we use present-day forcing modified by variable a^n and b^n (Fig. 4.6).

In the second one (magenta line in Fig. 4.5) the paleo-reconstructed forcing is modified as described above with variable a^n and b^n (Fig. 4.6). It is noteworthy that in the two SENS0-2 experiments the concept about a^n and b^n is the same, that is we suppose the same general change in the climate. In one of the experiments, this change modulates the present-day precipitation and evaporation, in the second one, it modulates the precipitation and evaporation constructed from proxy data. The latter does not well resolve the land-ocean contrasts.

The evolution of sea level (under enhanced contrast in climate) reveals two lows, one during the LGM and another one of ~ 104 m at about 11520 yr BP. The structure of the improved paleo-forcing (constructed using the concept of variable a and b) is very important, as demonstrated by the comparison between CTRL-2 and SENS0 experiments. The Black Sea level returns to sill depth (~ 40 m in our standard experiment) at about 8.8 ka BP, that is about the time of "catastrophic flood" as specified by Ryan et al. [2003] (8.4 uncalibrated ka BP is between 9 and 8.7 calendar ka BP when calibrated according to marine04.14 calibration curve [Hughen et al., 2004] with Calib software [Stuiver and Reimer, 1993]).

We recognise that the data used in the above computations have a very low temporal resolution. Furthermore, the possible time of reconnection with the Mediterranean depends on how we specify the sill depth (Fig. 4.7), therefore, we performed additional computations with various sill depths (40 m, 30 m, 20 m). Observed sea level rise for various sites according to Fairbanks [1989] and Tushingham and Peltier [1993] is also given in Fig. 4.7 (all data are plotted in calendar years).

Figure 4.8 shows the transport through the Bosphorus Straits for the CTRL-2 and SENSO-2 experiments. Maximal transport appears at 15 ka BP for all experiments with reconstructed paleo-forcing (CTRL-2: present-day a^n and b^n , and SENSO-2 paleo: variable a^n and b^n as given in Fig. 4.6), reaching a highest value of about $450 \text{ km}^3 \cdot \text{y}^{-1}$. This presents an about two-fold increase compared to the present-day situation (compare black and blue lines in Fig. 4.8 (outflow for reconstructed paleo-forcing) with red line (SENSO-2), which is outflow for the present-day forcing modulated by variables a^n and b^n).

One could ask the question about how accurate the estimates for sea level in inland basins can be. Knowing that estimates about precipitation and evaporation are among the most unreliable meteorological parameters, the answer of the above question seems not to be very optimistic. Considering the method presented in this chapter as a linear one, we could expect errors in the estimates of outflow through the straits, which are comparable to the errors in the water budget estimates. One rough example follows from the data presented by Cheddadi et al. [1997]: for 6 ka BP, $P - E$ in NW Europe including the Alps was $50\text{-}250 \text{ mm} \cdot \text{y}^{-1}$ less today, while in eastern Europe and western Asia $P_c - E_c$ was $50\text{-}200 \text{ mm} \cdot \text{y}^{-1}$ greater. Any errors comparable with the magnitude of changed climatic patterns would result in errors in budget (water outflow estimates) about 10 to 50 percent of the present-day values. Nevertheless, there is no place for pessimism here, but rather for motivation to deepen the understanding on the watersheds' hydrological budgets.

4.4 Discussion and Summary

The analysis given here demonstrates one step in bringing together meteorological, hydrological, and oceanographic approaches to address climate change in the last 20 ka. Reconstructions of hydrological changes in the Black Sea catchment area have been carried out using present-day data, paleo-observations, and theoretical considerations about hydrometeorological conditions of watersheds. The theory accounts in a very simple way for the changing land-sea contrasts in the large-scale evaporation and precipitation patterns. Water-budget analysis agrees quantitatively with some available geological observations.

According to Ryan et al. [2003] the low stand (105 m) of the Black Sea appeared between 13.4 and 11 ka BP. In our scenarios with enhanced aridity, a lowstand of 104 m is simulated at 11.5 ka BP, but our computations fail to identify the second low stand (-85 m) in this period (8.5 ka BP) suggested by those authors. In our simulations, the Black Sea reaches its outlet at 7.4, 8.2 or 8.8 ka BP depending on the sill depth (20, 30 and 40 m, respectively). According to various data sources [e.g. Fairbanks, 1989, Tushingham and Peltier, 1993], the Mediterranean sea level would have reached -40 m around 10.6 (Barbados), 9.5 (Gulf of Messenia) and 8.9

(Roussillon) ka BP. At those times, the Black Sea was 84, 51 and 41 m below the present-day sea level. For the sill depth at 30 m below the present-day sea level, Mediterranean sea water should have spilled into the Black Sea at 10.3 ka BP (Barbados) but for the observed sea-level rise at the Messenia and Roussillon sites reconnection would be more likely gradual because the two basins reached the sill level at about the same time, 8.2 ka BP. This scenario (sea level described by the observations in the Messenia and Roussillon sites) seems to be rather in agreement with statistical analysis of dinoflagellate cyst assemblages [Mudie et al., 2004] which does not support the idea of the sudden (shorter than 500-yr) flooding of the Black Sea. Obviously, more precise data would be needed to argue about the timing and nature of the Black Sea-Mediterranean connections. We recall that small changes in dryness could change the above conclusions.

The major results can be summarized as follows. Qualitatively both SENSO-2 (present and paleo) experiments give very similar results. Comparing sea levels for both simulations (Fig. 4.5) reveals that both minima appear at about the same time, the second minimum (Younger Dryas) having almost the same magnitude in the two experiments. The differences at the LGM between two experiments are probably due to uncertainties in initial conditions.

The qualitative agreement between both experiments and the support found in some observations give credibility of theoretical reconstruction, which replicates the major climatological oscillations since the LGM. The sensitivity experiments demonstrated that climatic conditions in the Black Sea area should significantly change in order to result in a descent of sea level of ~ 140 m below the present-day sea level. Such a transition could be possible only if *the decrease of precipitation and increase evaporation above the sea amount to at least ~ 1.7 times the present values*. Comparing this result with present-day observations (Fig. 5 of Stanev and Peneva [2001]) we see that the fresh water balance undergoes interannual changes with amplitudes larger than $10^2 km^3 \cdot y^{-1}$, which is more than half of the mean fresh water flux. Extremely high deviations from the mean of $\sim 2 \times 10^2 km^3 \cdot y^{-1}$ are observed during 1941 and 1981, however, these anomalous events had durations of several years only. Knowing that the hydrological conditions have changed in the past we cannot exclude a possibility of the low stand of the Black Sea level at the time of reconnection with the Mediterranean (note that ocean curves in Fig. 4.7 are above the Black Sea ones between 11 and 7 ka BP). Obviously, deeper and more accurate analyses are needed to answer the question about the paleo-evolution of the Black Sea level. We expect that new, well-dated geological measurements in this area will help to further constrain changes in the water budgets [Bahr et al., 2005].

4.5 Figures

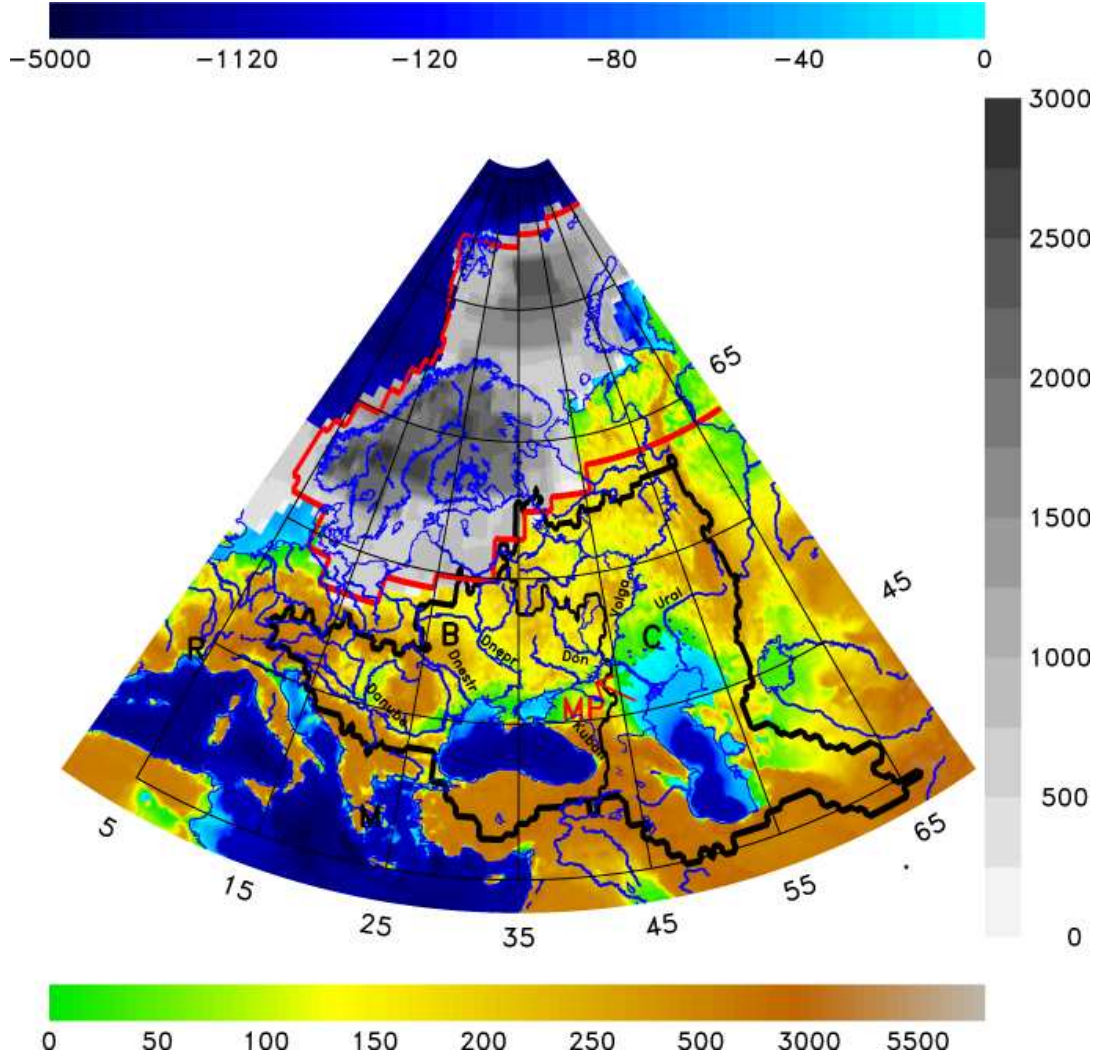


Figure 4.1: Orography, bathymetry, major rivers in the Black (B) and Caspian (C) Sea catchment areas and topography of the Eurasian ice sheet (EIS) at the LGM according to Peltier [2004]. Red line is Eurasian ice sheet margin at the LGM according to Peltier [1994]. EIS margin from Peltier [2004] is in good agreement with the LGM ice margin reconstructed by the QUEEN project [Svendsen et al., 2004, Siegert and Dowdeswell, 2004]. MP and the red arrow indicate the location of Manych Pass, 26 m ASL. R indicates Roussillon (42.7N, 3.1E) and M indicates Gulf of Messenia (37N, 22E), sites with paleo-observations of the Mediterranean sea level.

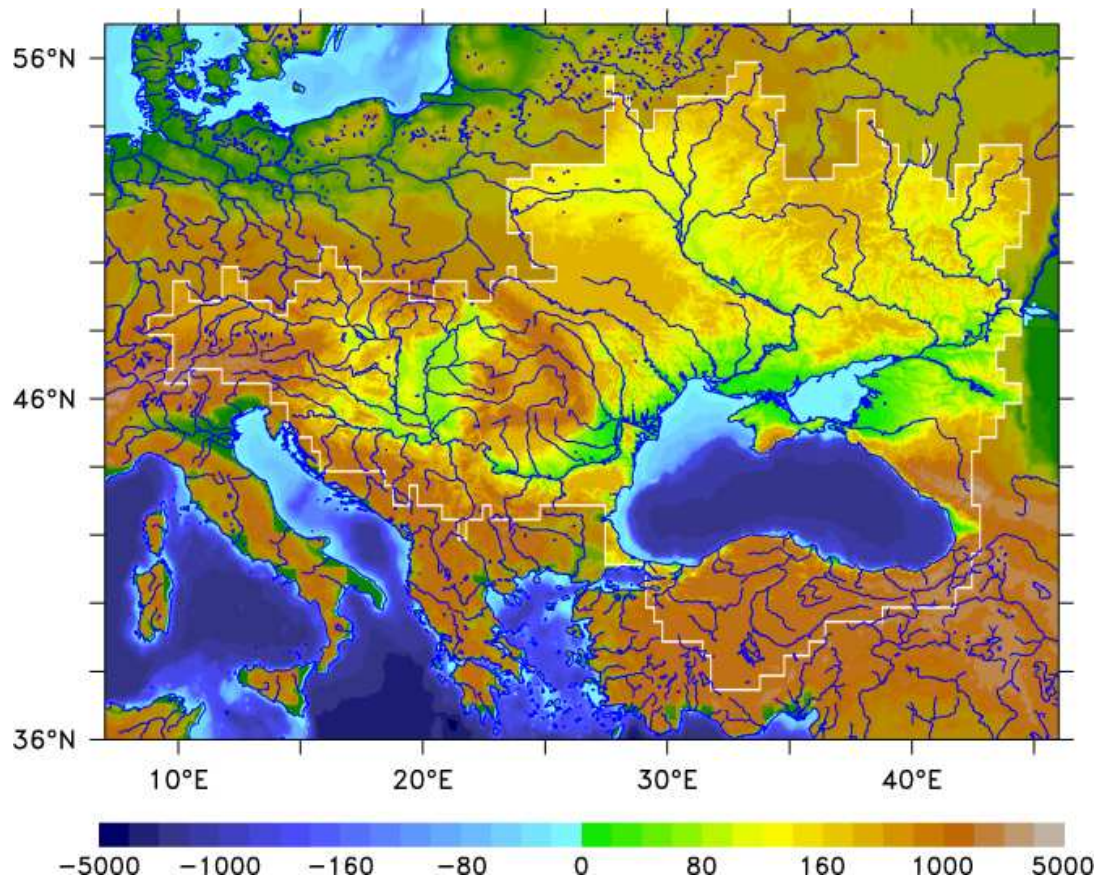


Figure 4.2: Orography, bathymetry and rivers of the Black Sea catchment area (lighter area). This map is used to calculate water fluxes in the Black Sea catchment area. Note that the color key applies only for the lighter area.

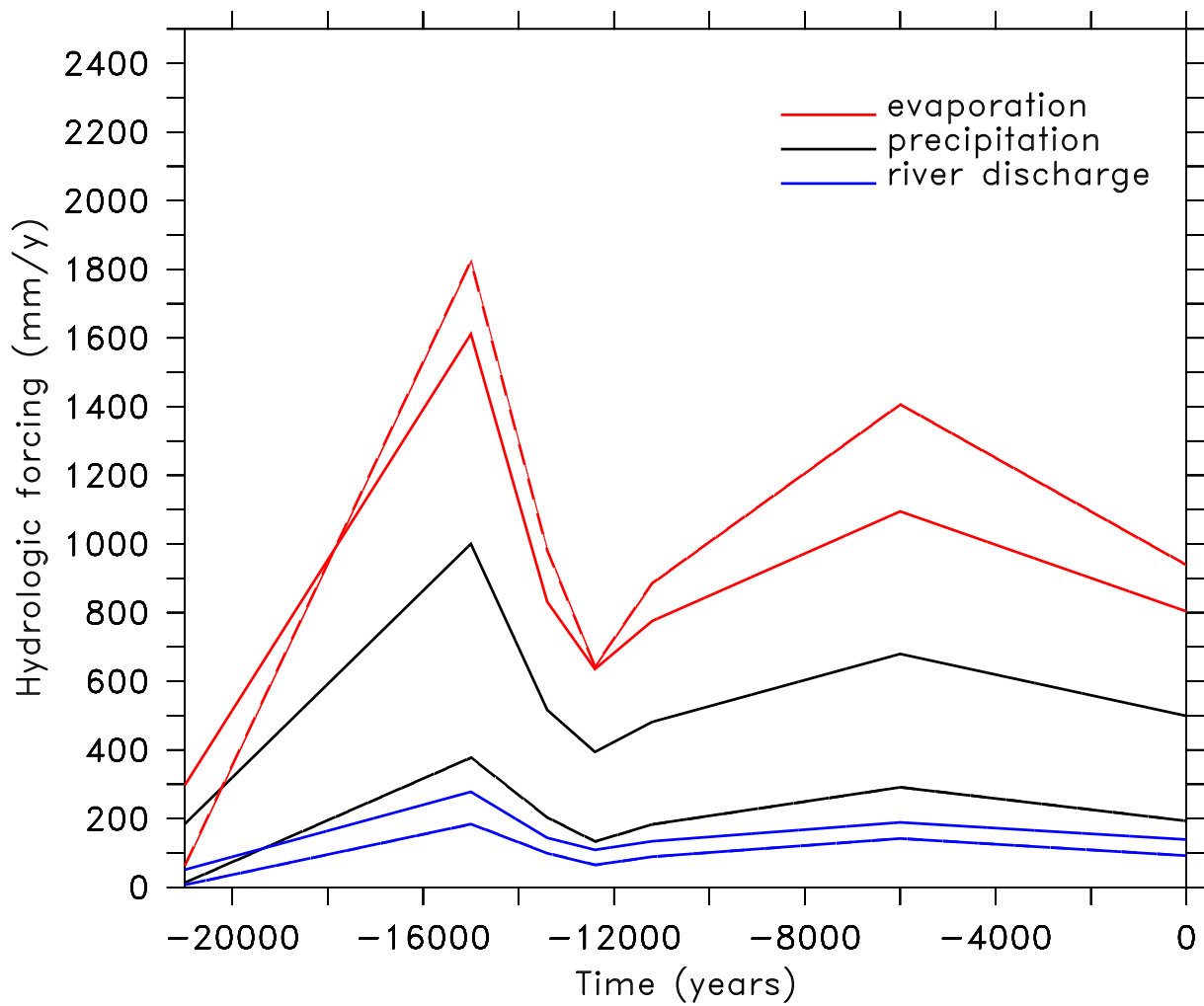


Figure 4.3: River discharge, precipitation, and evaporation in the Black and Caspian Sea as reconstructed in section 2.2.4. Full lines are for the Black Sea and dashed lines are for the Caspian Sea

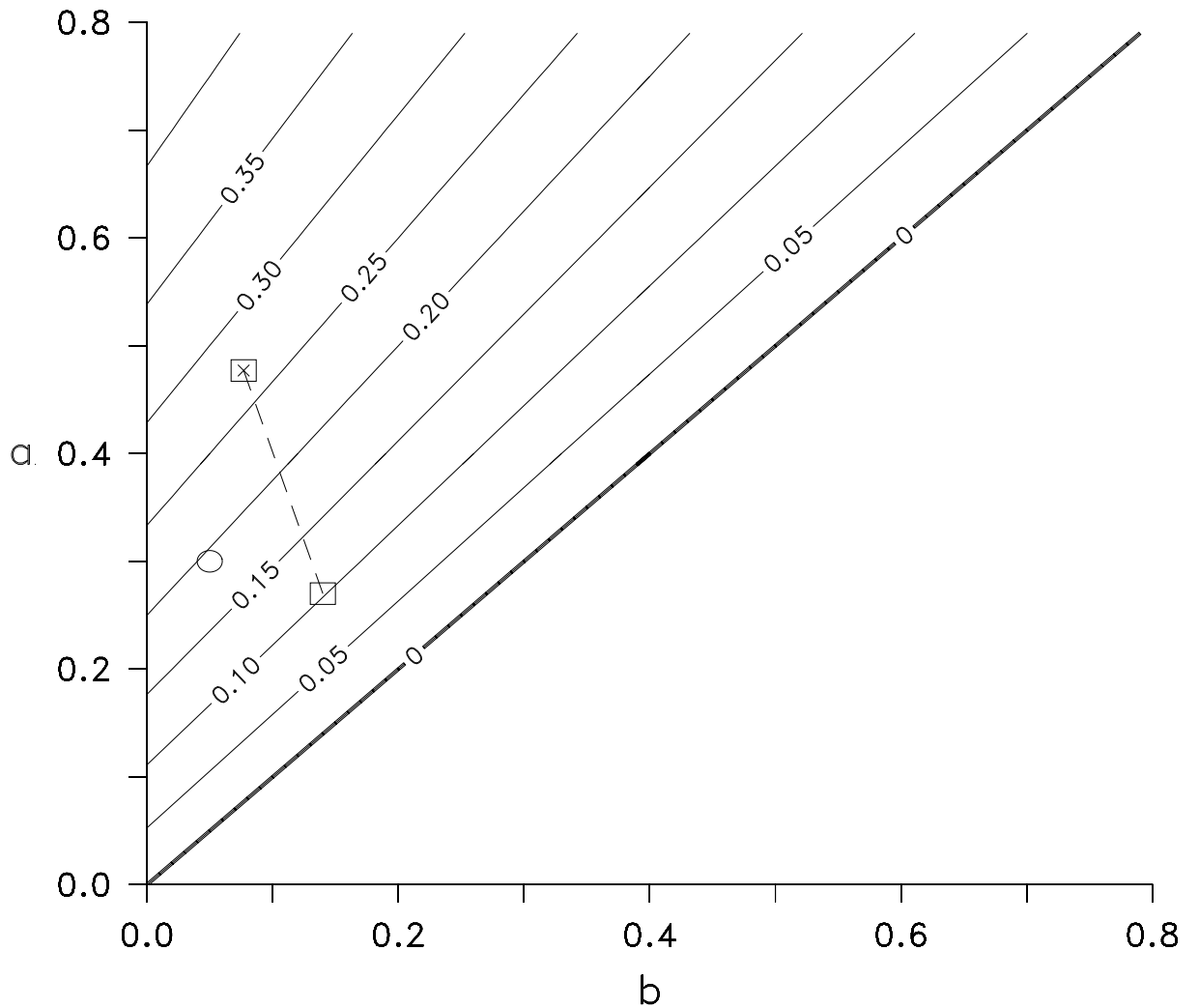


Figure 4.4: Phase diagram of climatic indices. This diagram gives an idea about the possible evolution of climates in the Black Sea and Caspian Sea area. The empty circle and square display the present-day states of Caspian and Black Sea, the crossed square gives the extreme Black Sea state that corresponds to the present-day state of Caspian Sea. Note that we show here indices which are not normalized. The full lines display runoff factor r computed from Eq. 4.4.

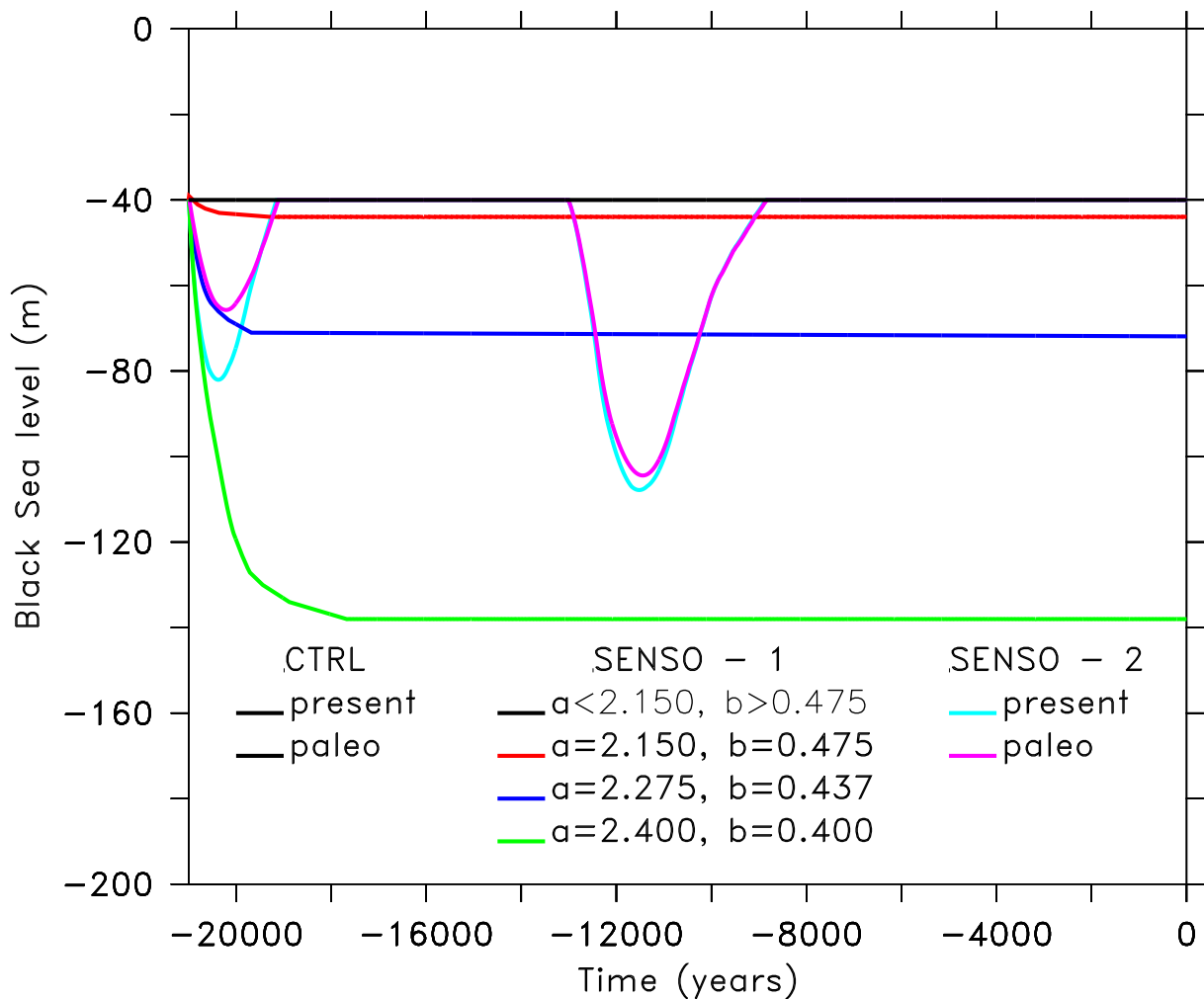


Figure 4.5: Black Sea level. The black, red, blue and green lines are results of the SENSO-1 set of experiments. The black line is valid also for both CTRL experiments. For CTRL and SENSO-1 experiments hydrological parameters a^n and b^n are constant throughout the whole period as given in Table 4.6. The light blue and magenta line represent results from the SENSO-2 experiments. In the latter experiment hydrological parameters a^n and b^n change in time (Fig. 4.6) to distinguish dry (LGM, Younger Dryas) and wet (onset of Lateglacial, Holocene to present transition) periods. The black line corresponds to the case with a^n and b^n taken from the first three rows in Table 4.6, the red, green, and blue lines correspond to the cases with a^n and b^n taken from the fourth, fifth, and sixth row in Table 4.6. The light blue line is for the present-day forcing modified by variable a^n and b^n (SENSO-2 present), the magenta line is for the paleo-reconstructed forcing modified by variable a^n and b^n (SENSO-2 paleo). First minimum in SENSO-2 experiments is shallower than the second one (unlike in some other paleo reconstructions) because the integration is initiated from -40m .

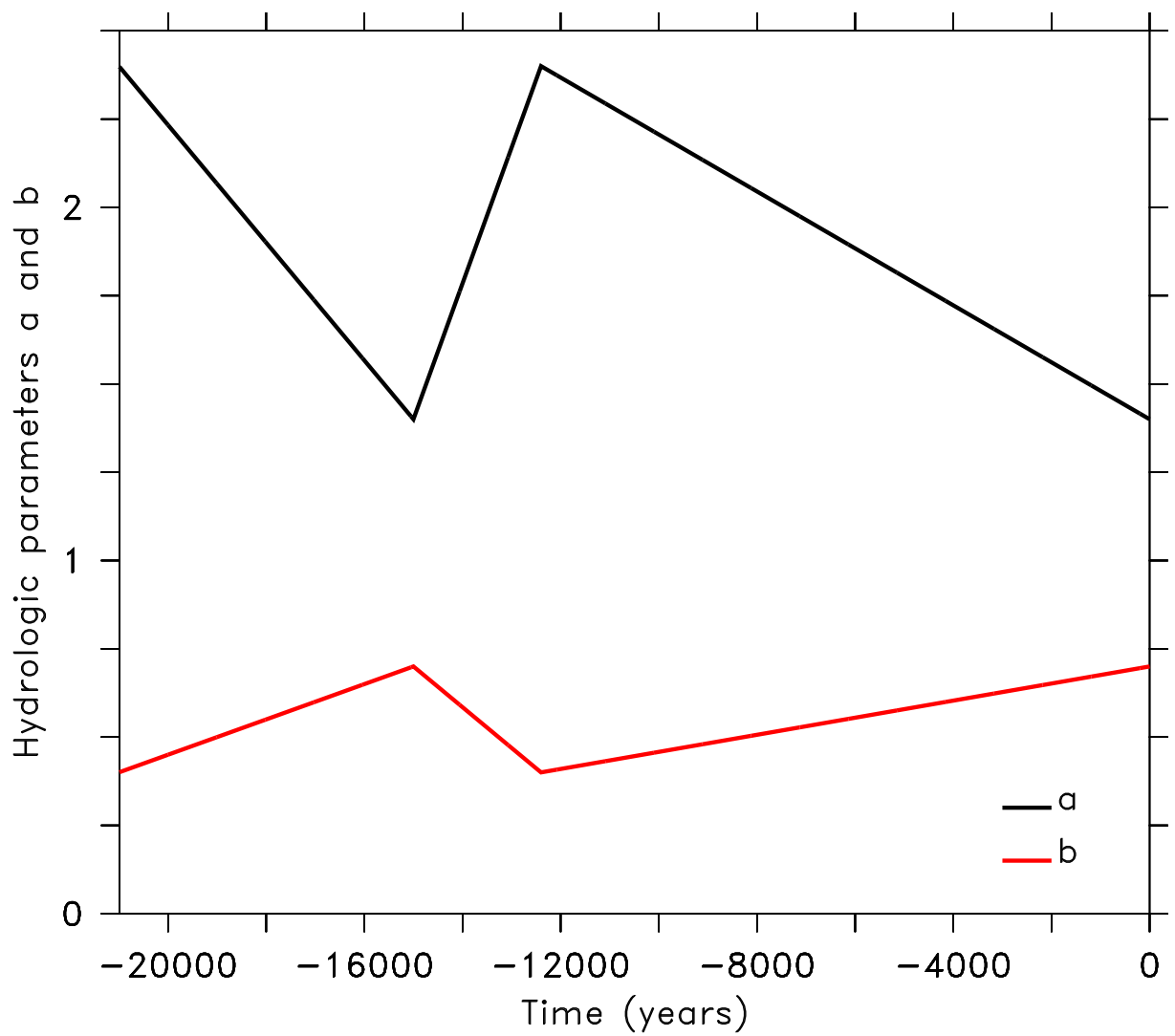


Figure 4.6: Variations of the hydrological parameters in the Black Sea catchment area. Dry conditions (large a^n , small b^n) correspond to LGM (21 ka BP) and Younger Dryas (13.4 ka BP), while wet (small a , large b) conditions correspond to onset of Lateglacial (15 ka BP) and to present-day.

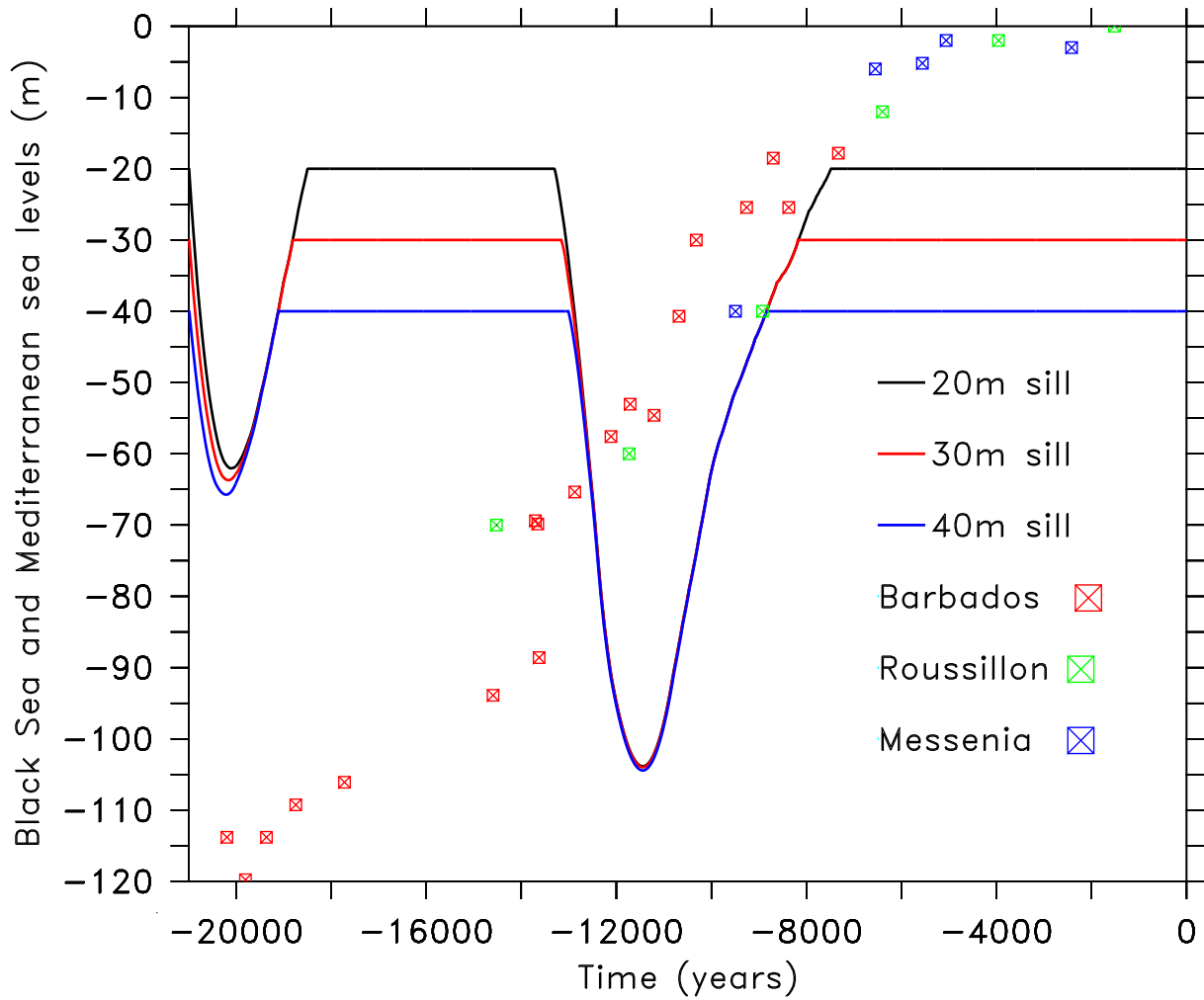


Figure 4.7: Black Sea level for various sill depths. Green rectangles represent global sea level rise as reconstructed by Fairbanks [1989] at Barbados. Red and blue rectangles represent sea level rise as reconstructed by Tushingham and Peltier [1993] at Roussillon (42.7N, 3.1E) and Gulf of Messenia (37N, 22E), respectively. See Fig. 4.1 for the location of two sites in the Mediterranean.

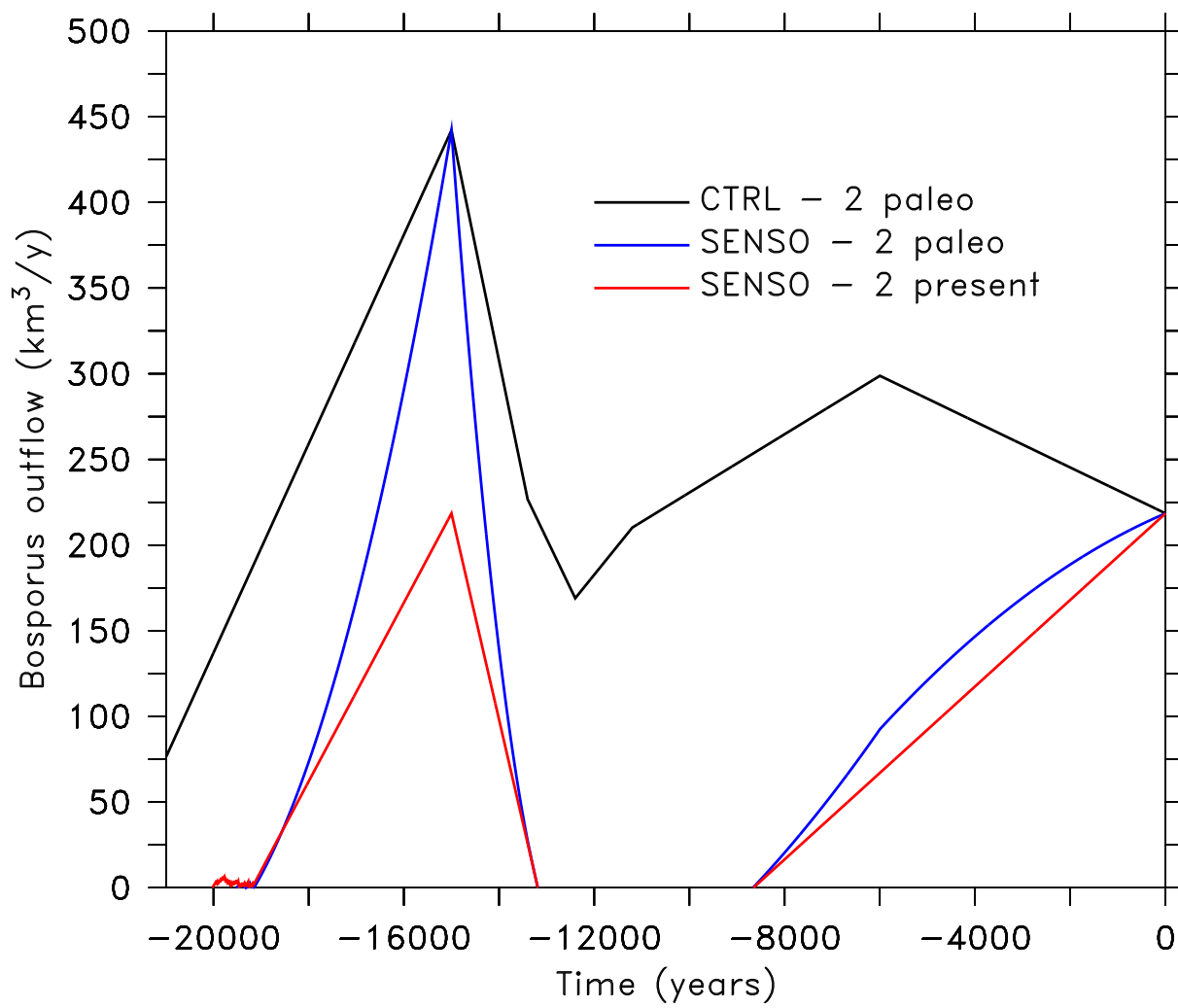


Figure 4.8: Outflow through the Bosphorus Strait for the CTRL - 2 and SENSO - 2 experiments.

Chapter 5

Black Sea level sensitivity to the changes of hydrologic cycle¹

Hypsometric and water budget analysis of the Black Sea basin is performed with topographic (ETOPO2) and hydrological (ERA-40 corrected with observation) data. According to a simple theoretical consideration one critical parameter controlling the Black Sea level could be the ratio between the continental and maritime area in the catchment area. Several idealized cases and two cases inferred from observations have been studied in order to investigate the sensitivity of the Black Sea level to the changes of components of the hydrological cycle. Our study indicates that it is possible to have the Black Sea level drop down for about 150 m in 1000 – 2000 years if precipitation decreases slightly more than evaporation. Furthermore, the sea level is more responsive to changes of continental components of hydrologic cycle (i.e. river discharge) than to changes of maritime exchange of water fluxes.

5.1 Introduction

Geological observations reveal that throughout the past two million years the Black Sea has predominantly been a freshwater lake interrupted only briefly by saltwater invasions coincident with a global sea level high-stand [Ryan et al., 2003]. Detached from the global sea and neglecting changes of the Black Sea catchment area due to the extension of the Eurasian ice sheet we can assume that changes of the Black Sea level depends only on the changes of the hydrological regime in the Black Sea catchment area. According to available observations [Mangerud et al., 2004, Svendsen et al., 2004], this is true at least since the Lateglacial inception (about 15 ka BP)

¹The manuscript based on this chapter is submitted for publication with the special issue of Quaternary International

to the possible time of the last reconnection of the Black Sea with the Mediterranean (about 8 ka BP). In our recent manuscript [Georgievski and Stanev, 2006], we provide a sensitivity study of the Black Sea level changes to the changes of the hydrological condition on the continental part of the Black Sea catchment area. Hydrological conditions were constrained with available paleo-observation [Tarasov et al., 1999, Sidorchuk et al., 2003, Klimanov, 1997, Velichko et al., 2002, Cheddadi et al., 1997]. Precipitation and evaporation above the Black Sea during that period (~ 15 –8 ka BP) remain unknown, therefore, for our sensitivity study, we assumed that the Black Sea level oscillations were driven by changes of the hydrological cycle above the sea only (increase of evaporation and decrease of precipitation during the cold period, and increase of precipitation and decrease of evaporation during the warm period). Since geological observations have low temporal (and spatial) resolution, and they are not available for all hydrological parameters, we are motivated to investigate sensitivity of the Black Sea level to the change of each of them i.e. maritime and continental precipitation (P_m, P_c) and evaporation (E_m, E_c). Simulation with EMIC described in chapter 2 motivate us to qualitatively estimate relation between continental and maritime hydrological cycle and their impact on the Black Sea water balance.

In the next section, we provide brief theoretical consideration about the sea level. In section 5.3 description of the data and methodology are provided. Results are described in section 5.4, followed by the discussion in section 5.5.

5.2 Theoretical consideration

We can get general ideas about the governing parameters for the sea level change, if we consider the rate of the change of sea level ($d\zeta/dt$) against the hydrological components (P_c, P_m, E_c, E_m):

$$d\zeta/dt = (P_m \cdot A_m/A_m - E_m \cdot A_m/A_m) + (P_c \cdot A_c/A_m - E_c \cdot A_c/A_m), \quad (5.1)$$

where "A" is area, index "m" is for maritime, and "c" for continental, "P" is for precipitation and "E" for evaporation. Both sides of the equation (5.1) could be divided by $E_c \cdot A_c/A_m$ in order to get a non-dimensional equation:

$$d\zeta^*/dt = \frac{E_m A_m}{E_c A_c} \cdot R_m^* + R_c^*, \quad (5.2)$$

where $R_c^* = P_c/E_c - 1$ is the continental contribution and $R_m^* = P_m/E_m - 1$ is the marine contribution to the non-dimensional relative sea level $\zeta^* = \frac{A_m}{E_c A_c} \cdot \frac{d\zeta}{dt}$. For the Black Sea $R_c^* > 0$ and $R_m^* < 0$. From Eq. 5.2 it becomes clear that for the constant hydrological conditions ($P_c, P_m, E_c, E_m = \text{const.}$) the critical parameter for the Black Sea level is the ratio between the maritime and continental area A_m/A_c .

5.3 Data and methodology

To estimate precipitation and evaporation in the Black Sea catchment area we use the European Center for Medium-range Weather Forecast (ECMWF) Re-analysis (ERA-40, Simmons and Gibson [2000]) data corrected with the present-day observation. The process of optimizing data is described into details in Georgievski and Stanev [2006], and for the purpose of our study we will use results from table 4 in that paper². The area of the basin (continental and maritime part) is calculated from watershed delineation and topographic data as described in Georgievski and Stanev [2006].

According to ETOPO2 data, at present days A_m/A_c is about 0.195, and for the sea levels 50, 100, and 150 m lower than today, it would be 0.151, 0.135 and 0.127, respectively. If we consider enclosed the Black Sea basin with the present-day values for P, E and A, the water balance of the basin would be positive. Thus, resulting in a sea level rise of about $16 \text{ mm} \cdot \text{y}^{-1}$. If we assume that the sea level is 50, 100, and 150 m lower then today, the ratio between maritime and continental contribution would be changed but water balance remains positive, and the sea level would rise 14.3 , 13.4 and $13 \text{ mm} \cdot \text{y}^{-1}$, respectively (Fig. 5.1). Although declining, the water balance remains positive and hydrological components need to be changed in order to result decrease in the sea level. If we assume that these changes are in the limits of their standard deviation for the present-day data calculated from ERA-40 reanalysis, it could, in some case result, in negative water balance. For example, if we assume that precipitation $P_{m,c} = \overline{P_{m,c}} - \sigma_{P_{m,c}}$ (over-line indicates average and σ is standard deviation) and evaporation $E_{m,c} = \overline{E_{m,c}} - \sigma_{E_{m,c}}$ are decreased to their lower values, the sea level would fall by $1.8 \text{ mm} \cdot \text{y}^{-1}$ for the present-day sea-land ratio (S0 line on the Fig. 5.1) but it would still rise by 0.7, 1.3 and $1.5 \text{ mm} \cdot \text{y}^{-1}$, respectively for the sea level at -50, -100, -150 m isobaths. However, if we assume that precipitation is decreased and evaporation increased for their respective standard deviation, it would result in an univocal sea level decrease, by 42.1, 29, 24.7, $22.8 \text{ mm} \cdot \text{y}^{-1}$. If we assume the case inferred from geological evidence, that is $150 \text{ mm} \cdot \text{y}^{-1}$ less precipitation and assuming that evaporation remains at the same value, sea level would drop down 19, 11.8, 9.6 and $8.6 \text{ mm} \cdot \text{y}^{-1}$ depending on the sea land distribution. Assuming that there was $450 \text{ mm} \cdot \text{y}^{-1}$ less precipitation, the sea level would decrease at the following rates: 89.2, 63.9, 55.5 and $51.7 \text{ mm} \cdot \text{y}^{-1}$ for initial levels 0, 50, 100, and 150 m below level of the present-day.

From the analysis presented above, we can conclude that there are certain hydrological conditions not so far from the observed one, even at the present-day, that could result with negative water balance on the annual time scale. However, what remains unknown is for how long should such a condition last to result in a significant sea level decrease. That issue would be considered in the chapter 6.

²Refer to Chapter 4 and Table 4.4 in this thesis

In order to test the sensitivity of the Black Sea level to the changes of the hydrologic cycle the same water balance equation for the closed basin as in Georgievski and Stanev [2006] is used. The time rate of change of the lake volume W

$$dW/dt = (P_m - E_m)A_m + R - D_l, \quad (5.3)$$

where $(P_m - E_m)A_m$ presents maritime components of the hydrologic cycle, i.e. *precipitation – evaporation* above the Black Sea (index m is for maritime); R is river discharge or the continental part of the hydrologic cycle, i.e. *precipitation – evaporation* above the continental part of the Black Sea catchment area; D_l is the transport through the Bosphorus Straits.

Our aim is to estimate how much should each component of the hydrological cycle in the Black Sea catchment area change in order to have a drop down of the Black Sea level about 100 m below the present day sea level as inferred by geological observation [Ryan et al., 2003]. In order that the sea level drops down precipitation should be decreased and evaporation increased, or what is more likely, precipitation has to be decreased slightly more than the decrease of evaporation. First, we investigate theoretical cases if only one of the components changes. That is, we will decrease only maritime or continental precipitation and increase evaporation (Table 5.1).

Table 5.1: Idealized experiment in which only one component of the hydrological cycle changes. All values are in $mm \cdot y^{-1}$. Signs “–”, “+”, “0”, indicate direction of change where “–” indicate decrease, “+” increase and “0” no changes of the hydrological parameter.

	maritime		continental	
	P_m	E_m	P_c	E_c
present day	509	$802 \text{ mm} \cdot y^{-1}$	713	574
P_m	–	0	0	0
P_c	0	+	0	0
E_m	0	0	–	0
E_c	0	0	0	+

Second, there is a possibility that the precipitation above sea and land decreases, but evaporation remains the same, or precipitation remains the same, but the evaporation above sea and land increases (Table 5.2).

The former case is suggested by Tarasov et al. [1999] for the Last glacial maximum (LGM). According to them at the LGM, there were 450 to $750 \text{ mm} \cdot y^{-1}$ less precipitation at several sites in the continental part of the Black Sea catchment area, while the drought index suggests similar or slightly wetter conditions compared to today. Furthermore, they suggest that for the regional water balance decreased precipitation was less important than decreased evaporation due to lower-than-present temperature. However, Ryan et al. [2003] suggest that a cold climate

Table 5.2: Experiments in which only maritime or continental components of the hydrological cycle changes for the same rate. All values are in $\text{mm} \cdot \text{y}^{-1}$. "–" indicate decrease, "+" increase and "0" no changes of the hydrological parameter.

	maritime		continental	
	P_m	E_m	P_c	E_c
present day	509	802	713	574
P_m, P_c	–	0	–	0
E_m, E_c	0	+	0	+
P_m, P_c and E_m, E_c	–	+	–	+

mode corresponded with an expanded lake and a warm climate mode with a shrunken lake. According to them, the Black Sea oscillations are mostly driven by an increase of evaporation during the warm period which predominate the increase of precipitation. However, none of aforementioned authors makes clear the distinction between the continental and the maritime part of the hydrological cycle. According to the simple theoretical consideration in section 5.2 water balance should be sensitive to the changes of the continental and maritime area. According to our sensitivity study [Georgievski and Stanev, 2006] and our results with the Planet Simulator (refer to Chapter 2), maritime and continental components of the hydrologic cycle should change non-linearly or quasi-linearly as a response to the change of the sea-land distributions. Therefore, in the third set of experiments, we are investigating cases when parameters of the hydrological cycle change non-linearly, i.e. evaporation is decreased slightly less than precipitation.

A similar approach is applied for available observations. Using available reconstructions of precipitation for the LGM [Tarasov et al., 1999] and Younger Dryas [Klimanov, 1997, Velichko et al., 2002] we have estimated how much should evaporation change in order to draw down the sea level to the observed value.

5.4 Results

Several sensitivity experiments are performed in order to test the response of the Black Sea level to changes of only one component of the hydrological cycle (Table 5.1 and Fig. 5.2). Considering precipitation only (Fig. 5.2(a) and 5.2(b)), it turns out that for the Black Sea level changes of continental fresh water fluxes are more important than the maritime ones. Fig. 5.2(a) indicates that even in the limiting case of very small maritime precipitation ($P_m \rightarrow 0$), if all other components remain the same, the Black Sea level drops down for 22–23 m and remains stable at that level. In the limiting case when $P_c \rightarrow E_c$, i.e. $R = 0$, the Black Sea disappears in about 7000 years ($0.805 \times P_c$ line on the Fig. 5.2(b) shows that the sea level drops down about 1000 m in

about 3500 years, it will take another 3500 years to dry out the Black Sea). It is also interesting to note that if P_c decreases by only 15% i.e. $107 \text{ mm} \cdot \text{y}^{-1}$, it will take about 2500 years to draw down the sea level to 150 m below the present day level ($0.85 \times P_c$ line on the Fig. 5.2(b)). Considering evaporation above the sea (E_m) similar results turn out for the double increase of E_m , i.e. the Black Sea drops down in 2000 years to -150 m ($2 \times E_m$ line on the Fig. 5.2(c)). For the increase of the continental evaporation (E_c) of $1.175 \times$ more than present-day E_c , the Black Sea level drops down 100 m below the present day level in 3500 years. In the limiting case $E_c \rightarrow P_c$, i.e. $R = 0$ same as before, the Black Sea disappears in 7000 years (compare $0.805 \times P_c$ line on Fig. 5.2(b) and $(1.242 \times E_c)$ line on Fig. 5.2(d). Considering the individual change of maritime and continental components of the hydrologic cycle one can conclude that the Black Sea level would have a more significant response to the changes of continental components i.e. river discharge than to the maritime components. Furthermore, considering only maritime components it turns out that changes of precipitation are negligible for the sea level compared to maritime evaporation. This is in accordance with Ryan et al. [2003] which claim that the Black Sea drop down is driven by evaporation. For the continental components the rate of change (increase of evaporation and decrease of precipitation) has a similar response of the Black Sea level. For example, one combination to achieve no-runoff conditions is the following: E_c has to be increased 24.2% and P_c has to be decreased 19.5%.

Fig. 5.3 (and Table 5.2) indicate cases when we test decrease of precipitation (P) and increase of evaporation (E). Fig. 5.3(a) is the case when P_m and P_c change for the same rate and evaporation remains the same. Fig. 5.3(b) is the case when E_m and E_c change by the same rate and P remains the same. Fig. 5.3(c) when (P) is decreased and (E) increased. Similarity of 5.3 with 5.2(b) and 5.2(d) indicates that continental (P_c and E_c) components of the hydrological cycle have a predominant role on the Black Sea level. However, changes of maritime components (P_m and E_m) amplify, i.e. speed up the process of decreasing the sea level. For the cases of no-runoff ($0.805 \times P$ line on the Fig. 5.3(a) and $1.242 \times E$ line on the Fig. 5.3(b)) Black Sea dries out in about 4000 and 5000 years, respectively. The latter is also the case when both (P) and (E) change (Fig. 5.3(c)). Comparing the results from Figs. 5.2 and 5.3, it becomes clear that river discharges play more important role for the Black Sea level than the maritime flux exchange.

Our third set of experiments is designed in accordance to our study with Planet Simulator (see Chapter 2). Results there indicate that changes of topography, sea-land mask and surface characteristic influence the non-linear response of the hydrologic components. For the globe, most of the experiments indicate that evaporation above the sea would increase, while the maritime precipitation would decrease. Exception is the PELT case. For continental components, in all of the experiments, E_c is decreased and P_c too, not only in the TOPO experiment (see Table 2.3 in Chapter 2). However, in the Mediterranean catchment area all experiments except TOPO show univocal decrease of all components of the hydrological cycle (see Table 2.5 in Chapter

2). This is in qualitative agreement with the geological observation for the Last Glacial Maximum (LGM) [Tarasov et al., 1999]. Therefore, here we perform a sensitivity study of the Black Sea Level response to the decrease of hydrologic cycle components. Fig. 5.4 shows three cases of weaker hydrologic cycles, i.e. both precipitation and evaporation are decreased by a certain amount. The former has to be decreased more than the latter in order to have a decrease in the sea level. Fig. 5.4(a) present cases in which precipitation (P) compared to present day is decreased from 35% to 95% and evaporation (E) is decreased from 25% to 94%. It is interesting when precipitation is decreased to 65% of its present-day value. This value is suggested for the East European Plain at Younger Dryas [Velichko et al., 2002]. It turns out that evaporation has to be decreased to 75% of its present-day value in order to have a decrease of the Black Sea level of 150 m in 4000 years. We have also investigated other theoretical cases in order to find out if there is a limiting case for which evaporation and precipitation could be decreased for the same amount to have a decrease in the sea level. It seems that such a case does not exist. P should be decreased more than E to cause a sea level drop down. If they decrease by the same rate, the sea level does not change.

Two interesting results were inferred from the geologic observations. The first case is for the LGM. According to Tarasov et al. [1999], there was $450\text{--}750 \text{ mm} \cdot \text{y}^{-1}$ less precipitation at the several sites around the Black Sea. We take a lower estimate as an average for the whole Black Sea catchment area, i.e. $450 \text{ mm} \cdot \text{y}^{-1}$ less precipitation than today. However, Tarasov et al. [1999] provide only qualitative estimates of evaporation, and it is not easy to interpret drought index. Here, we provide estimate of how much should evaporation decrease in order to make the sea level drop down (Fig. 5.4(b)). Another case is for Younger Dryas. Fig. 5.4(c) is exactly the same as Fig. 5.4(b), although it presents a different period (Younger Dryas) and changes of hydrologic components for different amounts. For example for $450 \text{ mm} \cdot \text{y}^{-1}$ less P and $350 \text{ mm} \cdot \text{y}^{-1}$ less E than present, the Black Sea level drops down by 150 in 1200 (Fig. 5.4(b)). The same sea level decrease could happened during the Younger Dryas for a decrease of $150 \text{ mm} \cdot \text{y}^{-1}$ in precipitation and $50 \text{ mm} \cdot \text{y}^{-1}$ less evaporation than at present (Fig. 5.4(c))

5.5 Discussion

There were several studies during the last 10 years discussing possible scenarios of the Black Sea reconnection with the Mediterranean (see Georgievski and Stanev [2006]) and reference therein). Those studies more often relied on geological observation than on numerical modelling. Therefore, results are controversial due to limitations of geological methods, for example dating remains uncertain, and there are sparse spatial and temporal resolutions. Based on the water balance equation and topography of the Black Sea catchment area, we provide

quantitative estimates of how much should components of the hydrological cycle in the Black Sea catchment area change in order to cause a sea level drop down. Our study indicates that is possible that the Black Sea level decreased by about 150 m in 1000 – 2000 years at LGM and Younger Dryas if precipitation decreases ($450 \text{ mm} \cdot \text{y}^{-1}$ and $150 \text{ mm} \cdot \text{y}^{-1}$ respectively) and evaporation decreases slightly less than precipitation. However, evaporation is even at present, one of the most elusive meteorological parameter. It is a function of temperature, wind, and humidity, all of which are interdependent. Regression (or multi-correlation) model between present day evaporation (and all the parameters that it depends on) and the past climate conditions inferred from available modelling study and data synthesis (Paleoclimate Modelling Intercomparison Project (PMIP) Joussaume and Taylor [2000]) could be the way to resolve the big question if there was a catastrophic flood on the Black Sea shelf or the gradual reconnection with the Mediterranean.

5.6 Figures

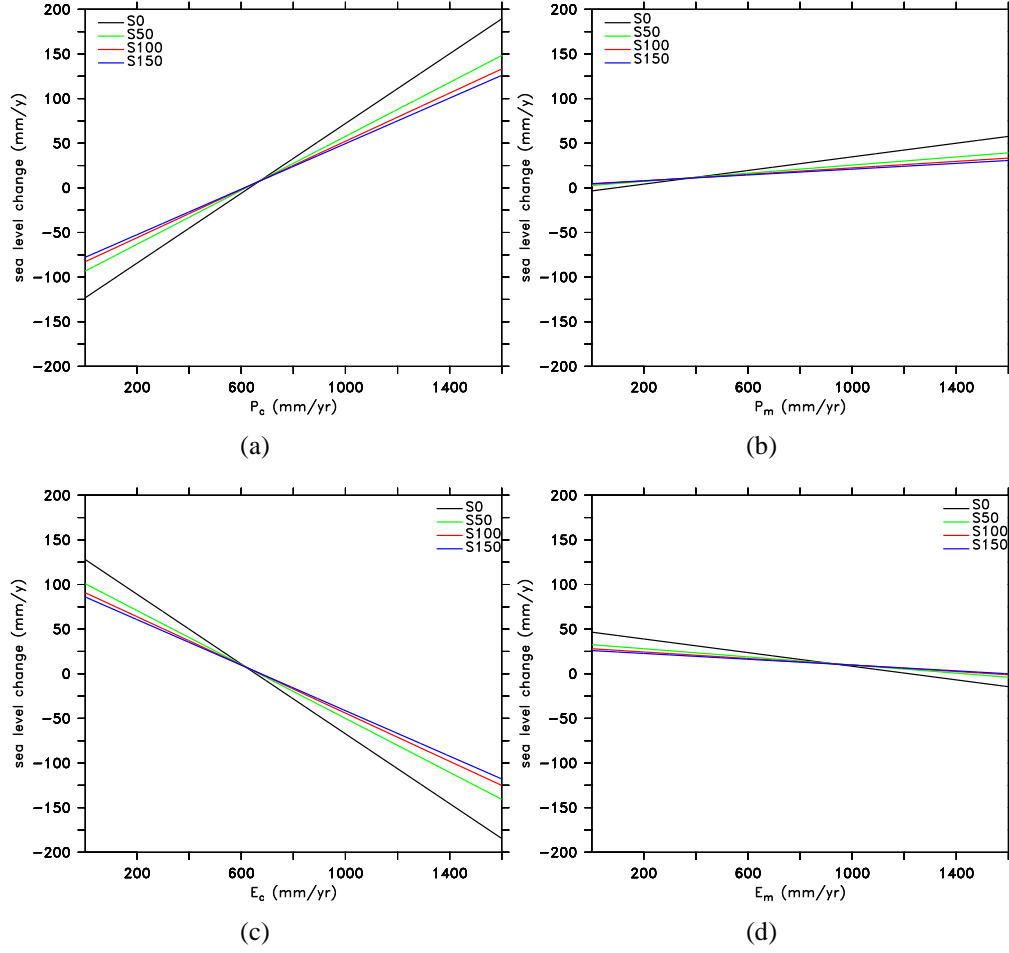


Figure 5.1: Changes of the sea level as a response to the changes of hydrological components ((a) P_c , (b) P_m , (c) E_c and (d) E_m in $\text{mm} \cdot \text{y}^{-1}$) and ratios between sea and land coverage. S0 is for the present-day sea level, S50, S100 and S150 for the sea level at 50, 100 and 150 m lower than today, respectively.

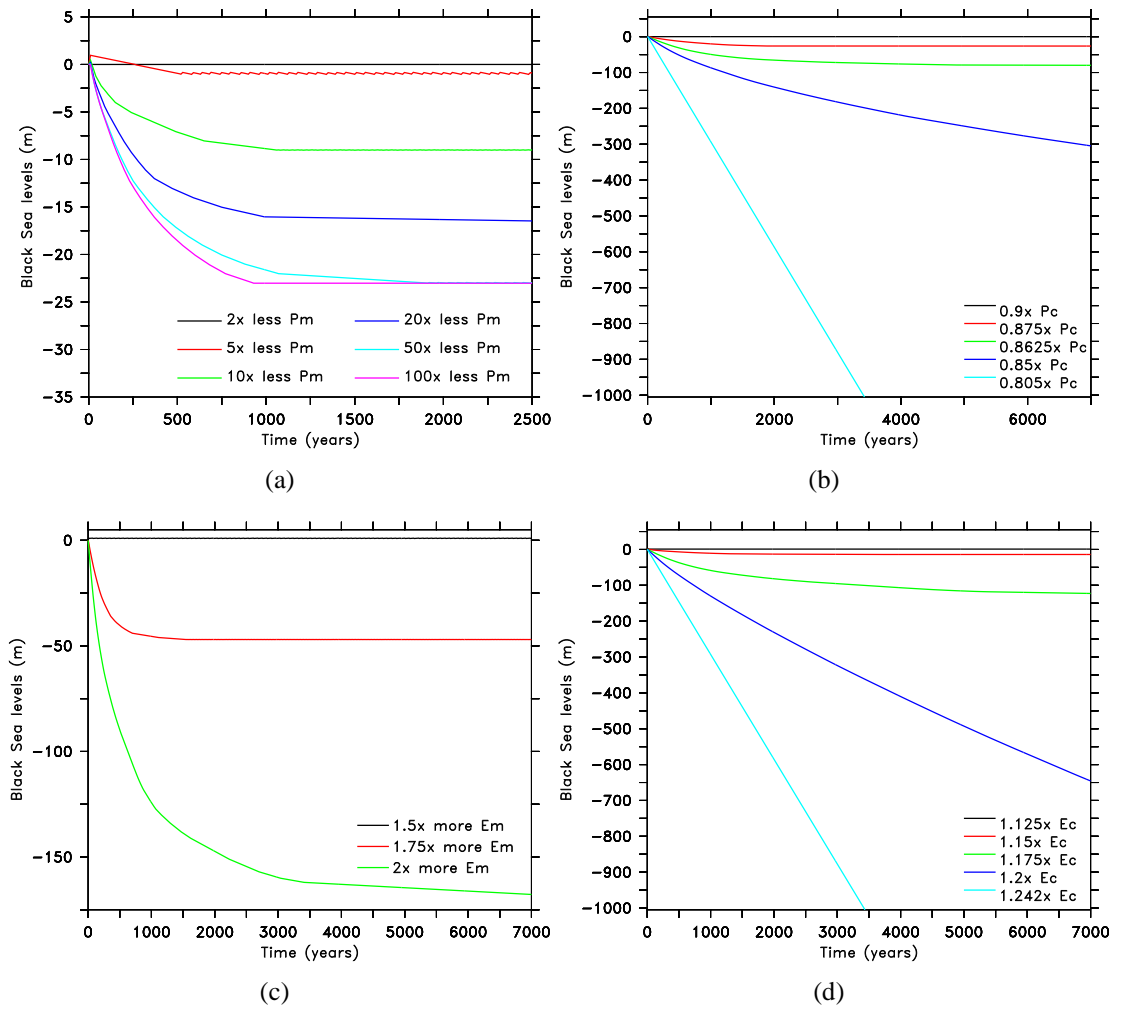


Figure 5.2: Changes of the Black Sea level, depending on change of only one component of the hydrological cycle a) maritime precipitation (P_m), b) continental precipitation (P_c), c) maritime evaporation (E_m) and d) continental evaporation (E_c).

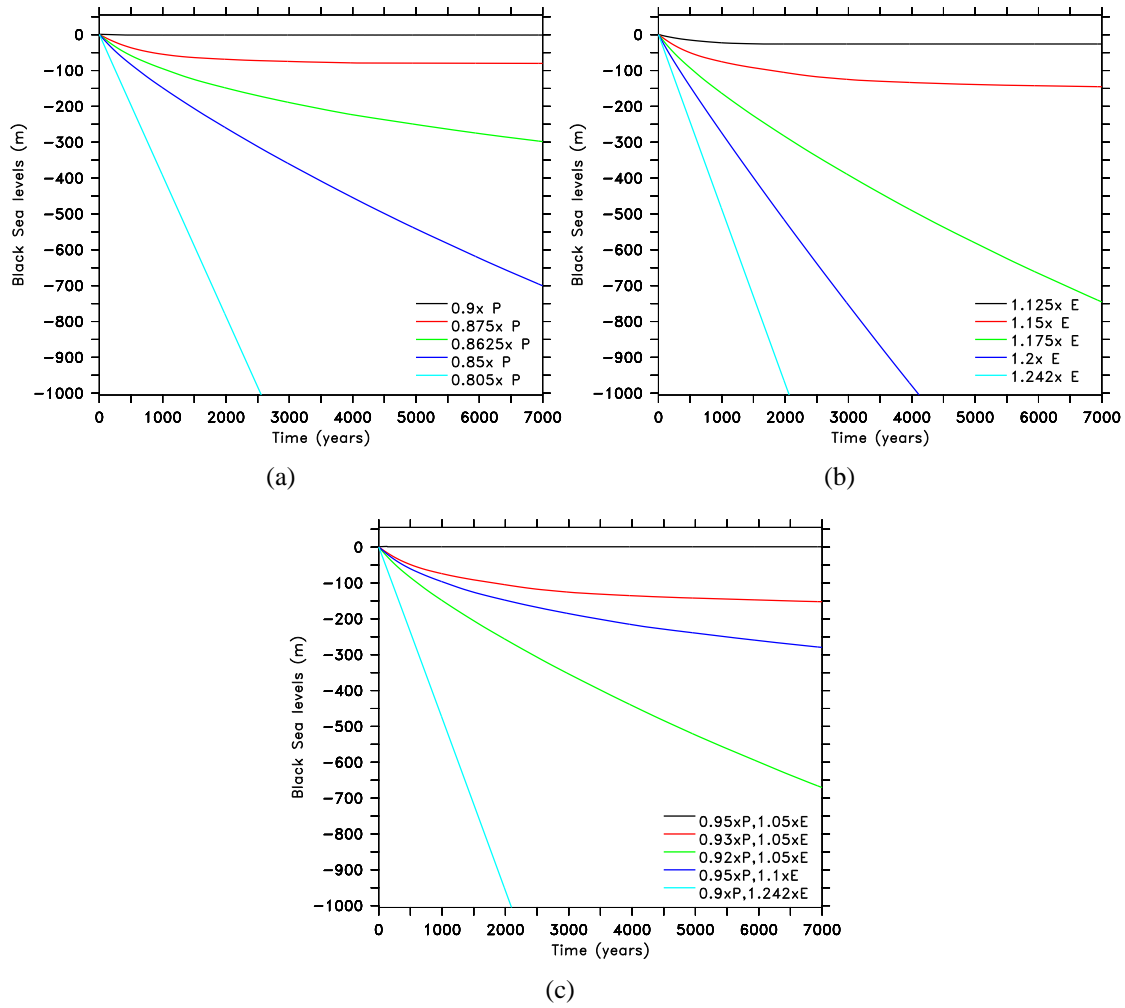


Figure 5.3: Changes of the Black Sea level, depending on change of a) less precipitation (P_c and P_m), b) more evaporation (E_c and E_m) and c) less precipitation (P_c and P_m) and more evaporation (E_c and E_m).

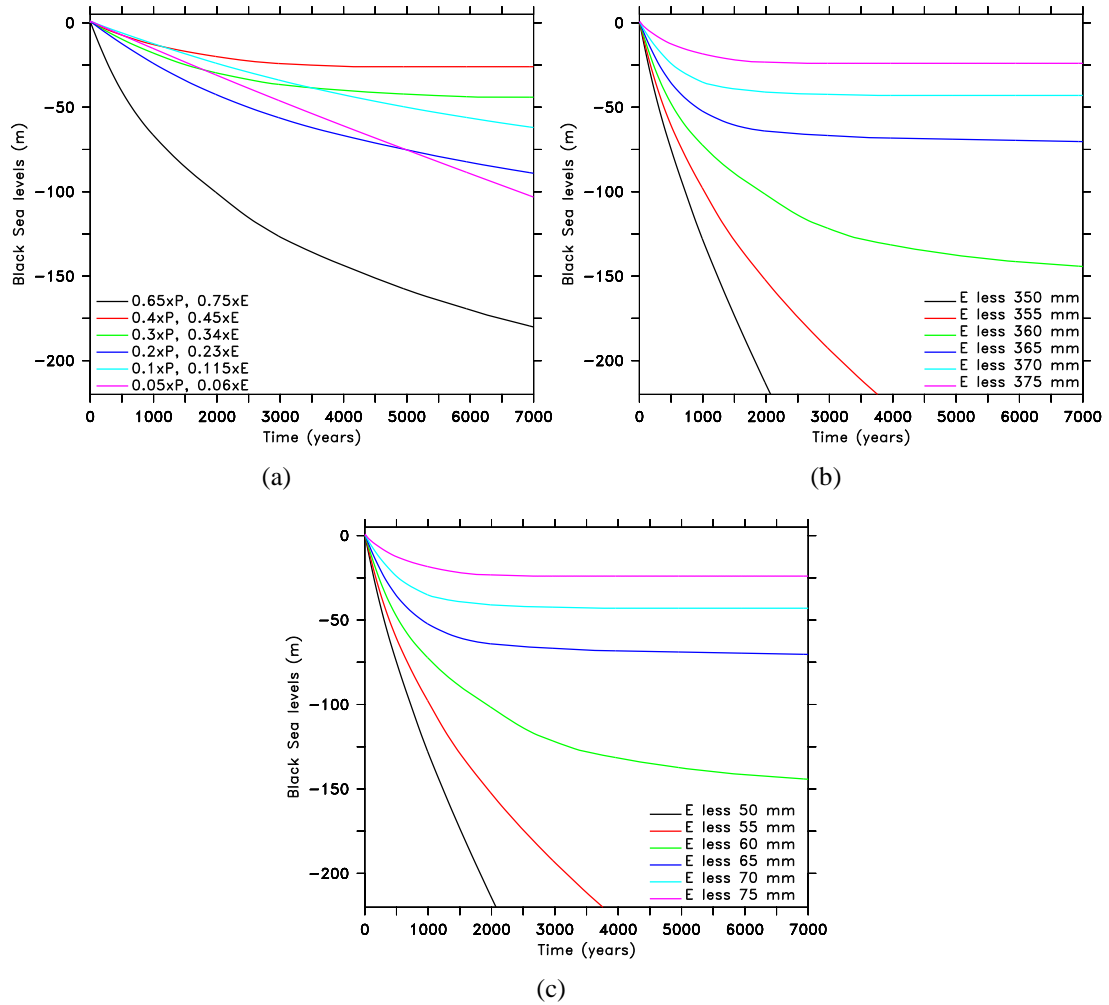


Figure 5.4: Theoretical changes of the Black Sea level as inferred from: a) Planet Simulator, b) geological observation [Tarasov et al., 1999] for LGM ($450 \text{ mm} \cdot \text{y}^{-1}$ less P than today and $350 - 375 \text{ mm} \cdot \text{y}^{-1}$ less evaporation than today), c) geological observation [Klimanov, 1997, Velichko et al., 2002] for Younger Dryas ($150 \text{ mm} \cdot \text{y}^{-1}$ less P than today and $50 - 75 \text{ mm} \cdot \text{y}^{-1}$ less evaporation than today)

Chapter 6

The Black Sea water balance during the past glacial cycle

The present-day hydrological data for the Black Sea catchment area are considered in parallel with the global and regional geological observations for the past ~ 160 ka. Using hypsometric function and water balance equation the Black Sea level and the Bosphorus outflow for the last glacial cycle are reconstructed. Our study indicates possible timing of the Mediterranean and Black Sea reconnection events. It yields that the reconnection during the last deglaciation was more likely gradual, while the penultimate deglaciation could result in a sudden infill of the Black Sea. Furthermore, we provide estimates of the transport through channels (Turgay, Uzboy, Manych and Bosphorus) between the Eurasian inland basins (Lake in the West Siberian Plain, Aral, Caspian, and Black Seas) at the time of their existence. From the analysis of reconstructed hydrological forcing it turned out that high frequency hydrological variations even with higher amplitudes do not cause substantial sea-level changes. However, a moderate hydrological shift towards dry climate would result in the sea-level decrease if it lasts for a sufficiently long time. Thus, for the Black Sea level, the duration of hydrological shifts towards dry climate is more important than the amplitude of change.

6.1 Introduction

The Eurasian inland basins and watersheds experienced dramatic changes during the Quaternary glacial cycles. At the present-day, the Caspian and Aral Seas are enclosed inland basins detached from each other, while the Black Sea is weakly connected with the Mediterranean through the Strait of Bosphorus. However, this was not a permanent configuration during the Pleistocene. Due to glacio-eustatic sea level changes of ~ 120 m the Black Sea detached several

times from the Mediterranean. Geological evidence indicates major changes of the Eurasian continental divide, including watersheds' extensions, changes of sea levels of the inland basins and the water transport through the passages between them [Mangerud et al., 2004, Ryan et al., 2003, Grosswald and Hughes, 2002, Boomer et al., 2000, Mamedov, 1997]. The region of our interest is shown on Fig. 1.1 (1°W - 116°E and 33°N - 86°N). These are the present-day Black, Caspian and Aral Sea catchment areas¹ and watersheds of rivers of the West Siberian Plain, Ob and Yenisei. The subject of our interest here is their evolution during the Late Pleistocene with the focus on the Black Sea level and the water transport through the Bosphorus Strait.

Recent research published by Ehlers and Gibbard [2004] has provided an invaluable resource for studying Quaternary glaciations. However, it does not go far beyond qualitative estimates of extensions of the ice-sheets and mountain glaciers. Quantitative understanding is still limited, e.g. the amount of melt water from mountains (Alps, Carpathians, Caucasus, Anatolian Mt., Altai and Kazakh hills, Ural, Pamir) that could contribute to the Black Sea water balance. To the best of the authors knowledge, by the time of preparing this text, quantitative reconstruction of the Alps Dome during the LGM is not available either. Apart from the sparse data, another source of limitations originates from the fact that geomorphology is influenced by tectonic activity and isostatic adjustment. Furthermore, heights of the possible water channels (passages) between inland basins appear to be areas of strong geologic activity, as well as sedimentation and erosion. Since these uncertainties present a huge limitation to an exact reconstruction of the evolution of Eurasian catchment areas we propose an alternative approach. Our approach is based on a positive correlation between $P - E$ and T established in the chapter 2 and sensitivity analysis described in chapter 4, complemented with available geological observations including $\delta^{18}\text{O}$ isotope oscillations identifying of wet and dry periods during the Late Pleistocene. Present-day topography is used for volumetric calculation and Glacial Melt Water (GMW) contribution is estimated from Peltier [1994] paleotopography. It is aim to bring these data together in order to reconstruct hydrological conditions in the Black Sea catchment area and its sea level for the past glacial cycle.

The text is organized as follows. Section 6.2 contains a brief summary of the geological processes in the region during the past glacial cycle. Data and methods are presented in section 6.3. Experimental setup is described in the section 6.4, followed by the results and discussion in section 6.5. Summary and outlook are provided in section 6.6.

¹To make our presentation more understandable we will use the following terminology: catchment area of the inland sea refers to the watershed and the basin, i.e. we use the term watershed to name the continental part of the catchment area and the term basin to name marine part (inland sea).

6.2 Extension of the Black Sea catchment area during the glacial cycle

During the extreme glaciation, the Eurasian Ice Sheet (EIS) and the geomorphological characteristic of the northern coast of Eurasian continent (Fig. 1.1) made it possible for north flowing rivers to be dammed and together with the Glacial Melt Water (GMW) re-directed to the south. One possible river route would form as a consequence of the Barents-Kara Ice Sheet advancing on the land, damming and re-directing rivers of the West Siberian Plain (Ob and Yenisei) to the southern inland seas (Aral, Caspian and Black Sea). According to a recent EIS reconstruction in the frame of the Quaternary Environment of the Eurasian North (QUEEN) project [Svendsen et al., 2004, Mangerud et al., 2004], the last time redirections of Arctic rivers happened 90 - 80 ka BP. However, there are authors [Grosswald and Hughes, 2002, for example] arguing that such an event happened even during the LGM. Support of the latter speculations can be found in Peltier's [1994] data, an earlier reconstruction of the ice sheet paleotopography (past 21 ka) based on glacial isostatic adjustment (GIA). However, a newer reconstruction of the same author [Peltier, 2004] is rather in agreement with the recent QUEEN's-project observations [Svendsen et al., 2004, Mangerud et al., 2004] and does not support damming and re-routing of Ob and Yenisei during the LGM. Transgression of the Arctic Ocean seems to be more likely during that time [Svendsen et al., 2004].

New waterways to the south could be created, if the margin of the EIS intersects borders of the Caspian or Black Sea catchment areas (from about 25°E to 55°E, see Fig. 1.1 for location), thus, blocking the route of the north-flowing rivers. The dating of these possible events is still a controversial issue, but according to geological observation it seems that one such event is dated about 18 - 17 ka BP [Mangerud et al., 2004]. At that time, rivers flowing to the Baltic Sea were dammed by the Scandinavian ice sheet, therefore melt-water from a considerable sector of the ice sheet and northwest flowing rivers were re-directed to the south to the Volga River. The above mentioned possibility has been supported by the recent ice sheet reconstruction at the LGM [Svendsen et al., 2004, Peltier, 2004]. Furthermore, according to Svendsen et al. [2004] the EIS advanced farther to the south during the Penultimate Glacial Maximum (PGM). It seems that, at that time, the Ob and Yenisei as well as the Volga river system contributed to the Black Sea water balance.

Not only little is known about the precise time, but also about how much glacial melt water was discharged into the northern Black Sea. Utilizing the concept of modern analogue channel geomorphology Sidorchuk et al. [2003] estimated that the river discharge of Severnaya Dvina, Mezen, Pechora, Volga, and Don during the last deglaciation amounted to twice their present volumes. Paleochannels connecting individual basins started to shallow at 15 to 14 ka BP.

Analyzing gravity cores from the continental slope in the northwestern Black Sea, Bahr et al. [2006] provide qualitative estimates of possible sources of Black Sea waters in the period 28.5 ka BP – 8 ka BP. Due to the Caspian transgression, these were glacial melt water. Dnepr and Don also drained proglacial waters. Danube showed variable discharge due to melting of the Alpine glaciers. Don lobe reached its maximum earlier in the Quaternary [Svendsen et al., 2004, Velichko et al., 2004].

Furthermore, extreme glaciation could probably provide a possibility for the rivers discharging at present in to the North Sea to be re-directed to the Black Sea. However, according to Ehlers et al. [2004] such a possibility was not likely during the past two major glaciations.

Apart from the geomorphological changes including glaciation, another factor that could influence the extension of the catchment areas and their water balances is the variability of the hydrological cycle. Furthermore, the above mechanisms are not independent one from another i.e. there is less precipitable water in the atmosphere during periods of huge extension of the ice sheets and vice versa.

6.3 Data and methods

In order to estimate water balances and extensions of the watersheds, we "corrected" available present day hydrological data using the global sea level curve and its proxies ($\delta^{18}O$ oscillation) to get theoretical values of precipitation and evaporation during the Late Pleistocene. This correction is based on a sensitivity study of the maritime precipitation and evaporation [Georgievski and Stanev, 2006], positive correlation between $P - E$ and T (chapter 2) and $\delta^{18}O$ oscillations. In the above mentioned research, the evaluation of the Black Sea catchment area for the period from the Lateglacial inception until the Holocene reconnection with the Mediterranean ($\sim 15 - 8$ ka BP) was addressed. Here, we extend results from that study for the Late Pleistocene (last glacial cycle) i.e. since ~ 120 ka BP until the recent Holocene reconnection of the Black Sea with the Mediterranean.

6.3.1 Present-day hydrology

For the present-day precipitation (P) and evaporation (E) in the Black and Caspian Seas catchment area, we use the European Center for Medium-range Weather Forecast (ECMWF) Re-analysis (ERA-40) data [Simmons and Gibson, 2000] constrained with the present-day observations on river discharges (R) [Stanev and Peneva, 2001, Stolberg et al., 2003]. The process of optimizing data (P, E, R) is described in detail by Georgievski and Stanev [2006] and results are

summarized in table 4 of that article. We will use the same values for the present-day P,E,R in the Black and Caspian Sea catchment areas as estimated there.

The Aral Sea gets most of its fresh water from Syr Darya and Amu Darya rivers, their discharge is $60.5 \text{ km}^3 \cdot \text{y}^{-1}$ [Fekete et al., 1999]. Since the hydrological cycle for the Aral Sea is not well resolved in the coarse resolution reanalysis data we use observations in 1960-s. One reason not to use present-day observation is that in the last 4 decades the natural hydrological state of this region has changed due to irrigation. Because the precipitation over the Aral Sea is small, it is often assumed that the evaporation of $\sim 880 \text{ mm} \cdot \text{y}^{-1}$ is balanced by the fresh water discharge [Stanev et al., 2004].

According to the Global Runoff Data Center (GRDC) report [Fekete et al., 1999] Ob and Yenisei (at present-day) discharge $965.1 \text{ km}^3 \cdot \text{y}^{-1}$ water into the Arctic ocean. For the $P_m - E_m$ (index "m" is for maritime, i.e. precipitation minus evaporation above the sea) above the West Siberian Plain which is supposed to have been transformed into a large lake during the Pleistocene, we use interpolated value between the present-day $P_m - E_m$ for the Kara and Caspian Sea, that is $P_m - E_m = 342 \text{ mm} \cdot \text{y}^{-1}$.

6.3.2 Palaeo hydrology

Precipitation and evaporation

On the glacial time scale, climate oscillates between cold and warm intervals, one consequence of which is the shift in the global hydrologic cycle. During cold-climate intervals sea level falls because water is evaporated from the oceans and stored on the continents in frozen phase (e.g. ice sheets and mountain glaciers). As the climate warmed, sea level rose because the melting of ice sheets returned their stored water into the oceans. This concept (i.e. positive correlation between $P - E$ and T proven in chapter 2) is used here to estimate paleo precipitation and evaporation from their present-day values. The correlation between the global sea level and the extension of ice sheet is revealed by the signature of marine and ice core record of the oxygen isotope. Therefore, we used marine (Raymo and Ruddiman [2004], see also Fig. 6.1(a)) and ice core (GRIP Members [1993] see also Fig. 6.1(b)) $\delta^{18}\text{O}$ isotope oscillation as an indicator of decrease of the hydrological cycle during glaciation and its amplification during the interglacial. We will also compare these results with global sea-level oscillations for the last glacial cycle from Lambeck et al. [2002] (Fig. 2a in that article).

For the continental precipitation P_c (index "c" is for continental), we assume a linear correlation

with $\delta^{18}O$, therefore:

$$P_c(t) = \frac{P_c^{LGM} - P_c^{PD}}{\delta^{18}O^{LGM} - \delta^{18}O^{PD}} \cdot (\delta^{18}O(t) - \delta^{18}O^{PD}) + P_c^{PD}, \quad (6.1)$$

where indexes "PD" and "LGM" stay for the present-day and the last glacial maximum values, respectively. Continental evaporation (E_c) is decreased by the same rate as P_c :

$$E_c(t) = E_c^{PD} \cdot \frac{P_c(t)}{P_c^{PD}} \quad (6.2)$$

Hydrological indexes "a" and "b" introduced by Georgievski and Stanev [2006], defining the ratio between maritime and continental parts of the hydrologic cycle ($a = E_m/E_c$ and $b = P_m/P_c$), are also linearly correlated to $\delta^{18}O$:

$$a(t) = \frac{a^{LGM} - a^{PD}}{\delta^{18}O^{LGM} - \delta^{18}O^{PD}} \cdot (\delta^{18}O(t) - \delta^{18}O^{PD}) + a^{PD}, \quad (6.3)$$

$$b(t) = \frac{b^{LGM} - b^{PD}}{\delta^{18}O^{LGM} - \delta^{18}O^{PD}} \cdot (\delta^{18}O(t) - \delta^{18}O^{PD}) + b^{PD}. \quad (6.4)$$

Non-linear changes of maritime components of the hydrologic cycle are taken into account:

$$E_m(t) = a(t) \cdot E_c(t), \quad (6.5)$$

$$P_m(t) = b(t) \cdot P_c(t) \quad (6.6)$$

Fig. 6.2 presents the reconstruction of the Black Sea fresh water fluxes. It reflects some differences between results based on an ice core $\delta^{18}O$ record (Fig. 6.1(b)) and marine oxygen isotope oscillation (Fig. 6.1(a)). Amplitudes of $\delta^{18}O$ oscillation are higher for the GRIP (the Greenland Ice Core Project) than for the MIS (Marine Isotope Stages) record. This feature is also reflected in the forcing functions (compare Fig. 6.2(b) and Fig. 6.2(c)). Differences between GRIP and MIS records are subject to continuous scientific debate but, are out of our scope here. For the purpose of this study it is sufficient to note that cores are sampled in different sites, MIS in the North Atlantic and GRIP in Greenland.

Glacial melt water

Paleotopography from Peltier [1994], presents one of a seldom publicly available quantitative reconstruction of the ice sheet volume with an evolution in time. Therefore, it is used here to estimate a glacial melt water (GMW) contribution to the Black Sea. The data set [Peltier, 1994] is available with 1° resolution for every 1000 years. The difference between ice volumes at

different time steps enables us to estimate the GMW, which is the contribution of ice melted from EIS to the global sea level rise per 1000 years. The part of the ice volume which would contribute only to the Eurasian inland basins is scaled by dividing the length of the EIS that intersects the individual catchment area with the perimeter of the EIS (see Fig. 6.3). There are three pathways of southern propagation of melt water: the ones of the Black Sea, Caspian Sea and to the lake in the West Siberian Plain. Table 6.1 shows the ice melted fluxes from EIS that contribute to the water balance of the Black Sea. The maximum of GMW appears at 16 ka BP, and this time is consistent with the estimate of Bahr et al. [2005], who found a good correlation of sedimentation events in the Black Sea and periods of large GMW. Between 15 and 14 ka BP, GMW drops to zero.

ka BP	TF	BF	CF	WSF
20	175156.8	42920.19	65221.95	67014.71
19	168027.7	41173.27	62567.31	64287.11
18	161302.3	39525.29	60063.02	61713.99
17	142354.5	34882.34	53007.55	54464.58
16	275962.2	67621.41	102758.2	105582.7
15	122152.5	-	-	122152.5

Table 6.1: GMW in $\text{km}^3 \cdot \text{y}^{-1} \times 10^{-3}$ entering the individual watersheds. BF is the Black Sea GMW, CF-Caspian, WSF-West Siberian, TF-the sum of all.

Maximum estimated values of GMW for the last deglaciation are about $270 \text{ km}^3 \cdot \text{y}^{-1}$. However, this value is not big enough to produce twice as much increase of river discharges as noted by Sidorchuk et al. [2003]. Permafrost melting is not included in that estimate, neither is the melt water contribution from the surrounding mountain glaciers. Our sensitivity study also indicates that at least $500 \text{ km}^3 \cdot \text{y}^{-1}$ is needed to have a Caspian transgression. Our conclusion is that during some short periods of the EIS retreat and permafrost melting a total of $500 \text{ km}^3 \cdot \text{y}^{-1}$ GMW was transported into the Caspian Sea.

6.3.3 Water budget

Hypsometric analysis of the Black Sea water balance is performed with ETOPO2 topography/bathymetry data. Watershed delineation is adopted from Oki and Sud [1998] as described in Georgievski and Stanev [2006]. Water balance equation is extended here to include the GMW and cascading waterfalls. The time rate of change of the lake volume W :

$$dW/dt = (P_m - E_m)A_m + R + GMW + D_u - D_l, \quad (6.7)$$

where $(P_m - E_m)A_m$ presents maritime components of the hydrologic cycle, i.e. *precipitation – evaporation* above the Black Sea (index m is for maritime, A_m is area of the basin, P_m is maritime precipitation, and E_m is maritime evaporation); R is river discharge or continental part of the hydrologic cycle, i.e. *precipitation – evaporation* above the continental part of the Black Sea catchment area; GMW is glacial melted water; D_u is water discharge from the upper lake in to the lower one and D_l is water export to the lower lake into the cascading sequence.

6.4 Experimental setup

According to our reconstruction [Georgievski and Stanev, 2006] based on the paleo-observation of the continental precipitation (since LGM to Holocene), the Black Sea water balance remains positive and therefore the only way to get a sea level drop down was to change maritime components of the hydrological cycle (decrease P_m and increase E_m), since they remain uncertain. Volumetric analysis is performed in accord with geological evidence [Mangerud et al., 2004, Svendsen et al., 2004], ice sheet topography [Peltier, 1994, 2004], present day topography (ETOPO2) and watershed delineation [Oki and Sud, 1998]. According to geomorphological properties of the region (Fig. 1.1), ice sheet advance at the West Siberian Plain would enable Ob and Yenisei to form an ice-dammed lake there. Due to geomorphological processes (sedimentation and erosion, isostatic adjustment, tectonic uplift) heights of the sill of the passages remain uncertain. Although the bedrock of Turgay Pass is about 40 m above sea level (asl) [Mangerud et al., 2004], we assume that due to limitation mentioned in section 6.1, the lake in the West Siberian Plain will overflow to Aral Sea when it reaches 126 m asl, i.e. present day height of the Turgay Pass. Similarly, the Aral Sea will spill over to the Caspian when its sea level reaches 53 m asl, that is the height of the Uzboy Pass. The Caspian Sea will discharge to the Black Sea when it reaches the height of the Manych Pass, that is 26 m asl. Boundary condition i.e. extension of the ice-sheet is taken from available literature.

6.5 Results

The focus is on the Black Sea level and the response of the transport through the Straits of Bosphorus to various forcing mechanisms such as ice melting water, rerouting the rivers of the West Siberian Plain and cascade transport between the Aral and Caspian Seas and Caspian and Black Seas.

6.5.1 Sea-land distribution

Distribution of the sea-land depending on the ice-sheet margin and according to our computation (Eq. 6.7) is shown in Fig. 6.4. Time slice at ~ 150 ka BP, corresponding to penultimate glacial maximum (PGM) is shown on Fig. 6.4(a). At that time, EIS advanced to the south on the West Siberian Plain and ice dammed lake was formed. Ob and Yenisei redirect their discharge to the south contributing thus to an increase in the Black Sea water balance. At the time of ice melting additional $500 \text{ km}^3 \cdot \text{y}^{-1}$ contributed to the Black Sea level rise. About ~ 90 ka BP (Fig. 6.4(b)), ice dammed lake is formed again, but there is no GMW contribution from the north of the Caspian and Black Seas. At the LGM, (Fig. 6.4(c)) some of the rivers discharging to the north were redirected to the Caspian Sea, and therefore, due to transgression, contributed to the Black Sea water balance.

6.5.2 Transport in the passages

Cascading transport constructed from three different forcing is shown in Fig. 6.5: Lambeck Fig. 6.5(a), MIS Fig. 6.5(b) and GRIP Fig. 6.5(c). In order to compare the results, they are shown for the whole analyzed period (140 ka for Lambeck forcing, 160 ka for GRIP and MIS forcing). However, the results (particularly the sea-level) for the first several thousands years should be taken with caution because of initialization problems. Cascading transports from the Lake in the West Siberian Plain to the Aral Sea (Turgay Pass) and then through the Uzboy Pass to the Caspian Sea and the Manych outflow to the Black Sea, are more or less the same for all three cases. However, the Bosphorus outflow reflects some features due to precipitation and evaporation changes. For the forcing constructed from the Lambeck sea-level curve (Fig. 6.5(a)) the Bosphorus outflow ceases only at the LGM, while the forcing constructed from MIS oscillation (Fig. 6.5(b)) allows for several thousands years a long shut off of the Bosphorus outflow at the PGM and LGM, as well as for the shut down associated with short episodes in between these two major events. According to forcing constructed from the GRIP (Fig. 6.5(c)), the major events of ceased Bosphorus outflow happened 60 ka BP and at LGM with several short episodes of closed strait in between and before that interval. Before PGM, estimate of the Bosphorus outflow ranges from about 500 to $650 \text{ km}^3 \cdot \text{y}^{-1}$ mostly due to the Arctic river redirection. At present-days, it ranges from 200 to $250 \text{ km}^3 \cdot \text{y}^{-1}$ depending on forcing (water fluxes constructed from MIS or GRIP). During the period 10 to 20 ka BP that is just after the PGM, which is considered to be a climatological similar period to the one after the LGM, the Bosphorus outflow was 250 to $450 \text{ km}^3 \cdot \text{y}^{-1}$. This is almost twice as much as when forcing is reconstructed from GRIP record. Our estimate of the Manych outflow is $520 \text{ km}^3 \cdot \text{y}^{-1}$ before PGM, about $30 \text{ km}^3 \cdot \text{y}^{-1}$ at 85 ka BP and $100 \text{ km}^3 \cdot \text{y}^{-1}$ at LGM. Just for the comparison, the

present-day river discharge into the Black Sea is about $340 \text{ km}^3 \cdot \text{y}^{-1}$.

6.5.3 The Black Sea sea-level

The variations in the Black Sea sea-level are shown on Fig. 6.6. Blue dashed line indicates the global sea level [Lambeck et al., 2002] and black line is the Black Sea level according to our reconstruction. In order to have an inundation of the Black Sea, the Mediterranean Sea level should be above the sill and the Black Sea should be below. Gradual reconnection takes place when the Black Sea is at the sill level, or higher (i.e. Bosphorus outflow exists). Comparing global and the Black Sea level curves for various forcing it turns out that flooding reconnection is likely to have happened at the penultimate deglaciation, according to MIS forcing. GRIP forcing provides more evidence for the gradual reconnection, while Lambeck forcing, should not be taken into consideration for the PGM since it spans for the past 140 ka, therefore not long enough to resolve initial conditions preceding the PGM. One interesting case is indicated by GRIP forcing at about 70 ka BP. At that time, the Black Sea was below the sill level and the global sea level was above the Black Sea level, but not above the Bosphorus sill. However, the height of the Bosphorus sill at that time remains uncertain. This case indicates that transient events of the Mediterranean waterfalls spilling over to the Black Sea are not to be excluded.

6.5.4 Error estimates and discussion

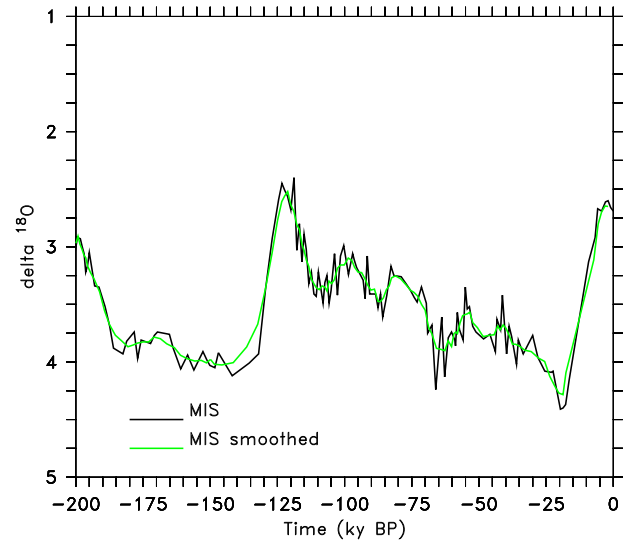
Comparing differences between the results inferred from MIS and GRIP forcing, the question of error estimates arises. Compared to the present-day changes of the hydrologic cycle, which are not well quantified, the situation for the past periods is even worse. For example, Tarasov et al. [1999] estimate $450\text{-}750 \text{ mm} \cdot \text{y}^{-1}$ less precipitation at the LGM than the present-day, while our estimate for the present-day is $P_c = 713 \text{ mm} \cdot \text{y}^{-1}$. Combining the maximum estimate ($750 \text{ mm} \cdot \text{y}^{-1}$ less precipitation and the same rate of change for the evaporation) for the LGM with the present-day P_c and E_c would result in negative river discharge, therefore our calculation are based on the minimum estimate (that is $450 \text{ mm} \cdot \text{y}^{-1}$ less precipitation than the present-day). Thus, any errors comparable with the range of change for the past hydrologic conditions would result in errors in water balance estimate about 10% to 50% of the present-day values. Nevertheless, there is even more to learn from the disagreement of MIS and GRIP results. One important conclusion could be drawn. High frequency oscillations seen on the GRIP record do not allow the Black Sea level to draw down. Although, the amplitudes of hydrologic shifts according to the GRIP forcing are higher than those seen in the MIS record, the shifts towards dry climate in the GRIP case do not last for very long, thus they can not cause a decrease the sea-level. If we apply smoothed GRIP forcing, the sea-level (figure not shown here) appear

similar to the result inferred from MIS forcing. This yields that for the Black Sea level it was more important how long the hydrologic shift lasted than how strong changes were.

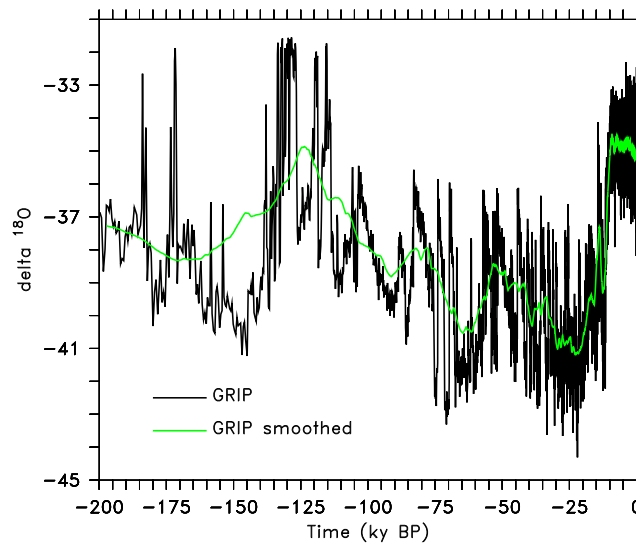
6.6 Summary and outlook

Geological observation reveal that throughout the past two million years the state of the Black Sea was predominantly of a freshwater lake interrupted only briefly by saltwater invasions coincident with global sea level high-stand [Ryan et al., 2003]. Combining the present-day data with available geological observation for the past glacial cycle we try to estimate the Black Sea level and the Bosphorus outflow for that period. Our results produce an idea of possible timing of the Mediterranean and Black Sea reconnection. Furthermore, they provide one step towards understanding how the Black Sea level responds to the changes of the hydrologic cycle in its catchment area. Although, according to this study the last reconnection of the Mediterranean and Black Sea happened gradually, the flood scenario can not be absolutely discarded. According to Ryan et al. [2003] the Black Sea flood happened after Younger Dryas or "8200 cold event", and these two events are not well resolved in our reconstruction. In order to make some progress, climatological proxy of evaporation would be needed to constrain hydrologic cycle more precisely, but this is not likely to become available in the nearest future. Furthermore, even the present-day hydrological cycle, in particular the distribution of evaporation and precipitation over the ocean is one of the least understood elements of the climate system. Non-linear changes of hydrologic cycle as a response to the changes of orography, surface characteristic and sea-land-ice distribution during the glacial cycle are even less understood. We only tackle those issues performing idealized experiments in order to isolate key mechanism controlling response of the hydrological cycle to the change of boundary conditions (chapter 2). Therefore, extensive sensitivity study with the Earth-system model of intermediate complexity (or even coupled OAGCM with fine resolution) is needed to deepen our understanding of global changes of precipitation and evaporation patterns, during glacial cycle. Further improvements could be expected applying regression analysis on climatological proxies from the Black Sea catchment area. Perhaps, one step could be to estimate potential evaporation from available temperature reconstructions by means of regression analysis. First step towards development of more complex model of the Black Sea catchment area on the glacial time scale would be to couple during the events of gradual reconnection the presented model with a simple hydraulic model of the type presented by Lane-Serff et al. [1997]. On the opposite side of the strait, model of similar complexity needs to be developed for sudden Black Sea infill with the Mediterranean water. Alternative would be to develop two layer shallow water model. In this way designed model, would provide more insight in the Black Sea stratification constrained by geological data.

6.7 Figures



(a)



(b)

Figure 6.1: Oscillation of $\delta^{18}O$ marine isotope according to data provided by Raymo and Ruddiman [2004] (a) and according to ice core record [GRIP Members, 1993], (b)

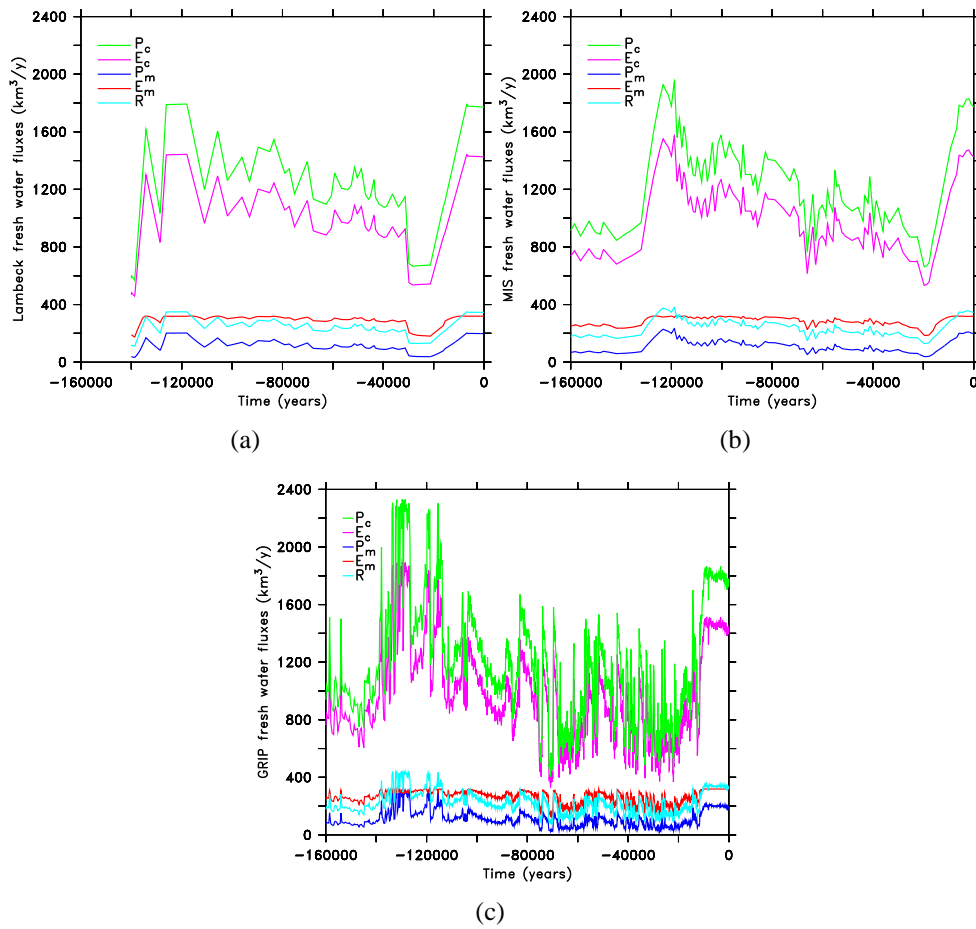


Figure 6.2: Black Sea fresh water fluxes reconstructed from (a) global ocean sea level oscillation Lambeck et al. [2002], (b) marine [Raymo and Ruddiman, 2004] and (c) ice core [GRIP Members, 1993] $\delta^{18}\text{O}$ isotope oscillation as an indicator of attenuation of hydrological cycle during glaciation and intensification during the interglacial.

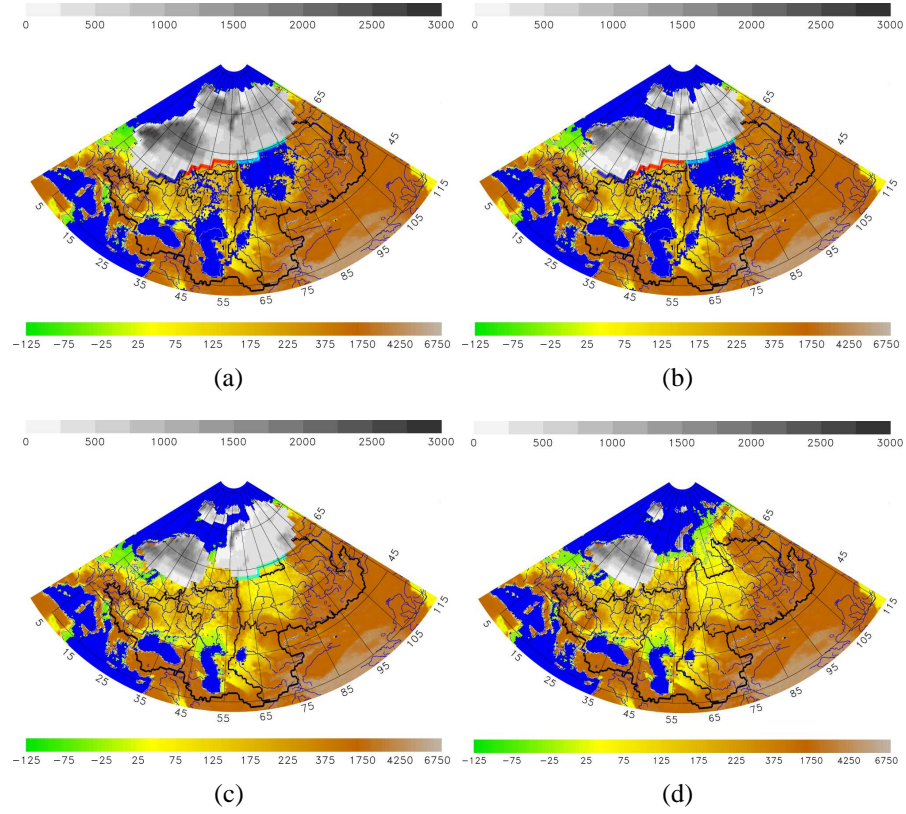


Figure 6.3: EIS retreat according to Peltier [1994], superimposed on the present-day topography (ETOPO2). Catchment area borders are adopted from TRIP. The tiny white lines indicate present-day coastline. The ice sheet topography is displayed by gray scale (0-3000 m with contour interval 250 m). The boundary of ice sheet where it intersects various catchment area is contoured with the thick blue, red and light blue lines to distinguish the contact zones with the individual watersheds: blue-Black Sea, red-Caspian Sea, light blue-the lake in the WSP. Land-sea mask is computed using the water balance model (see Eq. 6.7). (a) LGM 21 ka BP, (b) 16 ka BP, (c) 15 ka BP and (d) 14 ka BP. Corresponding GMW fluxes are given in Table 6.1.

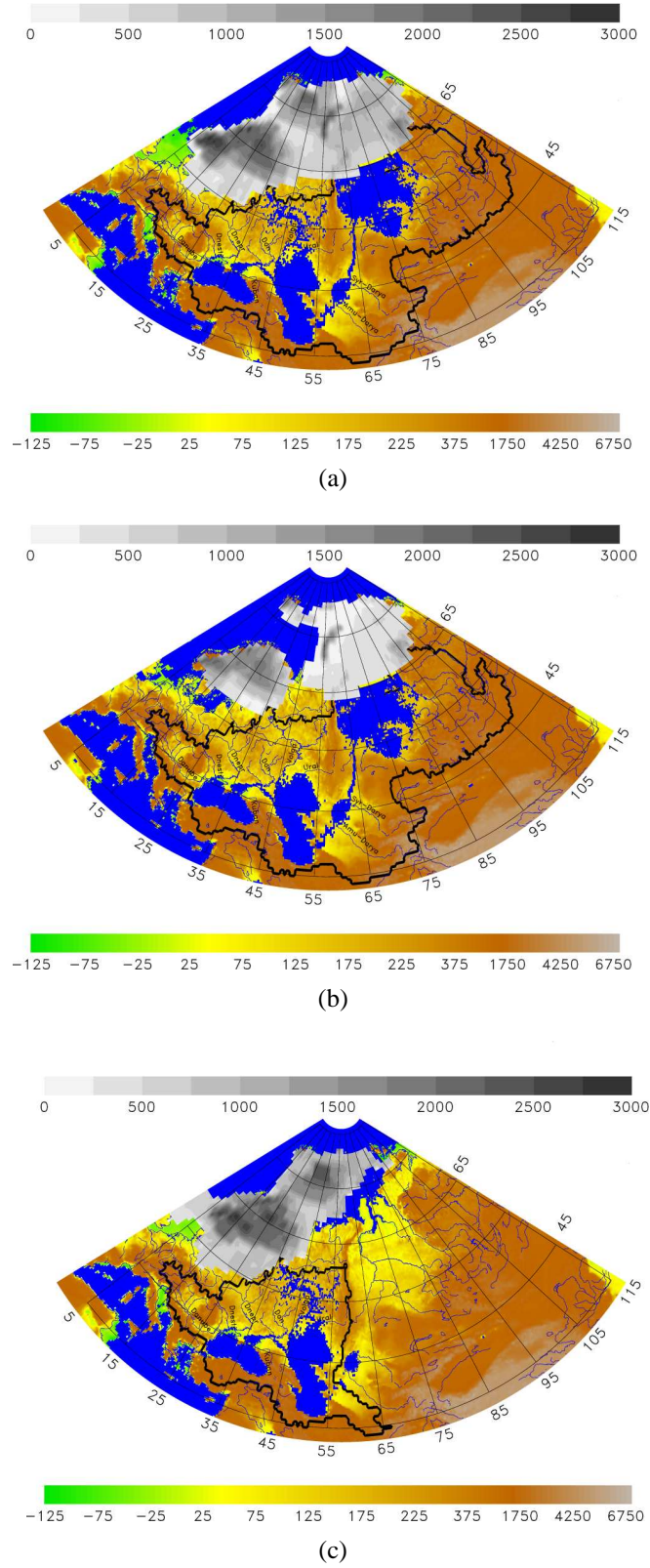


Figure 6.4: Theoretical portrayals of the sea-land and ice sheet distribution on the western Eurasian continent during the Late Pleistocene (a) penultimate maximum (~ 150 ka BP), (b) about 90 ka BP and (c) last glacial maximum (~ 20 ka BP).

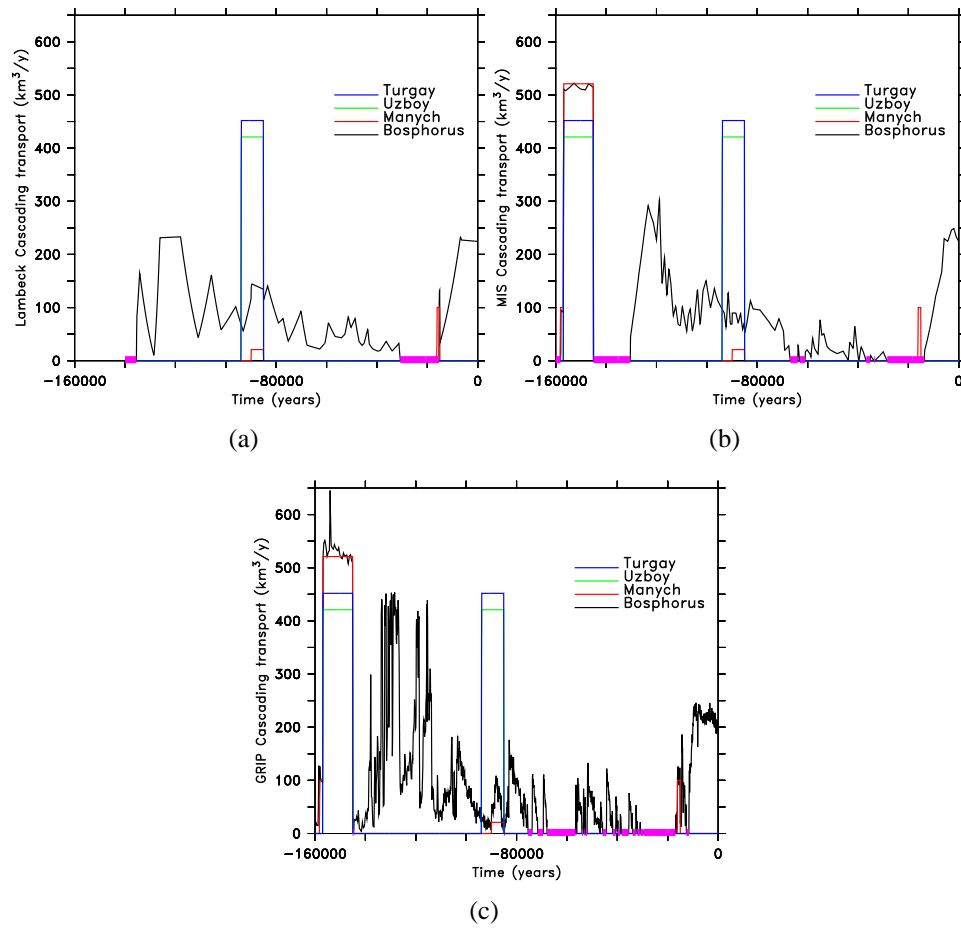


Figure 6.5: Transport through the passages and the Bosphorus Strait. Blue line is transport through the Turgay Pass (WSP to AS), green line is through Uzboy (AS to CS), red is through Manych Pass (CS to BS) and black line is Bosphorus transport (BS to Mediterranean): (a) Lambeck, (b) MIS and (c) GRIP forcing.

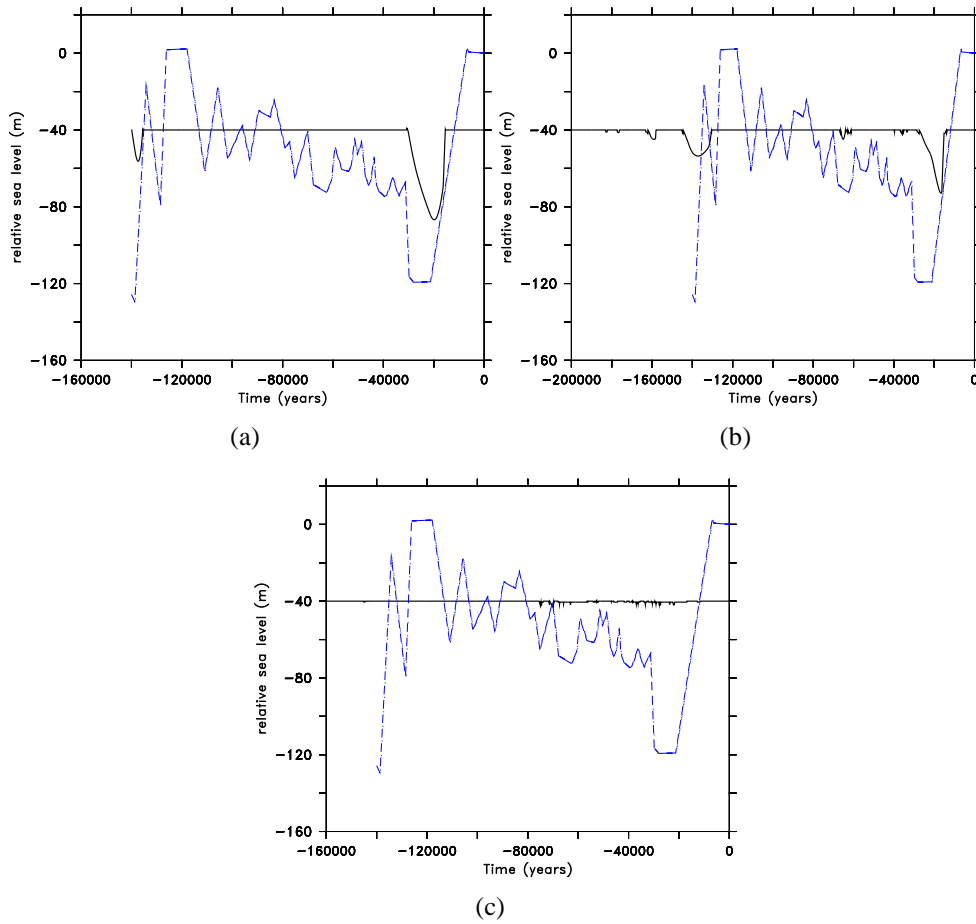


Figure 6.6: Black Sea (black) level since past 120 ka BP compared with global sea level (blue) from [Lambeck et al., 2002]. (a) with forcing constructed from [Lambeck et al., 2002], (b) with forcing constructed from Raymo and Ruddiman [2004] and (c) with forcing constructed from GRIP Members [1993]

Chapter 7

Summary and further perspectives

The Black Sea level fluctuation during the Holocene has been studied for more than 35 years. Perhaps there are even earlier works in Russian literature. However, during the last 10 years, one prominent event in the Black Sea history has attracted attention from an even broader community than the scientific one: the Black Sea reconnection with the Mediterranean. Two scenarios "catastrophic flood" and "gradual reconnection" have been proposed for the most recent (Holocene) intrusion of saline (Mediterranean) water into the Black Sea. The necessary (but not sufficient) condition for the catastrophic flood scenario to take place, is that the Black Sea level should at the time of re-connection be below the sill depth. The reconnection is gradual if the Black Sea level is above the sill i.e. the water balance of the basin is positive. To make things even more uncertain, the sill depth at the time of reconnection is not well known either. However, to the best of the author's knowledge, both of the reconnection scenarios are based either on geological observations or hydrodynamical properties of the flow. Furthermore, both methods provide support for the catastrophic and gradual reconnection. The controversy of geological interpretations comes from uncertainties with dating and low temporal and spatial resolution of observations, while the numerical modeling of hydrodynamical properties of the flow is biased since initial and boundary conditions are inferred from geological observations.

The problem arises from the fact that at the present state of knowledge glacio-eustatic sea level changes and changes of the hydrological cycle and their non-linear feed-backs in the climate system are not well understood. For example, the hydrological cycle, in particular the distribution of evaporation and precipitation over the ocean, is one of the least understood elements of the climate system. Therefore, hierarchy of numerical models and conceptual idealizations are needed in order to make progress integrating geological observations into theory. In this thesis, numerical simulations are performed with the Earth System Model of Intermediate Complexity (EMIC) - Planet Simulator (PS) in order to make some progress in our understanding of

the glacial hydrological shift and its regional implications. Furthermore, comprehensive analysis of available geologic observation in the Black Sea catchment area has been performed for the period from Last Glacial Maximum until the present-days. The hypsometric function with topographic data and the water balance equation with hydrological data were integrated to reconstruct the Black Sea level from LGM until the possible time of reconnection with the Mediterranean. An extensive sensitivity study has been performed to cover for unconstrained assumptions. Finally, all the results have been synthesized with the available geological observation in order to provide a reconstruction of the Black Sea level for the past glacial cycle.

The results presented could be classified according to several criteria. For example, qualitative and quantitative, global or regional. However, the most important results are summarized below in chronological order (how they appear in thesis). We demonstrate that topographic and surface property change connected with the glacial sea – land redistribution have a significant impact on the surface climate (2 m temperature, precipitation and evaporation). It is shown, that redistribution of sea – land can have a significant impact on regional climate. In particular, in the Mediterranean catchment area, where cooling due to the mountain uplift will cause the hydrologic cycle to shift towards dryer conditions, while warming due to the changed sea-land distribution will cause a shift towards wet conditions. Furthermore, it is shown that orography in the region between Minor Asia and the Alps could have a crucial role in the control of regional climatic patterns, in particular that of the EAWR. These results are used to constrain the Black Sea water balance. For that purpose, some problems with the ERA-40 data set in the Black and Caspian Sea hydrological cycle are recognized and corrected with available hydro-meteorological observations. According to our correction, precipitation above the continental part of the Black Sea catchment area is $713 \text{ mm} \cdot \text{y}^{-1}$, while evaporation is $574 \text{ mm} \cdot \text{y}^{-1}$. Above the sea, we have estimated $509 \text{ mm} \cdot \text{y}^{-1}$ precipitation and $809 \text{ mm} \cdot \text{y}^{-1}$ evaporation. Synthesis of available paleo-hydrological reconstructions indicate that the Black Sea water balance has been positive from LGM until today. Therefore, we performed sensitivity analysis to constrain the unknown components of the hydrological cycle. We have estimated that the increase of maritime evaporation and the decrease of maritime precipitation has to be 1.7 times the present-day values in order to achieve a sea-level drop down to 140 m. These results have motivated us to perform an extensive sensitivity study of the Black Sea level response to changes of each component of the hydrological cycle. It turned out that changes of maritime evaporation (E_m) have more control over the sea level than maritime precipitation (P_m). Even in the limiting case for a very small maritime precipitation ($P_m \rightarrow 0$), if all other components remain the same, the Black Sea level would reach the low stand at 22-23 m in less than 1000 years, and remain stable at that level. However, if E_m increases only twice as much as the present-day value, the Black Sea level would decrease for 150 m in about 2500 years. Furthermore, we have provided an estimate that is possible to have the Black Sea level drop down about 150 m in 1000 – 2000 years if evaporation decreases slightly less (or even remains the same) than precipitation. That

means for LGM or Younger Dryas if the precipitation decreases $450 \text{ mm} \cdot \text{y}^{-1}$ or $150 \text{ mm} \cdot \text{y}^{-1}$ respectively, evaporation has to decrease $355 \text{ mm} \cdot \text{y}^{-1}$ or less in the first case and $55 \text{ mm} \cdot \text{y}^{-1}$ or even less in Younger Dryas. These results together with geological observations for the last Quaternary glaciation (such as oxygen isotopes ratio ($\delta^{18}\text{O}$, maritime and ice core record) oscillation and Eurasian ice-sheet extension) as an indicator of hydrological regime change are used to provide theoretical portrayals of likely configurations of the Black Sea catchment area. Quantitative analysis of the Black Sea sea-level evolution and its reconnection history with the Mediterranean during the past $\sim 120 \text{ ka}$ is provided. Comparing our results with global sea-level, it turned out that reconnection at the penultimate glacial maximum could happen suddenly, while all recent reconnection were more likely gradual. The Black Sea water balance was positive almost all the time. Furthermore, from the analysis of reconstructed hydrological forcing it turned out that high frequency hydrological variations even with higher amplitudes do not cause substantial sea-level changes. In contrast to this, a moderate hydrological shift towards dry climate would result in the sea-level decrease if it lasts for a sufficiently long time period.

Our results provide one step towards understanding how the Black Sea level responses to the changes of the hydrologic cycle in its catchment area. Although, according to this study, the last reconnection between the Mediterranean and the Black Sea happened gradually, the flood scenario has not to be absolutely discarded. The problem is that we do not know how hydrological components change on the glacial-interglacial time scale. Geological proxy reconstruction of evaporation would be needed to constrain the hydrologic cycle more precisely. Since this is not likely in the near future, we admit that more extensive sensitivity studies are needed. In chapter 6 of this thesis, results from chapter 4 are combined with the $\delta^{18}\text{O}$ oscillations as an indicator of the hydrological shift in the Black Sea catchment area. However, if we combined results from chapter 5 with the $\delta^{18}\text{O}$ oscillations, results could be different. It is important to note that the former case is constrained with the geological observation and the change of hydrological parameters is gradual while the latter is a pure sensitivity study with the precipitation suddenly changed to the observed values and evaporation changed accordingly. Actually, there are plenty of possible combinations how the hydrological cycle could change but only some of them are plausible and have some evidence in geological observation or physical explanation. EMIC (or coupled AOGCM) simulations could be used to quantify global changes of precipitation and evaporation patterns during the glacial cycle. Further improvements could be expected using proxies from the Black Sea catchment area as an indicator of wet and dry periods and perhaps reconstructing potential evaporation from available temperature reconstructions by means of regression analysis. A similar approach could be applied for the Caspian Sea. This will provide more accurate timings of Caspian transgression. These are some indications how to refine presented results using the same or similar tools as used in this study. However, the program code written for the purpose of this thesis is designed in modern modular fashion and it will be

easy to implement other physical processes, either when more data become available or when we improve our understanding of certain phenomena to be able to model it. A first step towards a development of a more complex model of the Black Sea catchment area on the glacial time scale should be to couple the presented model with a hydraulic model during the event of a gradual reconnection with the Mediterranean. On the opposite side of the strait, a model of similar complexity needs to be developed for a sudden Black Sea infill with Mediterranean water. A model designed in this way, would provide more insight in the Black Sea stratification synthesized with the geological data. Further developments towards the integrated model of the Black Sea could be achieved by coupling with an ocean circulation module.

The sensitivity method (volumetric of the basin with the water balance equation for the catchment area) described in chapter 5 could be applied to some other regions of the world. For example if the precipitation and lake levels are known, the method could be used to constrain evaporation in the catchment basin. One possible investigation site could be the Prespa – Ohrid Lake system. One of the oldest and very unusual lake system in Europe unfortunately is not well investigated. However, its only outlet except the evaporation is the river Black Drin discharging into the Adriatic Sea. Therefore, reconstructing hydrological regimes in that region, including Albanian rivers, could be important even for the Mediterranean circulation since this is the area of the Adriatic Deep Water formation. Another complementary method to understand atmospheric variations during the past in the region in order to make a big picture of the past climate in the Mediterranean could be to perform analysis of the time series that could correlate with circulation patterns such as NAO and ENSO. This could be investigated on the Mediterranean microstromatolite timeseries, presented in a talk "Rediscovering pelagosome: a Mediterranean microstromatolite recording recent climate cycles" given by A. Monatanri as he was receiving the Jean Baptiste Lamarck Medal (2007). He suggested that the Holocene climate could be recorded in the pelagosome stratification.

I hope that in the near future there will be a chance to apply methods and results presented here in order to make progress towards deepening our understanding of climate change.

Bibliography

- A. E. Aksu, R. N. Hiscott, P. J. Mudie, A. Rochon, M. A. Kaminski, T. Abrajano, D., and Yasar. Persistent Holocene outflow from the Black Sea to the eastern Mediterranean contradicts Noah's Flood Hypothesis. *GSA Today*, 12(5):4 – 10, 2002.
- K. Arpe, L. Bengtsson, G.S. Golitsyn, I.I. Mokhov, V.A. Semenov, and P.V. Sporyshev. Analysis and modelling of the hydrological regime in the Caspian Sea basin. *Doklady Earth Science*, 4(366):552–556, 1999.
- R. Asselin. Frequency filter for time integrations. *Monthly Weather Review*, 100:487490, 1972.
- A. Bahr, F. Lamy, H. Arz, H. Kuhlmann, and G. Wefer. Late glacial to Holocene climate and sedimentation history in the NW Black Sea. *Marine Geology*, 214:309–322, 2005.
- A. Bahr, H. W. Arz, F. Lamy, and G. Wefer. Late glacial to Holocene paleoenvironmental evolution of the Black Sea, reconstructed with stable oxygen isotope records obtained on ostracod shells. *Earth and Planetary Science Letters*, 241:863–875, 2006.
- R. D. Ballard, D. F. Coleman, and G. D. Rosenberg. Further Evidence of Abrupt Holocene Drowning of Black Sea Shelf. *Marine Geology*, 170:253 – 261, 2000.
- G. Barnston and R. E. Livezey. Classification, seasonality and low-frequency atmospheric circulation patterns. *Mon. Wea. Rev.*, 115:10831126, 1987.
- I. Boomer, N. Aladin, I. Plotnikov, and R. Whatley. The palaeolimnology of the Aral Sea: a review. *Quaternary Science Reviews*, 19:1259–1278, 2000.
- M. A. Cane and S. E. Zebiak. A theory for the El Niño and the Southern Oscillation. *Science*, 228:10851087, 1985.
- R. Cheddadi, G. Yu, J. Guiot, S.P. Harrison, and C.I. Prentice. The climate of Europe 6000 years ago. *Climate Dynamics*, 13:1–9, 1997.
- P. U. Clark and A. C. Mix. Ice sheets and sea level of the Last Glacial Maximum. *Quaternary Science Reviews*, 21(1 - 3):1–7, 2002.
- M. Claussen, L. Mysak, A. Weaver, M. Crucifix, T. Fichefet, M.-F. Loutre, S. Weber, J. Alcamo, V. Alexeev, A. Berger, R. Calov, A. Ganopolski, H. Goosse, G. Lohmann, F. Lunkeit, I. Mokhov, V. Petoukhov, P. Stone, and Z. Wang. Earth system models of intermediate complexity: closing the gap in the spectrum of climate system models. *Climate Dynamics*, 18(7): 579–586, 2002.

- M. Conte, A. Giuffrida, and S. Tedesco. The Mediterranean Oscillation. Impact on precipitation and hydrology in Italy Climate Water. *Publications of the Academy of Finland, Helsinki*, 1989.
- A. Dai and K. E. Trenberth. Estimates of freshwater discharge from continents: Latitudinal and seasonal variations. *Journal of Hydrometeorology*, 3:660–687, 2002.
- E. T. Degens and D. A. Ross. Chronology of the Black Sea over the last 25000 years. *Chemical Geology*, 10:1 – 16, 1972.
- J. Ehlers and P. L. Gibbard. *Quaternary Glaciations – Extent and Chronology, part 1: Europe*. Developments in Quaternary Science, 2. Elsevier, Amsterdam, 2004.
- J. Ehlers, L. Eissmann, L. Lippstreu, H.-J. Stephan, and S. Wansa. Pleistocene glaciation of North Germany. In J. Ehlers and P. L. Gibbard, editors, *Quaternary Glaciations – Extent and Chronology*, volume 1, Europe, pages 135–146. Elsevier, Amsterdam, 2004.
- E. Eliassen, B. Machenhauer, and E. Rasmussen. *On the numerical method for integration of hydrodynamical equation with a spectral representation of the horizontal fields*, 1970.
- R.G. Fairbanks. A 17,000-year glacio-eustatic sea level record; influence of glacial melting rates on the Younger Dryas event and deep-ocean circulation. *Nature*, 342(6250):637 – 642, 1989.
- B.M. Fekete, C.J. Vorosmarty, and W. Grabs. Global composite runoff fields on observed river discharge and simulated water balances. Technical Report 22, Global Runoff Data Centre, Koblenz, Germany, 1999.
- K. Fraedrich, H. Jansen, E. Kirk, U. Luksch, and F. Lunkeit. The Planet Simulator: Towards a user friendly model. *Meteorologische Zeitschrift*, 14(3):299–304, 2005a.
- K. Fraedrich, H. Jansen, E. Kirk, and F. Lunkeit. The Planet Simulator: Green Planet and desert world. *Meteorologische Zeitschrift*, 14(3):305–314, 2005b.
- K. Fraedrich, E. Kirk, U. Luksch, and F. Lunkeit. The Portable University Model of the Atmosphere (PUMA): Storm track dynamics and low frequency variability. *Meteorologische Zeitschrift*, 14(3):735–745, 2005c.
- G. Georgievski and E. Stanev. Paleoevolution of the Black Sea Watershed: Sea Level and Water Transport through the Bosphorus Straits as an Indicator of the Lateglacial-Holocene Transition. *Climate Dynamics*, 26(6):631–644, 2006.
- N. Görür, M. N. Çağatay, Ö. Emre, B. Alpar, M. Sakinç, Y. İsalımoğlu, O. Algan, T. Erkal, M. Keçer, R. Akkök, and G. Karlik. Is the abrupt drowning of the Black Sea shelf at 7150 yr BP a myth? *Marine Geology*, 176:65 – 73, 2001.
- GRIP Members. Climate instability during the last interglacial period recorded in the GRIP ice core. *Nature*, 364:203–207, 1993.
- M. G. Grosswald and T. J. Hughes. The Russian component of an Arctic Ice Sheet during the Last Glacial Maximum. *Quaternary Science Reviews*, 21(1-3):121–146, 2002.

- S. Hagemann, K. Arpe, and L. Bengtsson. Validation of the hydrological cycle of ERA40. Technical Report 10, Max-Planck-Institute for Meteorology, 2005.
- B. J. Hoskins and A. J. Simmons. A multi-layer spectral model and the semi-implicit method. *Quarterly Journal of the Royal Meteorological Society*, 101:637655, 1975.
- K. A. Hughen, M. G. L. Baillie, E. Bard, A. Bayliss, J. W. Beck, C. J. H. Bertrand, P. G. Blackwell, C. E. Buck, G. S. Burr, K. B. Cutler, P. E. Damon, R. L. Edwards, R. G. Fairbanks, M. Friedrich, T. P. Guilderson, B. Kromer, F. G. McCormac, S. W. Manning, C. Bronk Ramsey, P. J. Reimer, R. W. Reimer, S. Remmele, J. R. Southon, M. Stuiver, S. Talamo, F. W. Taylor, J. van der Plicht, and C. E. Weyhenmeyer. Marine04 marine radiocarbon age calibration, 26 - 0 ka bp. *Radiocarbon*, 46:1059–1086, 2004.
- J. W. Hurrell. Decadal Trends in the North Atlantic Oscillation: Regional Temperatures and Precipitation. *Science*, 269:676679, 1995.
- S. Joussaume and K. E. Taylor. The paleoclimate modelling intercomparison project. In P. Brannonot, editor, *PMIP, Paleoclimate Modeling Intercomparison Project (PMIP): proceedings of the third PMIP workshop, Canada, 4-8 october 1999, in WCRP-111, WMO/TD-1007*, 2000.
- V. A. Klimanov. Late glacial climate in Northern Eurasia: the last climatic cycle. *Quaternary International*, pages 141 – 152, 1997.
- K. E. Kohfeld and S. P. Harrison. How well can we simulate past climates? evaluating the models using global environmental data sets. *Quaternary Science Reviews*, 19:321 – 346, 2000.
- S.O. Krichak, P. Kishcha, and P. Albert. Decadal trends of main Eurasian oscillations and the Eastern Mediterranean precipitation. *Theoretical and Applied Climatology*, 72:209220, 2002.
- Y. Kushnir. Interdecadal Variations in North Atlantic Sea Surface Temperature and Associated Atmospheric Conditions. *Journal of Climate*, 7:141157, 1994.
- H. Kutiel and Y. Benaroch. North Sea Caspian Pattern (NCP) an upper level atmospheric teleconnection affecting the Eastern Mediterranean: Identification and definition. *Theoretical and Applied Climatology*, 71:1728, 2002.
- K. Lambeck and J. Chappell. Sea level change through the Last Glacial Cycle. *Science*, 292: 679 – 686, 2001.
- K. Lambeck, T. M. Esat, and E.-K. Potter. Links between climate and sea levels for the past three million years. *Nature*, 419:199 – 206, 2002.
- G. Lane-Serff, E. J. Rohling, H. L. Bryden, and H. Charnock. Postglacial connection of the Black Sea to the Mediterranean and its relation to the timing of sapropel formation. *Paleoceanography*, 12:169 – 174, 1997.
- X. Liang, Y. Liu, and G. Wu. The role of land-sea distribution in the formation of the Asian summer monsoon. *Geophysical Research Letters*, 32, 2005.

- F. Lunkeit, S. Blessing, K. Fraedrich, H. Jansen, E. Kirk, U. Luksch, and F. Siehmann. *Planet Simulator: User's Guide*, April 2005a. Version 1.01.
- F. Lunkeit, M. Böttinger, K. Fraedrich, H. Jansen, E. Kirk, A. Kleidon, and U. Luksch. *Planet Simulator: Reference Manual*, September 2005b. Version 1.01.
- C. Major, W. Ryan, G. Lericolais, and I. Hajdas. Constraints on Black Sea outflow to the Sea of Marmara during the last glacial-interglacial transition. *Marine Geology*, 190(19):19 – 34, 2002.
- A. V. Mamedov. The Late Pleistocene-Holocene history of the Caspian Sea. *Quaternary International*, pages 161 – 166, 1997.
- J. Mangerud, M. Jakobsson, H. Alexanderson, V. Astakhov, G. K. C. Clarke, M. Henriksen, C. Hjorti, G. Krinner, J.-P. Lunkka, P. Möller, A. Murray, O. Nikolskaya, M. Saarnistou, and J. Svendsen. Ice-dammed lakes and rerouting of the drainage of northern Eurasia during the Last Glaciation. *Quaternary Science Reviews*, 23:1313–1332, 2004.
- P. J. Mudie, A. Rochon, A. E. Aksu, and H. Gillespie. Late glacial, Holocene and modern dinoflagellate cyst assemblages in the Aegean-Marmara-Black Sea corridor: statistical analysis and re-interpretation of the early Holocene Noah's Flood hypothesis. *Review of Palaeobotany and Palynology*, 128:143–167, 2004.
- P.G. Myers, C. Wielki, S. B. Goldstein, and E. J. Rohling. Hydraulic calculations of postglacial connections between the Mediterranean and the Black Sea. *Marine Geology*, 201(4):253–267, 2003.
- T. Oki and Y. C. Sud. Design of Total Runoff Integrating Pathways (TRIP) - A Global River Channel Network. *Earth Interactions*, 2(1):1–37, 1998.
- S. A. Orszag. Transform method for the calculation of vector-coupled sums: Application to the spectral form of the vorticity equation. *Journal of Atmospheric Sciences*, 27:890–895, 1970.
- J.P. Palutikof, M. Conte, J. Casimiro Mendes, C.M. Goodess, and F. Espirito Santo. Climate and climate change. In C. J. Brandt and J. B. Thornes, editors, *Mediterranean desertification and land use*. John Wiley and Sons, London, 1996.
- W. R. Peltier. Global glacial isostasy and the surface of the ice-age Earth: the ICE-5G (VM2) model and GRACE. *Annual Review of Earth and Planetary Sciences*, 32:111–149, 2004.
- W. R. Peltier. Global glacial isostasy and the surface of the ice-age earth: the ice-5g (vm2) model and grace. *Science*, 265:195–201, 1994.
- S. Philander. El Niño Southern Oscillation Phenomena. *Nature*, 302:295–301, 1983.
- S. Philander. El niño and la niña. *J. Atmos. Sci.*, 42:2652–2662, 1985.
- M. E. Raymo and W.F. Ruddiman. DSDP site 607 isotope data and age models, 2004.
- A. J. Robert. A stable numerical integration scheme for the primitive meteorological equations. *Atmos. Ocean*, 19:354–6, 1981.

- V. Romanova, G. Lohmann, K. Grosfeld, and M. Butzin. The relative role of oceanic heat transport and orography on glacial climate. *Quaternary Science Reviews*, 25:832–845, 2006.
- W. B. F. Ryan, W. C. Pitman III, C. O. Major, K. Shimkus, V. Moskalenko, G. A. Jones, P. Dimitrov, N. Görür, M. Sakiñ, and H. Yüce. An abrupt drowning of the Black Sea shelf. *Marine Geology*, 138(1-2):119–126, 1997.
- W. B. F. Ryan, C. Major, G. Lericolais, and S. L. Goldstein. Catastrophic flooding of the Black Sea. *Annual Review Earth Planetary Science*, pages 525 – 554, 2003.
- M. Siddall, L. J. Pratt, L. J. Helfrich, and L. Giosan. Testing the physical oceanographic implications of the suggested sudden Black Sea infill 8400 years ago. *Paleoceanography*, 19, 2004.
- A. Sidorchuk, A. Panin, and O. Borisova. The Lateglacial and Holocene Palaeohydrology of Northern Euroasia. In K.J. Gregory and G. Benito, editors, *Palaeohydrology. Understanding global change*, pages 61–76. Wiley, 2003.
- M. J. Siegert and J. A. Dowdeswell. Numerical reconstructions of the Eurasian Ice Sheet and climate during the Late Weichselian. *Quaternary Science Reviews*, 23:1273–1283, 2004.
- A. J. Simmons, B. J. Hoskins, and D. M. Burridge. Stability of the semi-implicit method of time integration. *Monthly Weather Review*, 100:405412, 1978.
- A.J. Simmons and J.K. Gibson. The ERA-40 project plan. ERA-40 Project Report Series. Technical Report 1, European Centre for Medium-Range Weather Forecasts, Reading, U.K., 2000.
- E. V. Stanev, E. L. Peneva, and F. Mercier. Temporal and spatial patterns of sea level in inland basins: Recent events in the Aral Sea. *Geophysical Research Letters*, 31, 2004.
- E.V. Stanev and E. L. Peneva. Regional sea level response to global climatic change: Black Sea examples. *Global and Planetary Changes*, 32:33–47, 2001.
- L. Starkel. Palaeohydrology of Central Europe. In K.J. Gregory and G. Benito, editors, *Palaeohydrology. Understanding global change*, pages 77–104. Wiley, 2003.
- F. Stolberg, O. Borysova, I. Mitrofanov, V Barannik, and P. Egtesadi. Caspian sea GIWA regional assessment 23. Technical Report 23, Global International Waters Assessment, Kalmar, Sweden, 2003.
- M. Stuiver and P. J. Reimer. Extended 14c database and revised CALIB radiocarbon calibration program. *Radiocarbon*, 35:215–230, 1993.
- J.-I. Svendsen, H. Alexanderson, V. I. Astakhov, I. Demidov, J. A. Dowdeswell, S. Funder, V. Gataullin, M. Henriksen, C. Hjorti, M. Houmark-Nielsenj, H. W. Hubberten, Ó. Ingólfsson, M. Jakobsson, K. H. Kjær, E. Larsenn, H. Lokrantz, J. P. Lunkka, A. Lyså, J. Mangerud, A. Matiouchkov, A. Murray, P. Möller, F. Niessens, O. Nikolskayat, L. Polyak, M. Saarnistou, C. Siegert, M. J. Siegert, R. F. Spielhagen, and R. Steins. Late Quaternary ice sheet history of northern Eurasia. *Quaternary Science Reviews*, 23:1229–1271, 2004.

- P. E. Tarasov, O. Peyron, J. Guiot, S. Brewer, V. S. Volkova, L. G. Bezusko, N. I. Dorofeyuk, E. V. Kvavadze, I. M. Osipova, and N. K. Panova. Last glacial maximum climate of the former Soviet Union and Mongolia reconstructed from pollen and plant macrofossil data. *Climate Dynamics*, 15(3):227–240, 1999.
- A. M. Tushingham and W. R. Peltier. Relative sea level database. Technical report, NOAA/NGDC Paleoclimatology Program, Boulder CO, USA, 1993.
- A. A. Velichko, N. Catto, A. N. Drenova, V. A. Klimanov, K. V. Kremenetski, and V. P. Nechaev. Climate changes in East Europe and Siberia at the Late Glacial-Holocene transition. *Quaternary International*, pages 75 – 99, 2002.
- A. A. Velichko, M. A. Faustova, Yu. N. Gribchenko, V. V. Pisareva, and N. G. Sudakova. Glaciations of the Eeast European Plain – distribution and chronology. In J. Ehlers and P. L. Gibbard, editors, *Quaternary Glaciations – Extent and Chronology*, volume 1, Europe, pages 337–354. Elsevier, Amsterdam, 2004.

List of Abbreviations

AGCM	– Atmosphere Global Circulation Model
AOGCM	– Atmosphere-Ocean Global Circulation Model
BP	– before present
CCM	– Coupled Climate Model
CR, CTRL	– Control Run
EAWR	– East Atlantic/West Russia, climatic index
ECHAM	– climate model, developed from the ECMWF model + comprehensive parameterization package developed at Hamburg
ECMWF	– European Centre for Medium-Range Weather Forecasts
EMIC	– Earth-system Model of Intermediate Complexity
ENSO	– El Niño-Southern Oscillation
ERA	– ECMWF re-analysis
GCM	– Global Circulation Model
GRIP	– Greenland Ice Core Project
ka	– kilo anno, 1000 years
LGM	– Last Glacial Maximum
MASK	– experiment with changed mask
MIS	– Marine Isotope Stage
NAO	– North Atlantic Oscillation
PELT	– experiment topography constructed from Peltier [2004]
PMIP	– Paleoclimate Modelling Intercomparison Project
POMA	– experiment with changed topography and mask
PS	– Planet Simulator
SG	– surface geopotential (orography)
SLM	– sea land mask
SR	– surface roughness
TOPO	– experiment with changed topography
SST	– Sea Surface Temperature

Acknowledgments

At the end of this eventful journey leading me to the completion of my thesis, it is the time to take a bow and to acknowledge all the helpful people that furnished me with their kind support along the way.

First of all, I am indebted to my supervisor Prof. Dr. Emil Stanev who invited me to join him to work together on the ASSEMBLAGE Project. He was also ensuring continuous funding for the first three years of my study, supported by the EC contract EVK3-CT-2002-00090. I would also like to express my gratitude for his friendly and permanent advice, meticulous guidance, pertinent encouragement, useful discussions and valuable suggestions throughout this investigation. I am grateful to Prof. Dr. Jörg-Olaf Wolff, Head of the Theoretical Physical Oceanography department at the Institute for Chemistry and Biology of the Marine Environment (ICBM), for his kind support whenever needed and providing a creative and friendly atmosphere in our department.

Additional funding that made me prolong my stay in Oldenburg has been supported from various sources that I would like to acknowledge. Thanks are due to Dr. Joanna Staneva. She kindly provided me with the opportunity to further develop and evaluate my software in cooperation with her on the Ferry-Box project. I was also awarded a DAAD stipend, thanks to the International Student Office committee in Oldenburg. A clever investment plan suggested by my brother Dalibor Georgievski made my life much easier. Hvala buraz!

I would also like to acknowledge the Wolfgang Schulenberg-Programm and European Science Foundation committee for the award of two travel grants to participate at the conferences and field trips in the frame of the IGCP 521 project: "Black Sea-Mediterranean Corridor during the last 30 ky: sea level change and human adaptation", in Istanbul (2005) and Kerch-Gelendzhik (2007). Additional travel grants were kindly ensured by Prof. Dr. Emil Stanev and Prof. Dr. Jörg-Olaf Wolff.

I really have to express my admiration and gratitude to Prof. Dr. Klaus Fraedrich and his colleagues from the Meteorological Institute (University of Hamburg), especially to the Planet Simulator (PS) development team for making the PS available to the scientific community.

ASSEMBLAGE workshops in Varna and Hamburg and IGCP 521 meetings were great opportunities to meet the colleagues and to work in a pleasant and stimulating atmosphere. I would like to thank them all for their valuable input, especially to the leaders of the projects, Gilles Lercolais (ASSEMBLAGE), Valentina Yanko-Hombach (IGCP 521) and those provid-

ing me with concrete suggestions, encouragements, and friendly support, Liviu Giosan, Olga Kwiecien, Andre Bahr, Elissaveta Peneva, Vanja Romanova, Preslav Peev, Petra Mudie, Ken Wallace, Anthony Brown, Marina Filipova-Marinova, Klaus Arpe, Andre Panin, Alexander Kislov, Ron Martin, Salomon Kroonenberg, Olga Lichodedova. I would also like to express my gratitude to Delcho Solakov for making me feeling like being at home in Varna and Philipp Konerding to provide me with a home in Hamburg.

Thanks are due to E. J. Rohling and an anonymous reviewer for their useful comments on chapter 4, as published with Climate Dynamics. I would also like to express my gratitude to Mrs. Mirjana Gabrić (English teacher) and Mrs. Adelheid Wegner-Demmer (English translator). They kindly provided assistance with English correction. Thanks are due to Jörg-Olaf Wolff and Sebastian Grayek for the German translation of the Abstract. I would also like to thank all the people of Free Software Foundation for providing GNU/Linux platform and tools to perform and present scientific research. Thank you guys for providing a free crunching time. I would also like to acknowledge support from the Ferret mailing list community. Ferret is a product of NOAA's Pacific Marine Environmental Laboratory. Almost all the graphics and some analysis in this thesis are performed with the Ferret program. I would also like to say "jedno zdrasti", to Dr. Elena Sokolova, for providing me with a L^AT_EX 2_ε template to produce this thesis, ZDRRRRASTi!.

A warm 'thank you' goes to all my colleagues at the ICBM especially those guys being members of our volleyball team members at the regular yearly Institute tournament. Special thanks goes to the members of Theoretical Physics/Complex Systems and Theoretical Physical Oceanography working group. They help me to gently adopt social activity of the North Germany, such as Bosseltouren. "I u nebo s njim i u pakao¹", goes to the one and only "Flying Burex", a football team and all the guys that were playing with us, breaking their bones and bleeding in the Soccerland arena. "SSSsshaaaj!" goes to my colleagues from the Sputnik Radio, Geistarbeiters DJ team.

I would also like to thank my parents for creating a careless environment even when going was tough, and Gaga for being far away so close.

¹To the heaven with them and staigh to the hell

Curriculum Vitae

Name.....: Goran Georgievski

Date of birth....: 9. 2. 1971.

Place of birth...: Zagreb, Croatia

Education

since 2004: Ph. D. student at the University of Oldenburg (Germany)

2002: graduated at Faculty of Science, Department of Physics (meteorology and physical oceanography), Zagreb (Croatia)

1989: Mathematical IT high school, course mathematician

Positions

since 2008: member of the chair of environmental meteorology in the Brandenburg technological university Cottbus

2003 – 2007: member of the Theoretical Physical Oceanography department at the Institute for Chemistry and Biology of the Marine Environment in Oldenburg

Erklärung

Hiermit erkläre ich, dass ich die vorliegende Dissertation selbstständig verfasst habe und nur die angegebenen Hilfsmittel verwendet habe. Teile der Dissertation wurden bereits veröffentlicht bzw. sind zur Verentlichung eingereicht, wie an den entsprechenden Stellen angegeben. Die Dissertation hat weder in Teilen noch in ihrer Gesamtheit einer anderen wissenschaftlichen Hochschule zur Begutachtung in einem Promotionsverfahren vorgelegen.

Oldenburg, im Januar 2008

Goran Georgievski